UNIVERSITY OF SOUTHERN DENMARK

Strategic Integration of Sustainable Gas to Liquid and Power to Liquid Pathways in the Danish Energy System in 2050

MASTER'S THESIS

ASGER VESTERGAARD LAURSEN

JEPPE BAY PEDERSEN

University Supervisor: Henrik Wenzel

Company Supervisor: Anders Bavnhøj Hansen

JUNE 2020

SDU
University of
Southern Denmark

ENERGINET

Authors

Asger Vestergaard Laursen

Student number: 427178

Master student, Energy Technology

E-mail: aslau15@student.sdu.dk

Jeppe Bay Pedersen

Student number: 84930519

Master student, Energy Technology

E-mail: jeppe15@student.sdu.dk

We hereby declare that the presented master thesis *Strategic Integration of Sustainable Gas to Liquid and Power to Liquid Pathways in the Danish Energy System in 2050* is written independently and without any other sources and aids than stated. Furthermore, we declare that we have cited each analogous applied passage.

Odense, June 16th, 2020

<table>
<tr><td>Asger Vestergaard Laursen</td><td>Jeppe Bay Pedersen</td></tr>
</table>

Educational Institution

University of Southern Denmark

Department of Maersk Mc-Kinney Moeller

Faculty of Engineering

Campusvej 55, 5230 Odense M

Please use the following reference to the whole report:

Laursen, Asger V. & Pedersen, Jeppe B., 2020: *Strategic Integration of Sustainable Gas to Liquid and Power to Liquid Pathways in the Danish Energy System in 2050.* University of Southern Denmark, Odense, Denmark

Abstract

For several years, greenhouse gas emissions, and the negative impact to the climate and environment that follows, has been an increasing concern to the global society as a whole. If the goal of the Paris Agreement that was signed in 2016 - limiting the global average temperature increase to well below 2.0 °C above pre-industrial levels while pursuing efforts in order to limit this temperature increase to 1.5 °C - is to be complied with, several measures have to be taken in every sector of every energy system. However, among others, one sector proves to be of a more challenging nature than others - namely the transportation sector.

This study investigates the prospects of adapting the gas-to-liquid (GtL) and power-to-liquid (PtL) pathways, for production of synthetic liquid fuels for the transportation sector, in the Danish energy system in 2050. The purpose is to give an overall recommendation of the most socioeconomically feasible production configuration, using GtL and PtL while utilizing the synergies that exist within sector coupling, in order to produce the Danish jet fuel demand of 50 PJ in 2050. Furthermore, the study answers questions related to the strain that is imposed on the Danish electricity network as a result of liquid fuel production through PtL, and the demand for negative CO_2 emissions towards a climate neutral energy system in 2050.

For the purpose of answering the stated research questions, a literature study of the different technologies that make up both the GtL and PtL pathways, have been conducted. This knowledge about the technologies has been applied in the development of an energy system model in Energinet's modeling tools Sifre and ADAPT. The model in Sifre has been used to simulate the production of jet fuel, in the Danish energy system in 2050, through different liquid fuel production plant configurations, including pure GtL, pure PtL and hybrid configurations between the two pathways. ADAPT has been used to simulate the most socioeconomically feasible investments in production capacities for the technologies applied in each liquid fuel production plant configuration. Furthermore, a sensitivity analysis has been conducted in order to investigate the robustness of the resulting jet fuel prices, when subjected to changes in key parameters of the GtL and PtL pathways.

From this study it can be concluded that, deploying hybrid configurations combining the GtL and PtL pathways, the entire Danish jet fuel demand can be produced at approximately double the price of jet fuel today, while not imposing significant strain on the existing infrastructure. Of these hybrid configurations, combining co-electrolysis with either steam-methane reforming (SMR) or partial oxidation (POX) results in the lowest jet fuel prices, when considering an average of upstream methane production from biogas upgrading and methanation of CO_2 in biogas, at 31.2 EUR/GJ. The results showed that, the jet fuel price in the pure GtL pathway with methane from biogas upgrading, that included POX, was lowest with a price of 25.2 EUR/GJ. However, in every variation the pure GtL pathway violates the biogas constraint meaning that the entire Danish demand of jet fuel can not exclusively be produced by GtL.

Preface

This master thesis has been conducted as a completion of the master education in Energy Technology at the Faculty of Engineering, University of Southern Denmark (SDU). The thesis has been conducted by Asger Vestergaard Laursen and Jeppe Bay Pedersen during the period of February 1st to June 16th 2020. The thesis corresponds to a workload of 60 ECTS points.

The primary supervisor at the University of Southern Denmark has been Henrik Wenzel. We would like to thank both Henrik Wenzel, and the main writer of *Nordic GTL* and Ph.D student at SDU at the time, Anders Winther Mortensen, for several hours of discussion, inputs and insights into the GtL pathway.

This thesis has been written in collaboration with the research department *System Perspective* at Energinet. We would like to thank our company supervisor, Anders Bavnhøj Hansen, who has contributed significantly with knowledge, inputs, discussions and competences to the working process.
A special thanks to the people at the department *Analyses and Models* at Energinet, who have contributed with several hours of supervision and assistance regarding Sifre and ADAPT. These people include Kasper Nybord, Bjarne Donslund and Jonathan Roskam-Hemmingsen.

Finally, we would also like to thank everyone else, that have contributed with knowledge and inputs to the whole process.

Contents

List of Figures

List of Tables

List of Abbreviations and Acronyms

AF19	The Danish Energy Agency's conditions for analyses for Energinet in 2019
ASU	air separation unit
BECCS	bio-energy carbon capture and storage
Biomethane	methane from a biomass feedstock
BNG	bio natural gas
bpd	barrels per day
CAPEX	capital expenditure
CC	carbon capture
CCS	carbon capture and storage
CCU	carbon capture and utilization
CHP	combined heat and power production
COP	coefficient of performance
CtL	coal-to-liquid
DAC	direct air capture
DEA	Danish Energy Agency
DH	district heating
DSO	distribution system operator
electrofuel	liquid fuel from a non-biomass feedstock
Electromethane	methane from a non-biomass CO_2 feedstock
ENTSO-E	European Network of Transmission System Operators for Electricity
ENTSO-G	European Network of Transmission System Operators for Gas
eSMR	electric steam-methane reforming
FT	Fischer-Tropsch
GCA	Global Climate Action
GHG	greenhouse gas
GtL	gas-to-liquid
HTFT	high-temperature Fischer-Tropsch
HTPH	high-temperature process heat
kt	kilo tonne
LTFT	low-temperature Fischer-Tropsch
LPG	liquid petroleum gas
LTPH	low-temperature process heat
LUP	long-term development plan
Mt	mega tonne
NSWPH	North Sea Wind Power Hub
O&M	operation and maintenance
OPEX	operational expenditure

PEM	polymer electrolyte membrane
PtL	power-to-liquid
PtX	power-to-x
POX	partial oxidation
RWGS	reverse water-gas shift
SDU	University of Southern Denmark
SMR	steam-methane reforming
SNG	synthetic natural gas
SOEC	solid oxide electrolyzer cell
ST	Sustainable Transition
syncrude	synthetic crude oil
syngas	synthesis gas
tCO$_2$	tonne CO_2
TSA	temperature swing adsorption
TSO	transmission system operator
TYNDP	10-year network development plan
UC	unit commitment
WtE	waste-to-energy
XtL	x-to-liquid

1   Introduction

Public awareness of the transportation's, and especially the aviation sector's, effect on the climate has accelerated in recent years, and the public is starting to demand more governance and sustainability in aviation. However, transitioning the aviation sector towards complete renewability is no easy task. The demand for aviation is still projected to increase - and by quite a margin [1]. No obvious replacement for liquid fossil fuel can currently be seen, though some promising studies suggest a pathway towards sustainable fuel production through the use of synthetic equivalents to conventional liquid fuels by the use of electricity, CO_2, biogas or methane, along with many more.

In Europe, aviation accounts for about 3% of the total greenhouse gas (GHG) emission and globally, that number is more than 2% [2], corresponding to around 700 $MtCO_2$ equivalents [3]. The International Civil Aviation Organization (ICAO) has projected that, in case no additional measures are made, jet fuel consumption could increase by an additional 300% by 2050 [4]. This puts even more pressure on policy-makers to support the development of sustainable production solutions to this potentially increasing emission source. In 2018, a study from the University of Southern Denmark found that renewable hydrocarbons could never be produced at the same cost of their fossil counterpart, and therefore, waiting for a solution that can compete on market terms seems unlikely [5].

The objective of the Paris Agreement, to keep the temperature-increase at a maximum of 2.0 °C compared to pre-industrial levels with an additional aim to limit this temperature-increase to 1.5 °C, will be an even bigger challenge in case no significant developments are made within the transportation sector. The aviation sector is a complex area to restructure and become sustainable due to the strict requirements for the fuels. This study focuses on measures to limit this worrying development in GHG emissions from aviation by replacing conventional fossil fuels with sustainable alternatives. This study aims at uncovering the more socioeconomic alternative to fossil liquid jet fuel by the use of the well-known Fischer-Tropsch technology currently deployed several places in the world.

This study seeks to minimize the extra cost as much as possible, by exploring synergies that can be found by locating the production facilities on or near current combined heat and power production (CHP) sites in order to utilize the strong infrastructure and connection to the valuable district heating networks that are a special part of the Danish energy system, and could make Denmark a front runner in production of sustainable liquid jet fuel. Furthermore, with a goal of installing in the range of 180 GW of renewable electricity production in the North Sea [6], utilizing excess electricity for jet fuel production could help minimize the socioeconomic cost.

In this study, the production of the entire Danish jet fuel demand in 2050 has been the primary focus, and a case study of a fuel production plant located in Odense on Funen has been done in order to investigate

potential electricity network constraints and limitations in different production configurations.

The pathway towards sustainable aviation has been considered with a perspective such that elements of the value chain for liquid fuels can be implemented earlier than 2050 with a focus of reducing GHG emissions from e.g. gas system supply, as reductions in international flight is excluded from the goal for 2030 reductions [7].

2 Problem Statement

The goal of the energy system becoming completely renewable by 2050 is no new notion, and has been of central focus for many years now. Until now, transitioning electricity and heating has been largely in focus. At Energinet, the Danish transmission system operator (TSO) of both the gas and electricity transmission systems in Denmark, this has been referred to as the first half of the transition [8]. In the second half, other sectors that are more challenging will be the primary focus, such as the transportation sector, that traditionally has had a longer temporal scope of full sustainability than producing renewable electricity and heating. This is largely because a portion of the sector can not be electrified and alternatives must be discovered - alternatives that are often significantly more expensive. This has brought attention to renewable liquid fuels that are produced by electricity, gas and biomass. Fuels based on electricity are often referred to as electrofuels due to its non-biomass feedstock. Biomass is expected to be a limited resource in the future with increasing demand, and therefore, the biomass consumption for the production of fuel must also be limited, and some alternative carbon resource must be utilized.

This study will focus on the part of the transportation sector that has traditionally been regarded as a more challenging sector to restructure, aviation, since there are few alternative propellants for long-range aviation. This brings up the challenge that is demand for liquid fuels which, if they are to be renewable, are significantly more expensive than their fossil counter-part - though necessary nonetheless. Therefore, this study investigates the socioeconomic feasibility of different pathways for producing these fuels in order to reduce the gap between fossil and renewable liquid fuels.

In recent years, and as recently as 2019, gas-to-liquid (GtL) has been receiving increasingly more attention due to its technical advancement and its prospects for economic feasibility, compared to other renewable fuels - which was brought further into the spotlight in [9]. The GtL pathway is based on commercial technologies and expected developments towards 2050. The aim of this study is to identify the most socioeconomically feasible configuration of a fuel producing plant, while still considering resource constraints, and therefore, combining pathways with electricity has been included in the analysis as well.

2.1 Research Questions

This study aims to answer the following research questions:

Which method of producing jet fuel is the more feasible?

Identifying the more feasible configuration of jet fuel production is central to the challenge of the transition towards renewability. Since production of renewable liquid fuels are currently more expensive than traditional fossil fuels [9], minimizing the gap of production costs is important for expanding the production capacity of renewable fuels.

Which synergies can be found by locating fuel production at central locations that are currently running combined heat and power plants?

Of a more qualitative nature, this question helps describe why the jet fuel price changes with configurations and provide policy-makers and system operators with understanding of the optimal locations for the fuel production.

What level of strain does fuel production put on the electricity network, and which measures can be utilized for mitigation of this network strain?

Not all liquid fuel production technologies use methane as a primary input. Some technologies could potentially create a significant demand of electricity for liquid fuel production and these technologies might cause bottlenecks in the electricity network. Based on a case study of Odense on Funen, does the fuel production cause bottlenecks in the electricity network, and if so, what measures can be found to help mitigate these bottlenecks?

Which parameters and framework conditions show high sensitivity in the production and the resulting price of jet fuel?

In order to evaluate the validity and robustness of the results of this feasibility study, investigating key parameters is necessary, and can help identify pit falls and opportunities in the value chain.

Which carbon resources should be utilized for jet fuel production?

As biomass will be a limited resource, alternative carbon sources will be investigated. Here, a future market for CO_2 and CO_2 reductions will be investigated and modelled and simulated more in-depth.

2.2 Project Scope and Delimitation

This study will focus on the production of renewable jet fuel, as it is perhaps the most challenging form of energy to produce economically competitive. The synergies of jet fuel production to the energy system is essential to get deeper understanding of the prospects for producing jet fuel in Denmark, and therefore, these are included in the modelling.

The study has been delimited to the development of an energy system model, the *Fuel Production Model*, using Energinet's modelling tool *Sifre*, in which an hourly optimization of jet fuel production, based on producing the entire demand of jet fuel without infrastructural constraints, can be simulated. The purpose of developing this model is to evaluate the generally more feasible production pathway in Denmark. Investigating technical constraints in the energy system has been delimited to a case study in order to understand the potential challenges that could arise from liquid fuel production, while not uncovering all constraints in

the Danish infrastructure. This also means, that required capital investments in both electricity and gas infrastructure, which are necessary as a consequence from the production of synthetic liquid fuels, have not been included in the analyses.

In the *Fuel Production Model*, biogas has been assumed as a primary energy, i.e. the production of biogas has not been modelled. This is due to the modelling of the biogas production not providing significant additional value to the simulation of jet fuel in order to match the required modelling time. Furthermore, thorough analyses of the biogas potential in different regions of Denmark has been made in recent years [10], [11] which provides key knowledge on the potential for biogas production and the geographical location of this biogas, making the modelling of biogas production unnecessary.

3   Methodology

This section will serve as a description of the methodology of which the study has been conducted, along with how each research question will be answered. The results and intermediate steps towards answering the research questions can be found throughout the report.

The approach of this study is a holistic energy system analysis with the Danish perspective for producing jet fuel within the projected energy system. An essential aspect of this analysis has been to utilize the synergies that can be found in sector coupling between jet fuel production and the power, gas and heating systems in order to reduce the production costs. Sector coupling is of highest focus in most newer energy system analyses, including the newest strategy from Energinet [8]. In energy system analyses, satisfying the aviation demand is usually an efficient place to start, since there are often by-products from jet fuel production that can be utilized in other sectors. Many studies with a focus on jet fuel production within energy system analysis has been released in recent years, and elements and considerations from all these have been included in this study [1], [5], [12]–[20].

Based on a literature study of the field - done prior to any modelling - the technology data has been determined for all conversion technologies used in the model. In order to present a more realistic technical and economic analysis, literature based on practical experiments has been preferred in order to account for inefficiencies that inevitably arise in practical applications. For all conversion technologies higher heating values have been used as basis for calculations. Energy balances for all conversion technologies can be seen in Appendix B. Many studies focus on the individual conversion technologies and the operation of these, and specific values has been taken from some promising studies, while others have served more as a source of general knowledge of the pathway for sustainable hydrocarbons [21]–[48]. Central to the study has been to use the technology of Fischer-Tropsch (FT), as it is a well-known technology to produce jet fuel. In FT synthesis, a comparable product to fossil crude oil is produced, and in the refining of this several by-products, such as gasoline, are produced. While it would be more accurate to model the market for gasoline as well as any other energy flows, it has been assumed that by-products such as gasoline and ethanol are sold at a fixed market price. This revenue is then deducted from the cost of production and part of the final price of jet fuel.

The economic analysis has been conducted in accordance with standard socioeconomic procedure [49], since this yields the *true* socioeconomic price of jet fuel. To calculate the socioeconomic jet fuel price, which is a representation of the socioeconomic production cost, the operation of the jet fuel production pathway has been simulated on an hourly optimization time-step using Energinet's modeling and simulation tool *Sifre* along with the socioeconomic investment-optimization module *ADAPT*.

As mentioned, this study aims on identifying the most feasible jet fuel pathway, and to answer some significant questions regarding resource use, constraints and more. Therefore, modelling has been split into two parts;

main scenarios with best estimates and sensitivity scenarios to evaluate the influence of key parameters.

Fuel Production Model   refers to the model developed in this study, which contains a series of simulations for producing the total Danish jet fuel demand with different configurations of liquid fuel production. A simulation is done for each configuration in order to evaluate and compare each result including possible unquantifiable benefits - and to evaluate the margin of difference between configurations. These simulations are done with resource constraints on national levels in order to identify the more feasible configuration of a fuel plant, taking the use of resources into consideration. Here, biogas, biomass, waste and electricity are primary energies, meaning that the production of these have not been simulated and therefore, prices have been defined prior to simulations. This has been done as modelling the production of these does not add further value to the evaluation of jet fuel production.

The aim of the simulations is to evaluate the resulting jet fuel price of different plant configurations in the context of the total Danish energy system, and to uncover relevant and important synergies within the different liquid fuel production pathways. Therefore, the only fixed demand to be satisfied is a 50 PJ jet fuel demand. The technical simulation results for all scenarios modelled is the result of a prior investment simulation in which all production capacities are products of a socioeconomic optimization conducted by the investment-optimization module ADAPT, in Sifre. This includes capacities of interconnection lines and storages. This results in the lowest possible jet fuel price for each plant configuration. Furthermore, each plant configuration is modelled with both biomethane and bio- and electromethane as upstream feedstock in order to evaluate the effect of the methane price.

For each configuration, specific parameters are then further analyzed by fixing and manually changing them - and thereby removing them from the optimization - to evaluate their influence on the system.

Naturally, simulating liquid fuel production in a model resembling the entire Danish energy system would yield more accurate results, but using the *Fuel Production Model* helps analyze specific parameters and their effect on the fuel price in order to help identify economically feasible alternatives.

4   Framework Conditions

The purpose of this section is to provide the reader with an understanding of the underlying framework conditions of the modelled scenarios for production of synthetic liquid fuels in Denmark. This includes a description of Energinet's long-term development plan (LUP), potentials, demands and constraints related to the production of synthetic liquid fuels and finally, assumed market prices in the energy system.

4.1   LUP Framework

The Danish energy system is undergoing a rapid transition towards a more renewable system and Energinet's part in this transition is to ensure that the electricity and gas transmission network are capable of transporting the necessary amounts of energy. Therefore, Energinet wishes to work out a LUP every second year to address the need for development in the electricity and gas transmission network in Denmark towards 2040. LUP describes two possible scenarios, or development tracks, Blue and Yellow, towards different political objectives including the objective of a 70% reduction of emissions in 2030. This is because it is generally political objectives that sets the framework for the development. Towards 2040 it is expected that the development is primarily driven by:

- The Energy Agreement 2018 [7] which is a driver between **2020-2024**.
- The objective of 55% renewable energy in the system and a 70% reduction in emissions in 2030 drives the development between **2020-2030**.
- The objective of being independent from fossil fuels in 2050 drives the development in the period from **2030-2040**.

The rapid transition of the energy system makes it difficult to predict the layout of the future energy system. Especially, the interest in large-scale wind and solar power, GtL and power-to-x (PtX) in general can create great difficulties in the energy system if they are not timed correctly.

As mentioned, the LUP framework only stretches towards 2040, but since this study deals with production of 100% renewable jet fuel in 2050, some assumptions have been made regarding the framework. This is due to the fact that LUP is currently one of Energinet's most accurate and available frameworks for the future Danish energy system. This means, that the electricity, heating and gas consumption are assumed to be the same in 2050 as in 2040. The same goes for the capacities of production units and infrastructural connections and market prices. The capacities of infrastructural connections will be elaborated in Section *4.2.8 Network Constraint* and market prices relevant to the production of jet fuel, including the electricity price, will be elaborated in Section *4.3 Market Prices*.

4.1.1   Blue and Yellow LUP Scenarios

General for the Blue and Yellow scenario is, that they are developed on the basis of The Danish Energy Agency's conditions for analyses for Energinet in 2019 (AF19) [50] and *Systemperspektiver ved 70%-målet og Storskala Havvind* [17]. Furthermore, the scenarios are developed with data from the European Network of Transmission System Operators for Electricity (ENTSO-E)'s European scenario called *Sustainable Transition*

(ST) in the 10-year network development plan (TYNDP) from 2018. Both scenarios explore potential challenges within the Danish electricity network by only incorporating the Danish energy system and the demands of energy in Denmark. Therefore, the scenarios can be used to explore how much of Danish renewable energy that can be utilized in Denmark, but not how big a role Danish renewable energy plays in the rest of Europe.

The main difference between the two scenarios is the production of renewable energy - both electricity and liquid fuels. In the Blue scenario the electricity production is more centralized by implementing large-scale offshore wind power. A consequence of this is centralized large-scale hydrogen production and liquid fuel production by PtX. In the Yellow scenario the electricity production is more decentralized with higher amounts of locally placed solar power capacity and lower amounts of offshore wind power capacity. Methane has a more central role in the Yellow scenario than in the Blue given a high amount of local methanation of CO_2 in biogas. A result of this methanation is a higher amount of local hydrogen production compared to the Blue scenario. The methane is utilized in large-scale GtL plants placed centrally where there is a connection to the gas grid and a district heating (DH) network so that excess heat can be utilized. In the Blue scenario methane is not utilized in GtL. The biogas is upgraded to methane by conventional biogas upgrading, as explained in Section *5.3.1 Biogas Upgrading*, and primarily used in the industry, heat production and for balancing the electricity grid. These methane consumers are also present in the Yellow scenario, since electrification isn't possible in part of the industry, and dispatchable production units are still required in a system with a high amount of renewable production units.

Generally, the specific consumptions are kept constant between the Blue and Yellow scenario. Is is primarily the production units and the distribution of the production units that changes between the scenarios. The capacities of renewable electricity production of onshore and offshore wind power and solar power in the Blue and Yellow LUP scenarios can be seen in Figure 4.1.
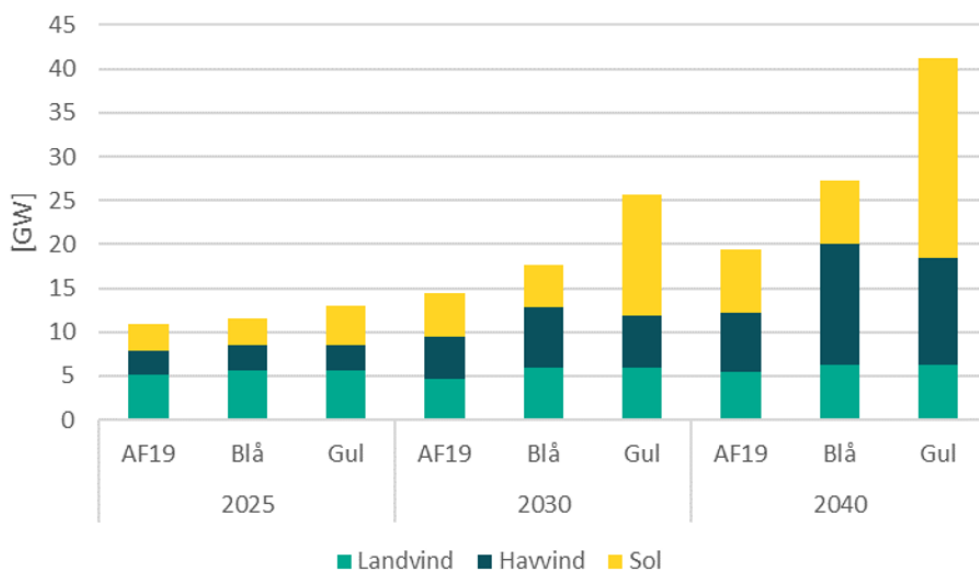
Figure 4.1: *The figure shows the capacities of renewable electricity production of onshore and offshore wind power and solar power in the Blue and Yellow LUP scenarios compared with AF19 between 2025-2040. Source: Energinet.*

Even though the distribution of electricity production is not present, it can be seen how solar power plays a larger role in the Yellow scenario while offshore wind power plays a smaller role.

4.1.2   Role of the LUP Framework

Because of the more decentralized production of renewable electricity, and the fact that methane plays a larger role in the Yellow scenario than in the Blue, it has been chosen to use the Yellow scenario as the framework for the Fuel Production Model. The Yellow scenario includes aspects that favour the production of liquid fuels through GtL. With that said, it does not mean that the model developed in this study contains every aspect of the existing LUP model for the Yellow scenario. Generally, the model contains electricity prices which are a result of the existing LUP model. Electricity prices are a central aspect of liquid fuel production both in regards to production of hydrogen for methanation of biogas, but also when considering production of syngas purely from electricity and CO_2. The electricity price used will be elaborated upon in Section *4.3.1 Electricity.*

Furthermore, this study contains an analysis of strain in the electricity network as consequence of liquid fuel production. For this analysis Funen will be used as a case study, and some central elements of the LUP framework will be implemented in the Fuel Production Model for this purpose. These elements include the electricity production capacities for onshore wind and solar power, and the production profiles from the LUP framework. Also the electricity demands for different sectors on Funen are implemented together with their respective demand profiles. Finally, in order to analyze the strain on the connection lines connecting Funen with Southern Jutland and Western Zealand, capacities for these connection lines are implemented. The resulting production and demands of electricity, and strain on the connections lines will be presented in Section *8.2 Case Study of Funen.*

4.2   Demands and Constraints

4.2.1   Aviation Fuel Demand

Traditionally, when analyzing energy systems, producing jet fuel is one of the first elements that must be considered. This is due to the limited options of producing jet fuel and the fact that production of jet fuel is associated with production of other liquid fuels, gasses and heat as by-products. Therefore, figuring out how to produce jet fuel most feasibly greatly impacts the remaining energy system.

The most commonly used aviation fuel is called jet fuel and is used to power gas turbine engines. Amongst jet fuels, the most common types are Jet A and Jet A-1. Jet fuel is a mixture of a longer range of hydrocarbons, while the specific ratio is difficult to define. The range of the hydrocarbons are defined by the technical requirements such as freezing and flash point. Kerosene-type jet fuel, which is the focus of this study, ranges from carbon numbers 8 through 16. It is assumed that the jet fuel produced in FT comply with the requirements of Jet A-1, which will be further evaluated in Section *5.6.3 Fischer-Tropsch Fuel.*

In 2010, the major airports along with some of the largest Scandinavian airlines formed *Brancheforeningen*

Dansk Luftfart, the Danish Aviation Trading Association. Through personal communication with their Chief Consultant, the Danish demand for sustainable jet fuel in 2050 has been estimated to be 50 PJ [51].

4.2.2   District Heating

Utilizing excess heat from liquid fuel production can, as mentioned, help reduce the overall production costs. Locating the fuel production plants at locations with large DH networks is a way of utilizing this excess heat. As the Fuel Production Model has been used to simulate an aggregated Danish energy system, an aggregation of the DH demands from the five largest DH networks has been used as well, which can be seen in Table 4.1. Simulating the specific sites could potentially show different results. This has been further investigated in the case study of Funen, where the specific DH of the DH network in Odense has been used.

Table 4.1: *District heating demands in the five largest DH networks in Denmark in 2018.*

Location	Operator	Demand
Copenhagen	CTR, HOFOR, VEKS [52]–[54]	29.1 PJ
Aarhus	AffaldsVarme Aarhus [55]	11.8 PJ
Odense	Fjernvarme Fyn [56]	9.4 PJ
Aalborg	Aalborg Varme [57]	6.8 PJ
Triangle Region	TVIS [58]	6.0 PJ
Total		63.1 PJ

4.2.3   Biogas Potential

Biogas is an increasingly more important element of the Danish energy system and in the Danish goals for a renewable energy production. Furthermore, biogas production has some derived positive effects for the Danish agriculture that makes biogas a desired energy.

In 2012, the Danish Parliament agreed on a subsidy scheme for the production and use of biogas in Denmark. Here, companies could receive a subsidy for the use of biogas for industrial processes or for the use in transportation. The scheme also subsidised upgrading and scrubbing of the biogas in order for it to be fed into the natural gas grid along with the use of biogas to produce electricity.

Since the first subsidy was paid in 2014, the utilization of biogas has been steadily increasing from approximately 6 PJ to a projected 15 PJ in 2020, as shown on Figure 4.2.

In 2015 however, it was politically agreed on that the use of energy crops in biogas units should be limited. From the beginning of August 2015 to the end of July 2018, in order to be eligible for receiving subsidies for the biogas production, the use of energy crops could not exceed 25% of the total weigh of biomass, and from August 2018 to July 2021, the use must not exceed 12% [59].

For upgrading of biogas and electricity production, the scheme is confined to plants that are operational before the 1st of January 2020.
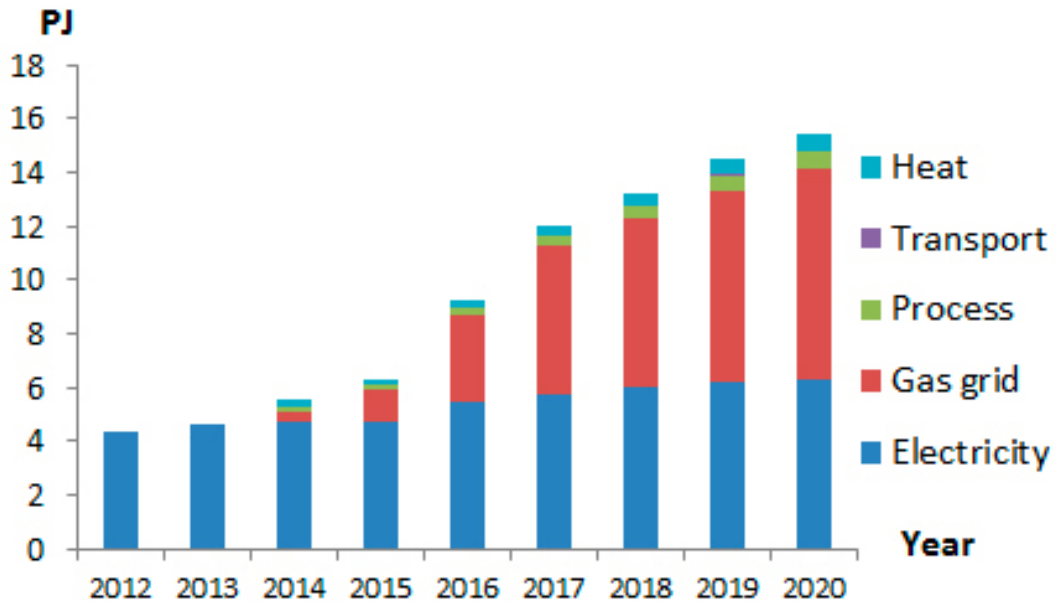
Figure 4.2: *Biogas Production in Denmark from 2012 to projection of 2020 in PJ split into end use. The specific values given in the legend has not been used, but it should serve as an indication of where the biogas potential is located. Source: Danish Energy Agency [60].*

The full potential of biogas production has been discussed in many cases, and many studies have been conducted to map this potential, since not all biomass resources are economically feasible to use for biogas production.

In 2015, SEGES and AgroTech released a report made for the Biogas Taskforce from the Danish Energy Agency (DEA) aiming to map the economically feasible locations of future biogas plants using available biomass resources and limiting the use of crops for biogas production [10]. Here, 75 currently commissioned plants were identified as well as 16 potential plants, of which some will be completed and some will be abandoned. These 91 identified plants will be able to consume a total of 11.9 mega tonne (Mt) of biomass every year, of which 82% will be found on the already existing plants. In the study, 30 different types of biomass was identified and the business case of using all types were evaluated. The types that resulted in the lowest methane production cost was some organic waste, straw, bedding and manure. The study found that most of the feasible locations for biogas plants are located in the southern and western part of Jutland which is evident on Figure 4.3, in which the potential for biogas production on a municipal level shows that especially the aforementioned parts of Jutland would be feasible locations due to the high potential. The potential biogas production distribution, expressed in percentages, can be seen in Appendix A.

While this study focuses on the national energy resources rather than geographical locations of them, it is relevant to account for since the renewable methane production would, in case of biogas upgrading, produce a large amount of CO_2, which can be utilized for fuel production, which will be further discussed in the next section. The price of this potential carbon source would be dependent on the geographical location of the biogas production since the transportation cost is linearly dependent on distance, e.g. when trucking or
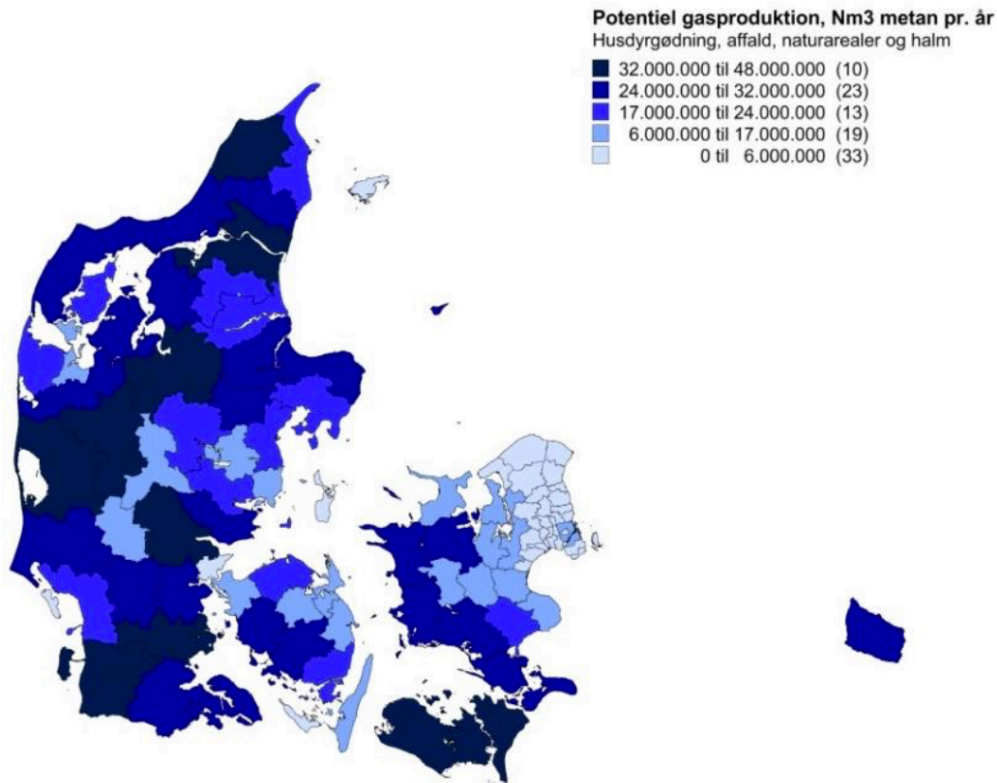
Figure 4.3: *The figure shows the distribution of potential biogas production on a municipal level in Denmark [10].*

piping the CO_2. Therefore, in this study, costs associated with transporting CO_2 has been included, and resulting CO_2 prices as a result of transportation by different means and distances will be presented and discussed in Section *8 Simulation Results*.

In January 2020, the University of Southern Denmark (SDU) and SEGES released a report with their estimation of the total biogas potential including a mapping of the potential for biogas production if all excess biomass resources in Denmark were to be collected and used to produce biogas regardless of economic feasibility [11]. The report was made to evaluate the consequences of limiting the allowed use of energy crops to produce biogas as mentioned earlier. In this report, seven types of biomass was classified; manure and fertilizer, straw, bedding, industrial waste, discarded energy crops, organic waste and sustainable agricultural waste. These seven types of biomass amounts to a full potential of 94 PJ of biogas. Based on these inputs of biomass to biogas, the gas will constitute approximately 60% methane and 40% carbon dioxide. However, the report has been made in order to classify every and all biomass for biogas. In reality, a portion of this biomass would not be economically feasible to collect and produce biogas from, e.g. scraping stables for remaining bedding. Therefore, it has been assumed that 85% of all biogas potential will actually be produced, which means that from the 94 PJ potential, 80 PJ has been assumed to be produced in 2050.

In 2018, Energinet released an analysis with their projection of a possible future energy system *Systemperspektiv 2035* [61]. Here, many different aspects of the energy system were modelled and simulated for the three different European development frameworks *Distributed Generation*, *Sustainable Transition* and *Global*

Climate Action, in which a modification of the consumptions of biogas related to the Global Climate Action scenario has been the basis in this study.

In [61] the consumption of renewable gasses was assumed to be roughly 12 PJ for the industry that will likely require gas for high-temperature processes or as part of the chemical processes. The electricity network would also be demanding gas, which would be used for balancing of the supply and demand by the use of gas turbines. This demand was found to be roughly 17 PJ. The individual heating has been assumed to be fully electrified, and would not consume any renewable gas by 2050. These consumptions has been subtracted from the 80 PJ of assumed biogas production to account for other demands for gas. The remaining gas has been assumed available for liquid fuel production in this study and will be part of the Fuel Production Model. In [61], 25 PJ renewable gas was assumed consumed by the transportation sector for heavy duty transportation. However, in 2020, a new analysis from Energinet has shown hydrogen to be more economically feasible for heavy transportation, and therefore, it has been assumed that, in 2050, there will be no demand for biogas in the transportation sector. This results in a total available biogas resource of roughly 50 PJ in 2050.

While aviation is one major consumer of liquid fuels, other sectors will likely require liquid fuels as well, e.g. the shipping sector, which should be taken into account when assigning bio-resources for fuel productions. The challenge of reducing the emissions of the shipping sector is very similar to those of aviation. However, the shipping sector is currently investigating a few more options. The demand for liquid fuels in the shipping sector is very similar to aviation with a demand of 50 PJ in 2050 - but recent advancements in ammonia production, e.g. from [62] could potentially mean that the shipping sector would not consume any hydrocarbon-based fuels, and therefore would not require the carbon resources from biogas. In this study, it has been assumed that since aviation requires hydrocarbons - and likely more than shipping - the entire biogas resource is made available for jet fuel production, and that the shipping will be using ammonia as fuel. Maersk has also identified ammonia as one of the more promising fuels for the shipping in the future [63].

Grid Injection of Upgraded Biogas   As mentioned in Section *2.2 Project Scope and Delimitation*, added investments related to expansion of the gas infrastructure in Denmark, as a consequence from the production of liquid fuels, have not been included in the analyses. However, the cost of compressing the upgraded biogas, i.e. methane, to transmission pressure, which is generally a significant part of the investment and fixed operation and maintenance (O&M) costs related to producing methane from biogas and injecting it into the gas grid, have been included in the analyses. The added investment related to compression is 0.196 MEUR/MW-upgraded biogas, and the added fixed O&M is 5000 EUR/MW/year [64]. For methane produced by conventional biogas upgrading the cost of compression constitutes 44% of the total investment cost and 45% of the total fixed O&M. For methane produced by methanation of CO_2 in the biogas, the cost of compression constitutes 27% of the total investment cost and 20% of the total fixed O&M [64].

4.2.4 CO$_2$ as a Resource

The future energy system will likely see CO$_2$ as a valuable commodity. Today, 230 Mt of CO$_2$ is consumed in different industries [65]. Using CO$_2$ to produce liquid fuels has become increasingly more interesting to governments, industries and investors, while technologies have yet to become fully commercialized. The idea of using pure CO$_2$ arises from the sustainability issue of the biomass resource, and therefore, in order to produce the consumption of liquid hydrocarbon fuels, an alternative carbon source has to be found. Capturing the CO$_2$ from the air or from point sources such as waste incineration or biomass-fired heat units could both reduce emissions from the incineration and mitigate the demand for carbon from biomass resources. Capturing CO$_2$ from these sources are necessary to produce liquid fuels classified as electrofuels.

Due to this potential use of CO$_2$, a synergy between waste and biomass incineration plants and liquid fuel production arises, which will be further described in Section *6.1 Plant Configuration*. The amount of CO$_2$ that could potentially be captured from waste and biomass incineration has been based on [47], [66].

For **Waste Incineration**, the DEA has projected the future capacity in Denmark towards 2035, and the potential for CO$_2$ capture has been based primarily on [47]. Figure 4.4 shows the projected evolution of the total Danish capacity for waste incineration.
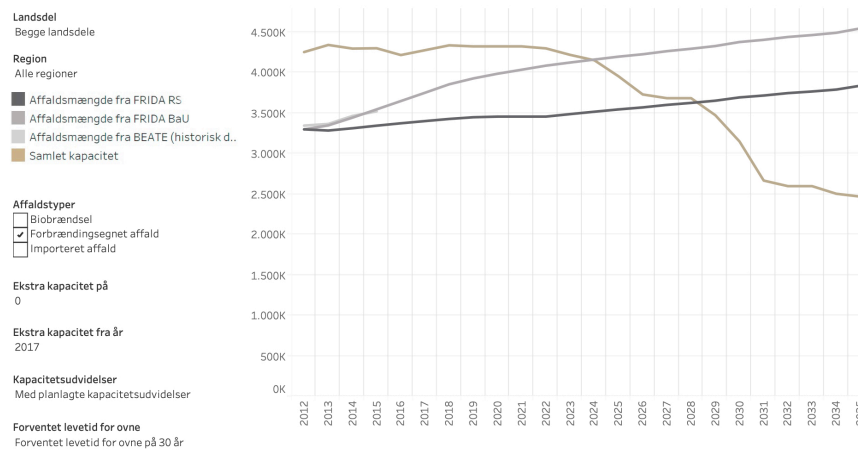
Figure 4.4: *Projection of Danish generation of waste along with the capacity for incineration towards 2035 [66]. The grey lines illustrate the actual amount of waste, while the brown line illustrates the plant capacity for incineration. These projections are made with two different models; BEATE and FRIDA. Generally, FRIDA projects a smaller amount of waste throughout the period, but the projection of BEATE seems to fit more accurately with historical data, as evident from the lighter grey line illustrating BEATE with historical data from 2012-2015, which is almost identical to the projection of BEATE with business as usual policies.*

Here, it can be seen that while the generation of waste is projected to increase, the capacity of incinerating is projected to be reduced by more than 40%. This can likely be explained by the increasing focus on recyclability, which has been stated by 2013 government's *Denmark Without Waste* [67], which is still in effect. While the strategy aims for no waste, some waste is very similar to biomass and suitable for incineration - and would be more so, if the CO$_2$ would be used for fuel production. It has been assumed that the waste

and biomass incineration will generally be located on the central locations, i.e. at the same locations as fuel production, in order to utilize synergies.

The Danish Council on Climate Change, in corporation with NIRAS, has projected a total of 1.7 Mt of biogenic CO_2 being feasible for capture from waste incineration, which will be the assumption made for this analysis as well. Assuming a higher heating value of 10.6 MJ/kg, a CO_2 content of 95.1 kg/GJ waste and a feasible amount captured of 75% [47], this would result in a total amount of waste of approximately 2.25 Mt of waste, which is fairly close to the estimation made in [66].

For **Biomass Incineration**, the Danish Council on Climate Change and NIRAS has projected a total consumption of 34.6 PJ of biomass in the energy system. While the CO_2 from biomass is generally regarded as neutral, physical CO_2 is available for capturing. While the potential for CO_2 capture should be investigated individually for each plant, in this study, the total potential has been assumed in the model. 34.6 PJ of biomass would result in approximately 2.45 Mt of biogenic CO_2 [47]. Capturing CO_2 from smaller plants is technically possible, but it has been assumed that it would not be economically feasible to capture CO_2 from gas turbines and other peak load production units due to their low number of full-load hours. The investment cost of the capture units would not be justified by the captured amount of CO_2.

4.2.5   Carbon Capture

In order to utilize CO_2 from waste and biomass incineration it must be captured from the flue gas. The Global CCS Institute expects that the price of capturing CO_2 in waste-to-energy (WtE) applications will fall to between 31.7-45.3 EUR/tCO_2 as a result of current development in solvent innovation and process integration and intensification [44]. The upper limit of this price interval, 45.3 EUR/tCO_2, has been assumed for the cost of carbon capture (CC) in this study. The price of CC from biomass incineration plants has been assumed to be the same as for WtE incineration plants.

4.2.6   Transport of CO_2

In today's energy system, there is no infrastructure to transport this CO_2 from especially biogas, which means that in order to utilize it at central locations, remotely located from the biogas plant, it is necessary to investigate the feasibility of different means of transporting it. In this study, two different means have been included; trucking and piping, and been directly compared. In order to directly compare the cost of these, the same distances must be assumed. In the main scenarios, the transport of CO_2 has been assumed to be 60 km, which is an approximation of the weighted average distance from a biogas plant to a central location assumed for jet fuel production in Denmark. However, to further investigate the influence of distance, both transporting 30 km and 100 km have also been analyzed. 30 km transport has been assumed to be the lower limit for the distance and is what can be assumed for collecting CO_2 at e.g. Funen, which would cover most biogas plants with transport to Odense. As mentioned, to investigate the influence of distance, 100 km would be assumed as the upper limit, which is comparable to collecting all CO_2 from biogas at Zealand and transporting it to Copenhagen.

Trucking of CO$_2$ Advantageous for trucking is that it does not require larger investment costs for the producer or the consumer of CO$_2$. However, usually, trucking will be more costly as the distance increases. The cost of trucking has been done in such a manner, that it will be linearly dependent on the distance of transportation. The calculation of the cost of transporting CO$_2$ on a truck has been done in cooperation with *Nature Energy* [68]. In order to estimate the cost of providing this transportation service, it has been assumed that a truck costs 80 EUR per hour per truck. If it is assumed that a truck drives with an average speed of 40 km per hour, and consumes what corresponds to 0.11 EUR worth of fuel per km, the total cost per km will be 2.1 EUR. However, the cost of trucking becomes more feasible the more CO$_2$ can be transported per truck, and therefore, it has been assumed that an average truck can transport 25 tCO$_2$. This results in the cost of trucking CO$_2$ being 0.084 EUR per tonne per km.

The cost of trucking CO$_2$ then becomes 2.53 EUR per tonne for a distance of 30 km, 8.43 EUR for a distance of 100 km. The weighted average cost of trucking, at 60 km, results in a cost of 5.06 EUR per tonne.

Piping of CO$_2$ The cost of piping CO$_2$, has been based on [69], [70]. Here it was reported that for onshore CO$_2$ pipes with a yearly capacity of 3 Mt the transportation cost would be approximately 11.1 USD per tonne per 250 km in 2015. Correcting for inflation at an average rate of 2%, this becomes 12.1 USD in 2020, corresponding to 11.1 EUR per tonne per 250 km. As the cost is generally linearly dependent on the distance, the cost in EUR per tonne per km becomes 0.044 EUR per tonne per km. This results in a cost of 1.33 EUR per tonne for a distance of 30 km, while the cost becomes 2.67 and 4.44 EUR per ton for 60 km and 100 km, respectively. Table 4.2 shows an overview of the costs of trucking and piping for different distances.

Table 4.2: *The cost of transporting CO2 from both trucking and piping in EUR per tonne. It can be seen that the cost for piping is generally significantly lower than the cost of trucking by almost half [68]–[70].*

	30 km	60 km	100 km
	EUR/tCO$_2$		
Trucking	2.53	5.06	8.43
Piping	1.33	2.67	4.44

4.2.7   Heat from Waste and Biomass Incineration

Many of the production units used for jet fuel production requires heat at high temperatures, which will be further described in Section *5 Synthetic Fuel Value Chain*. When locating incineration of waste and biomass close to fuel production to utilize the CO$_2$, it would be relevant to evaluate the business case in utilizing the heat that is produced from incineration as process heat instead of selling it as DH, which naturally has a lower value due to its more limited applications. It has been assumed that both waste and biomass incineration plants can generate heat at a temperature of approximately 450 °C - this temperature can be boosted by the use of an additional burning of gas, such as methane, hydrogen or fuel gas. However, in order

to produce heat at these temperatures, the turbine in CHPs would be by-passed, which means that in order to produce process heat from incineration, it must assumed that the plants do not produce electricity. In this study, it has been assumed that all waste and biomass is incinerated in a boiler rather than in CHPs, since electricity can easily be produced from other sources, and peak load can be supplied by gas turbines using renewable methane, hydrogen or excess gasses from other processes. DH, similar to electricity, can be produced from other sources.

Based on the capacity for waste incineration from [66], and assuming a general efficiency of incineration of 90%, the total Danish production of process heat from waste incineration would be approximately 23 PJ - much of which would likely be placed in Copenhagen due to the size of the DH grid.

Assuming the same parameters for biomass, incinerating 34.6 PJ of biomass would produce approximately 31 PJ of process heat.

4.2.8   Network Constraint

A part of this study is to research the strain in the electricity network as a consequence of production of liquid fuels in the Fuel Production Model for the Funen case study. Therefore, connection lines with a limited amount of electricity transfer capacity has been implemented in the model. In the existing LUP model the only connection lines in the electricity network is a consequence of the interconnectors between electricity price areas, such as the connection across the Great Belt connecting DK1 with DK2. However, this does not give the ability to observe potential bottlenecks between Funen and Southern Jutland. Therefore, the Danish electricity network has been divided into 11 electricity price areas, called *bidding zones*, instead of only the two real price areas, DK1 and DK2. These 11 bidding zones are; Bornholm (Bornholm), Funen (Fyn), Copenhagen (KBH), Northern Jutland (NordJL), Northern Zealand (NordSJ), North Western Jutland (NordvestJL), Southern Jutland (SydJL), Southern Zealand (SydSJ), Western Jutland (VestJL), Western Zealand (VestSJ) and Eastern Jutland (ØstJL). A map showing how the bidding zones are distributed can be seen in Figure 4.5.
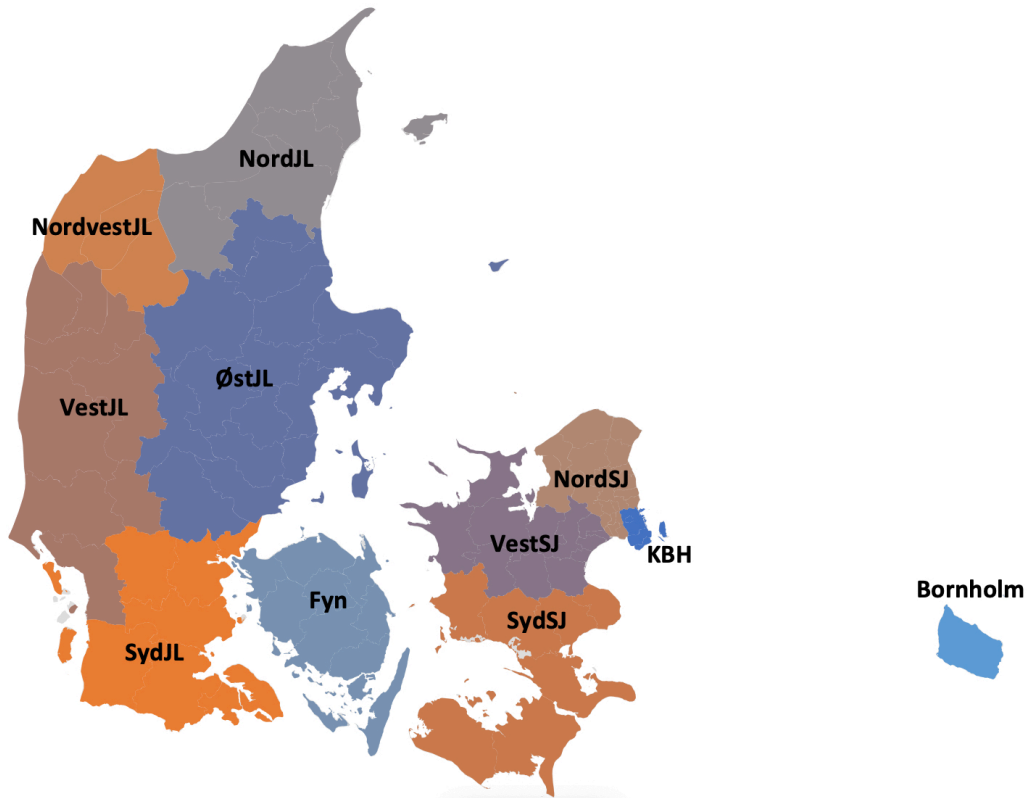
Figure 4.5: *The figure shows how the bidding zones are distributed within Denmark.*

The interconnection line capacities between these bidding zones are based on an estimated expansion of the electricity network towards 2040. The capacities can be seen in Table 4.3.

As can be seen, the capacity between the bidding zones in the central and southern part of Jutland are relatively large. The connection lines between these bidding zones are not expected to be relevant for investigating potential bottlenecks in the electricity network as a consequence of liquid fuel production on Funen. As can be seen, the capacity between Southern Jutland and Funen are more limited with a capacity of 1116 MW. Also the capacity between Funen and Western Zealand is limited to 600 MW. These two capacities will be used for investigating potential bottlenecks in the connection lines as a consequence of liquid fuel production on Funen in 2050.

The capacities resemble the N-1 capacity. This means, that the actual capacity between the bidding zones are larger, but since the Danish electricity network is operated with a N-1 security, only the total interconnection line capacity minus the capacity of the largest interconnection line can be utilized. Effectively, the electricity network is able to carry the strain in case of a breakdown on the largest interconnection line between two bidding zones.

It should be mentioned, that these capacities are merely indicative and reflect a 2020 estimation of the electricity network in 2040. The capacities are generally subject to changes in the future.

Table 4.3: *The table shows N-1 capacities of the interconnection lines between bidding zones. Source: Energinet.*

Bidding zones		N-1 Interconnection Line Capacity (2040)
Zone 1	*Zone 2*	*MW*
Bornholm	NordSJ	70
Fyn	VestSJ	600
NordJL	NordvestJL	569
NordJL	ØstJL	3677
NordSJ	KBH	1400
NordvestJL	VestJL	574
NordvestJL	ØstJL	382
SydJL	Fyn	1116
VestJL	SydJL	2788
VestJL	ØstJL	4334
VestSJ	NordSJ	2500
VestSJ	SydSJ	1000
ØstJL	SydJL	4699

4.3   Market Prices

4.3.1   Electricity

The electricity price used in the Fuel Production Model is different from the electricity price in the existing LUP model. In the existing LUP model the electricity prices in DK1 and DK2 is a result of, among other factors, the electricity prices in the neighbouring price areas that DK1 and DK2 are connected to. These prices, called *External Area Prices*, serves as an input to the existing LUP model. They are based on European data from the ENTSO-E's European scenario called *Sustainable Transition* in the TYNDP from 2018. Electricity price duration curves of the external area prices can be seen in Figure 4.6.

It can be seen that the electricity price of every external area is quite steady between 60-70 EUR/MWh in a significant number of hours during the year. Furthermore, the prices do not show a significant amount of outliers except for a couple of hours in the UK where the price goes up to 277 EUR/MWh, but the electricity price in the UK is generally higher than in the other neighbouring price areas. It should be noticed that even though negative electricity prices is a possibility for the actual price areas, the predictions of the future electricity prices does not operate with this possibility.
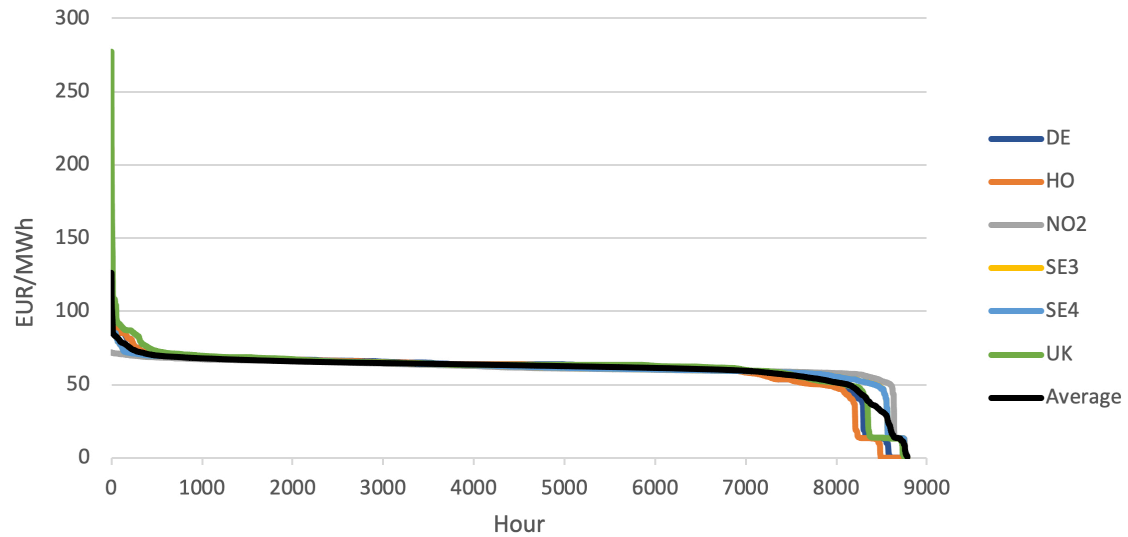
Figure 4.6: *The figure shows duration curves of the neighbouring electricity price areas, which serves as an input to the existing LUP model. The electricity price used in the Fuel Production Model is, among other factors, a result of these external electricity prices. Source: Energinet.*

The electricity price used in the Fuel Production Model is a result of a simulation in the existing LUP model of the Yellow scenario in 2040. Since the Fuel Production Model only operates with a single electricity price, even though there are two electricity price areas in Denmark, an average of the resulting electricity prices in DK1 and DK2 has been used as the electricity price in the Fuel Production Model. This hourly electricity price can be seen in Figure 4.7. It can be seen that, similar to the electricity prices of the external price areas in 4.6, the price remains rather constant between 60-70 EUR/MWh for a significant number of hours during the year. However, the duration curve also shows that the price seems to drop down to 0 EUR/MWh for slightly more hours than the external price areas.
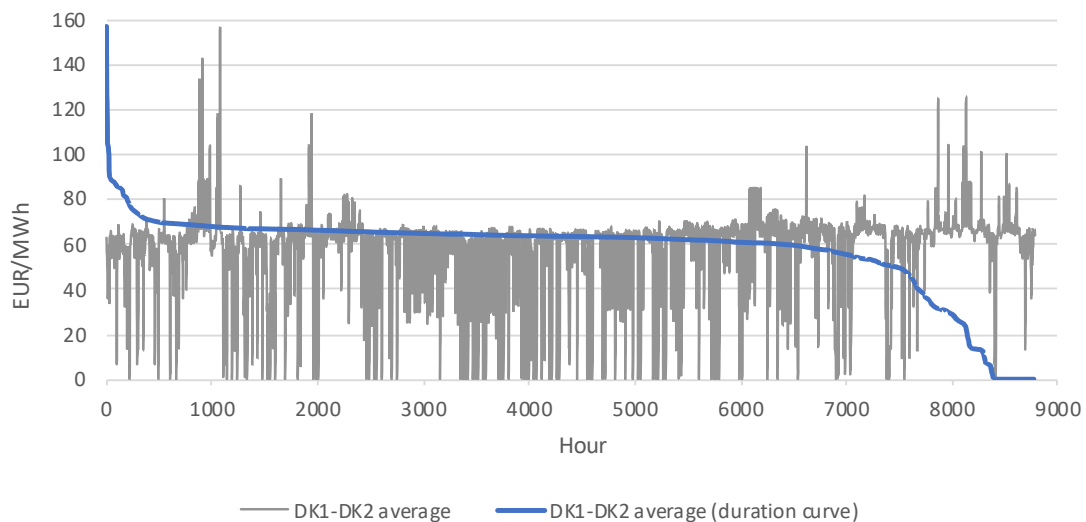
Figure 4.7: *The figure shows a duration curve of the electricity price used in the Fuel Production Model.*

Some statistics related to the electricity prices in the Fuel Production Model and the existing LUP model have been summarized in Table 4.4. The table shows the effect of more hours with lower electricity prices and more variation in the prices, as the ones used in the Fuel Production Model, by a lowest average price of 57.8 EUR/MWh and a highest standard deviation of 18.0 EUR/MWh. Regarding the prices used in the existing LUP model, it is seen that the average price of the external price areas are more or less the same. It should be mentioned that the average price of the external price areas is not used in the existing LUP model. The average is only displayed to give an overview of the external area prices.

Table 4.4: *The table shows average, minimum, maximum and standard deviation of the electricity prices used in the Fuel Production Model and the existing LUP model. DE = Germany, HO = Netherlands, NO2 = Norway 2, SE3 = Sweden 3, SE4 = Sweden 4, UK = United Kingdom.*

[EUR/MWh]	Fuel Production Model	Existing LUP Model						
	DK1-DK2 average	DE	HO	NO2	SE3	SE4	UK	Average
Average	57.8	60.3	59.7	61.6	61.5	61.5	61.9	61.1
Minimum	0.0	0.0	0.0	2.0	0.0	0.0	0.0	0.4
Maximum	157.2	157.1	211.9	72.0	108.7	108.7	277.3	126.2
Std. deviation	18.0	14.6	16.0	7.7	9.6	9.6	14.3	10.6

Additional to the spot price on electricity, a consumer pays tariffs for the transportation of electricity in the grid. Tariffs are split up in two categories; system- & transmission tariffs and distribution tariffs, since not all consumers pay all tariffs. In this study it has been assumed that consumption on central locations, i.e. the fuel production plants will be charged only the system & transmission tariff, while all decentral consumption will be charged both tariffs. This differentiation has been assumed due to the fact that central locations are likely connected at a higher voltage level that is classified as transmission and therefore, does not use the distribution grid. However, decentral plants are usually smaller, and therefore likely connected at a lower voltage level. The transmission tariff has been assumed to be 13.183 EUR/MWh, i.e. the same as in 2020, which is paid to Energinet [71]. The distribution tariff is not constant for all areas, and varies with the individual distribution system operators (DSOs). Here, the distribution tariff has been assumed to be 2.648 EUR/MWh, which is generally used internally at Energinet. This tariff is similar to the tariff paid to *Radius* as an *A-high* customer that is connected to the electricity grid at 50/30 kV.

4.3.2   Excess Heat

Since the demand for DH is dependent on the outside temperature, the value of the excess heat from fuel production changes during the year due to the alternative cost of producing heat. To account for this, a rough estimation of season-dependent heat prices has been assumed. These prices can be seen in Figure 4.8. Naturally, the heat is most valuable during winter, when peak production units are producing.
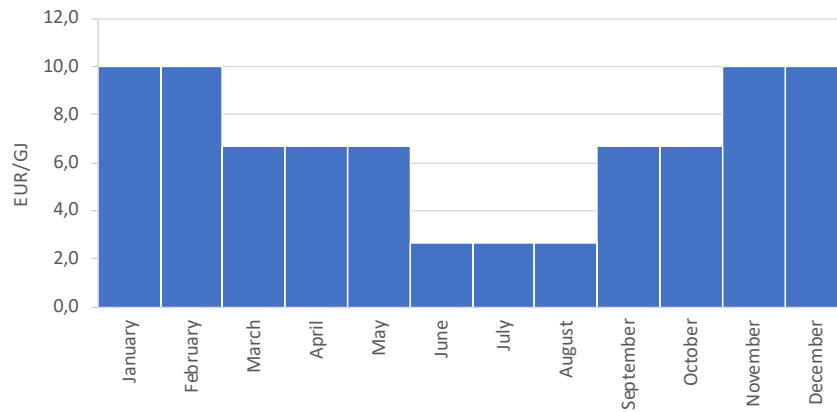
Figure 4.8: *The figure shows the assumed selling price for excess heat in the DH grids per month.*

4.3.3 Additional Prices

A part from the electricity prices and tariffs and the prices of excess heat, the remaining market prices can be seen in Table 4.5.

As can be seen in the table, the price of biogas has been set to 17.6 EUR/GJ. This price is based on the production cost of biogas in 2030. The socioeconomic price of biogas in 2019 was 18.9 EUR/GJ and this is expected to decrease to the aforementioned 17.6 EUR/GJ, which is also assumed to be the price of biogas in 2050 [49], [72].

Table 4.5: *The table shows market prices used in the Fuel Production Model. Biogas, Wood chips and Waste serve as inputs to the modelled plants while Gasoline, Ethanol, Fuel gas and Oxygen serves as outputs from the modelled plants.*

	Market price	Unit
Biogas	17.6	EUR/GJ
Wood chips	7.5	EUR/GJ
Waste	0.0	EUR/GJ
Gasoline	37.7	EUR/GJ
Ethanol	37.7	EUR/GJ
Fuel gas	8.8	EUR/GJ
Oxygen	0.0	EUR/tonne

For the purpose of producing low-temperature process heat (LTPH) and CO_2 for the liquid fuel production and to satisfy the demand for CO_2 reduction, as described in Section *4.2 Demands and Constraints*, both a biomass and waste boiler are implemented into the Fuel Production Model. The fuel price of wood chips has been assumed for the fuel input to the biomass boiler and this price is an estimate by the DEA. However, generally the projection of fuel prices in Denmark do not stretch further than 2040, so the price in 2040 has been assumed to also be the fuel price in 2050. This gives a resulting price of wood chips of 7.5 EUR/GJ, which reflects the price of wood chips being consumed at a heat producing unit [49]. The price of waste which

is the fuel input to the waste boiler has been set quite differently. This is because the fuel price of waste can range from negative to positive depending on the energy content, ease of handling, harmful substances etc. [73], [74]. Therefore, an average fuel price for waste of 0.0 EUR/GJ has been assumed in this study.

Both gasoline, ethanol and fuel gas are side products from the production of jet fuel. The prices of gasoline and ethanol have been assumed to follow the production cost of 2. generation bioethanol at 37.7 EUR/GJ [9]. The price of fuel gas, however, is different. Fuel gas is not a pure product but a mixture of gaseous hydrocarbons. It might contain a part of methane, but since it is not pure it can not be used in e.g. steam-methane reforming (SMR), but only for heat production purposes. The value of fuel gas has therefore been assumed to be half the price of biogas i.e. 8.8 EUR/GJ.

The price of oxygen has been assumed to be 0.0 EUR/GJ. There might be a market for oxygen in the future where the price would lie somewhere around the production cost of oxygen in an air separation unit (ASU). However, since oxygen is also a side product from hydrogen production in solid oxide electrolyzer cell (SOEC) electrolysis or co-electrolysis this might lower the market price of oxygen. It is however quite difficult to give a reasonable estimate of and therefore the price has been set to 0.0 EUR/GJ.

5   Synthetic Fuel Value Chain

This section will provide the reader with an understanding of the value chain of synthetic jet fuel and will cover the description of key characteristics of kerosene-based jet fuel produced by Fischer-Tropsch (FT), which is the main focus of this study and the output that dictates the value chain from biogas, CO_2 and electricity to liquid fuel. In order to understand the value chain of synthetic jet fuel, the relevant conversion technologies will be evaluated from carbon source to final liquid fuel product.

An overview of energy balances for all conversion technologies can be seen in Appendix B.

5.1   Biogas Production

As described in Section *4.2.3 Biogas Potential*, biogas will become an increasingly more important element in the Danish energy system as it can provide many of the same properties as fossil natural gas through simple conversions. Biomass resources are utilized to generate a methane-rich gas that can be converted to natural gas and used for the same applications while being sustainable. Biogas can be directly burned to generate heat and power, directly used in transportation or be converted to methane.

Usually, a biogas plant is located near agriculture in order to use agricultural waste, manure, bedding and more as feedstock at the plant since these are biodegradable biomasses. At the plant, the biomass undergoes an anaerobic process called anaerobic digestion.

In anaerobic digestion, biomass is contained in a large tank that is heated to 40-50 °C, depending on the type of process, in order to speed up the bacterial process. In this tank, microorganisms - bacteria - are added to break down the biomass and produce biogas - this process is called degassing.

While only around half of the organic matter is actually degassed to form biogas in the reactor, producing biogas from anaerobic digestion leaves a digestate that can be recirculated to the fields as a high-quality fertilizer of a better quality than manure due to mineralization of nitrogen [75]. Additionally, the methane slip from handling and storing of slurry is reduced when manure is used to produce biogas. While anaerobic digestion of organic waste is the most common way of producing biogas in Denmark, some biogas is also produced from water treatment and landfill plants. However, these will not be of further focus. As described in Section *3 Methodology*, the anaerobic digestion has not been modelled and simulated, and the price of biogas has been pre-defined. However, the understanding of how biogas is produced serves a purpose in the sustainability concern of producing synthetic liquid fuels.

As mentioned in Section *4.2.3 Biogas Potential* utilizing all biomass resources to produce biogas, the composition would be 60% methane and 40% CO_2.

5.2   Hydrogen Prodction

Hydrogen is still a relatively new form of energy in the energy system, mainly due to its high production costs and the fact that the current gas infrastructure only allows for a certain amount of hydrogen mixture. This is due to the very small size of the hydrogen molecule compared to the methane molecule which is the

main component of the natural gas in the gas grid today [76], [77]. However, the development in hydrogen producing technologies is regarded as one of the most important developments towards a sustainable energy system because of the synergy it can create between the gas and electricity systems and being the central to PtX, which inevitably will be a major part of the future energy system. Hydrogen production can be used to balance the power system in hours of excess renewable electricity production and store it for future use as gas, or to produce electricity later in a turbine. The production of hydrogen is mainly done through electrolysis, which uses electricity to split water into oxygen and hydrogen. Electrolysis will especially be relevant with the potential for offshore wind farms in the Danish part of the North Sea being 10 GW [78], and even more so with the current international target of installing 180 GW in the North Sea by 2045 as part of the large-scale North Sea Wind Power Hub (NSWPH) [6].

Electrolysis is usually divided in three types; polymer electrolyte membrane (PEM), Alkaline and SOEC in which PEM and alkaline are both commercially proven technologies, while SOEC is still in development due to its more demanding technical setup and high operation temperature of around 700 °C. These three technologies are also the ones included in [64]. In this study, it has been assumed that SOEC will become commercially viable in the period from 2030 to 2050, and therefore, it has been assumed that the entire capacity of electrolysis in 2050 will be based on SOEC. From 2030, the investment costs are projected to be relatively similar for SOEC and alkaline electrolysis, while SOEC is projected to be more efficient in terms of electricity to hydrogen [64].

5.3   Methane Production

In today's energy system, methane is used for a wide range of applications but is most commonly used to produce high-temperature process heat (HTPH) due to the low price and relatively high efficiency of gas boilers along with its ease-of-use. Furthermore, alternatives to producing HTPH are limited. Today, the gas grid in Denmark flows with natural gas, of which methane is the main component, making up 91 mol% in 2019, while various slightly longer hydrocarbons make up most of the remaining 9% along with impurities like nitrogen, carbon dioxide and sulphur [79]. Henceforth, methane has been assumed to be indifferent from natural gas in terms of quality, and mentioning either natural gas or methane refers to the same type of gas.

Methane is a fossil gas due to the origin of the carbon in the molecules. While the gas is fossil, it is still widely used as it has a range of advantages compared to renewable gasses such as hydrogen, e.g. the burning rate and the price. Since the gas grid today contains mostly methane, which has the same chemical composition regardless of the origin of the carbon, renewable methane can easily be transported in the existing gas grid without major adjustments. The gas grid can be used to transport methane over long distances without any major losses as compared to electricity, and can even be used as a large storage, which reduces the need to build external storage units for methane [80]. Furthermore, methane is a desirable energy form as it is the primary feedstock for SMR and partial oxidation (POX) as will be described in the Section *5.5 Synthesis Gas Production.*

Today, methane is primarily extracted from large gas fields, such as Tyra, which is located in the North Sea. However, there are ways of producing methane sustainably, e.g. through the use of biogas from renewable biomass resources, as mentioned in Section *4.2.3 Biogas Potential.* This study will focus on the prospects of using biogas to produce methane by either biogas upgrading or methanation of carbon dioxide using hydrogen.

5.3.1 Biogas Upgrading

In biogas upgrading, the 40% carbon dioxide is removed from the biogas, leaving methane in the gas and thereby *upgrading* the heating value. This can be done by the use of biogas scrubbing, membrane technology, pressure swing absorption, and more, with the most commonly used technology being water-scrubbing [64]. Here, biogas is put in contact with water, either by spraying water or by bubbling water through the biogas, which reacts with the CO_2, separating the methane. Methane produced by upgrading of biogas is commonly referred to as biomethane, or bio natural gas (BNG), since it is based on a biogenic resource. In this study the technical and economic characteristics of biogas upgrading has been based on the water-scrubbing technology.

5.3.2 Methanation of Biogas

Methane can also be produced by *mixing* biogas with hydrogen, which is called methanation or hydrogenation. Here, CO_2 in the biogas reacts with the hydrogen to increase the methane yield of biogas. When producing methane with this method, there will be no need to handle CO_2 from the biogas, and effectively electricity can indirectly substitute some biogas production, which can easily be required due to the limited biomass resource for biogas production. Given a CO_2 content of the aforementioned 40 vol% the energy output of methane from methanation of biogas can be increased by approximately 60% [81]. Methane from methanation using hydrogen is commonly referred to as bio- and electromethane, or synthetic natural gas (SNG), since it contains both biogenic carbon and hydrogen from electricity through electrolysis. However, SNG can also be produced purely with electricity as input, called electromethane, which is also usually referred to as SNG. This can be done by capturing CO_2 from a point source such as waste incineration, or from filtering it from the air by direct air capture (DAC). This CO_2 reacts with hydrogen in a chemical process, which could be the Sabatier process shown in Equation 5.1.

$$CO_2 + 4\,H_2 \longrightarrow CH_4 + 2\,H_2O \tag{5.1}$$

5.4 CO_2-Capture

In the future, carbon could also come from capturing CO_2 from different sources. In this study, three different ways of acquiring CO_2 has been included. These are capturing from waste and biomass incineration, biogas and from ambient air. Capturing CO_2 from waste and biomass incineration is referred to as carbon capture and utilization (CCU), capturing CO_2 from ambient air is done through DAC and CO_2 from biogas

is assumed to be collected as part of the upgrading process described in *5.3.1 Biogas Upgrading*. Based on the report from SDU from 2020 [11], from which the total economically feasible potential for biogas production in Denmark was assumed to be 50 PJ when considering other demands, as described in Section *4.2.3 Biogas Potential*, this biogas would contain almost 1,000 kilo tonne (kt). Capturing CO_2 from the air would naturally be considered limitless as long as renewable electricity is available. However, capturing CO_2 from the air is still a relatively costly technology, with producers such as *Climeworks* [82] and *Carbon Engineering* [83] currently developing and testing increasingly larger plants.

As described in Section *4.2.4 CO₂ as a Resource*, CO_2 can be transported from biogas upgrading plants to the fuel production plant either by a dedicated CO_2 pipe or by trucking, and the cost associated to the different CO_2 sources will be evaluated in Section *8 Simulation Results*.

5.5   Synthesis Gas Production

Synthesis gas, commonly referred to as syngas, is a fuel gas that primarily consists of hydrogen and carbon monoxide, H_2+CO. Today, syngas is produced from fossil natural gas, coal, liquid petroleum gas (LPG), woody biomass, etc. [84]–[88]. Syngas can be produced by a wide range of conversion technologies, a few of which will be described later in this section. In the future, it is likely that syngas will be produced primarily with a feedstock of methane, electricity and CO_2. The advantage of using methane comes with the utilization of the natural gas grid, as it can be transported over great distances, and has a large storage capacity in the linepack of the grid.

Electricity will be the backbone of the future energy system, and the potential for producing renewable electricity from offshore wind farms are expected to be more than 10 GW within the Danish territory, as mentioned in Section *5.2 Hydrogen Prodction*. This means that there will be hours where the system is in need of ancillary services, and these could also be provided, to some extent, from the fuel production plants by using this excess electricity to produce liquid fuels that can more easily be stored. Furthermore, using biogenic CO_2 that would otherwise be emitted for liquid fuel production, would result in the output fuel being CO_2 net-neutral, as it displaces .

Syngas is the main feed in the FT synthesis reactor, which is used to produce liquid fuels. FT will be further described in the following section. When using FT, according to multiple sources, one should aim for a H_2:CO ratio of 2:1 [12], [24], [25], [89]. In this project, four different technologies to produce syngas has been evaluated and modelled; steam-methane reforming, partial oxidation, reverse water-gas shift and co-electrolysis.

5.5.1   Steam-Methane Reforming

Steam-methane reforming (SMR) is perhaps the most commonly known of the four technologies, as it has a long history of producing hydrogen. Today, SMR accounts for the majority of the worlds pure hydrogen production [90]. However, with technologies such as electrolysis that use electricity to produce hydrogen being

developed and commercialized, SMR units can be used to produce syngas instead. SMR is an endothermic process in which methane and steam is mixed and heated to 700-1000 °C in which the steam and methane react, producing syngas with a ratio between hydrogen and carbon monoxide of 3:1 [25]. The ideal chemical reaction can be seen in Equation 5.2:

$$CH_4(g) + H_2O(g) \longrightarrow 3\,H_2(g) + CO(g) \qquad \Delta H_f^\circ = +206\text{kJ/mol} \tag{5.2}$$

SMR is usually operated with a reverse water-gas shift (RWGS) unit in order to adjust the ratio of hydrogen and carbon monoxide. When applied in a FT application the ratio is adjusted to 2:1 instead of 3:1, which is the optimal ratio for FT, as earlier mentioned. According to [21] the efficiency of typical SMR units is 80-90%, and therefore, 85% has been assumed in this study.

5.5.2   Partial Oxidation

Partial oxidation (POX) is, as well as SMR, a known technology but has not attracted as much attention as SMR. Opposite SMR, POX is an exothermic chemical process in which steam and methane is combusted with a sub-stochiometric amount of oxygen (partially oxidated) in a reformer. Since there is a lack of oxygen, the reaction does not complete to form CO_2. According to [24] the POX unit is usually operated at around 700 °C - slightly lower than the SMR and has a CO selectivity of 95%, which is a measure of conversion efficiency. The ideal chemical reaction of POX can be seen in Equation 5.3:

$$CH_4(g) + \frac{1}{2}\,O_2(g) \longrightarrow 2\,H_2(g) + CO(g) \qquad \Delta H_f^\circ = -36\text{kJ/mol} \tag{5.3}$$

The syngas produced using POX has a H_2:CO ratio of 2:1, as evident in the equation. This means that the syngas produced using POX does not need to be adjusted and can be used directly in FT. However, it requires a feed of oxygen, which, if supplied through an ASU, could be costly and spacially demanding.

5.5.3   Reverse Water-Gas Shift

As well as adjusting the H_2:CO ratio in syngas from SMR, the reverse water-gas shift (RWGS) reaction could become an important element in the future production of liquid fuels, since it can also be used to produce syngas isolated. Based on the stochiometric chemical reaction, RWGS would produce carbon monoxide and water with a feed of carbon dioxide and hydrogen, as evident in Equation 5.4.

$$H_2(g) + CO_2(g) \rightleftharpoons CO(g) + H_2O(g) \qquad \Delta H_f^\circ = +41\text{kJ/mol} \tag{5.4}$$

However, operating the RWGS with an excess of hydrogen, the process can be used to produce syngas and water in which it is assumed that the hydrogen does not react in the unit but mixes with the output carbon monoxide. The RWGS unit would preferably be operated with an excess of hydrogen resulting in a syngas ratio of 2:1, but could be modified to produce with any desired ratio by adjusting the amount of

feed hydrogen. Using RWGS to produce syngas enables a plant to operate purely on electricity, making it possible to produce pure electrofuels if the carbon source is captured from the air or from a point source using electricity as well.

5.5.4   Co-electrolysis

Another way of producing syngas purely based on electricity, is through a modification to the SOEC in which the unit is fed with both water and carbon dioxide, called co-electrolysis. A schematic of the co-electrolysis of water and carbon dioxide can be seen on Figure 5.1. Water and carbon dioxide is fed to the cathode in which an oxygen atom is separated from the CO_2 molecule creating carbon monoxide, and thereby syngas, and oxide. From the cathode the oxide travels through the electrolyte creating oxygen at the anode. To produce syngas with a H_2:CO ratio of 2:1, extra water can be supplied. The stochiometry of this configuration can be seen in Equation 5.5. Excess oxygen from the anode can be collected and used in processes like POX. While co-electrolysis is still in development stages, it has been assumed that the technology will mature towards 2050 [9], [64] - similar to electrolysis of water using SOEC.

$$2\,H_2O\,(g) + CO_2(g) \longrightarrow 2\,H_2(g) + CO\,(g) + 1.5\,O_2(g) \tag{5.5}$$
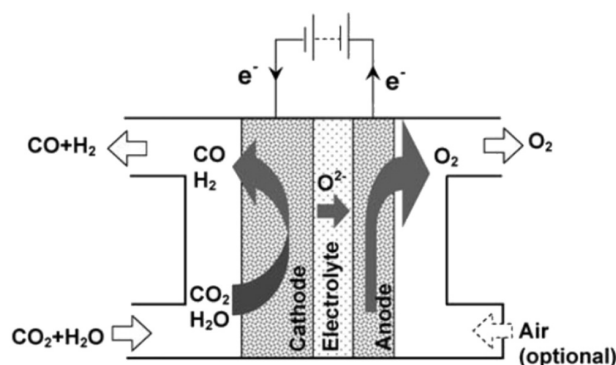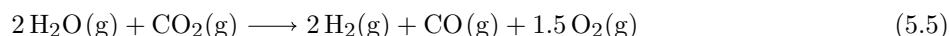
Figure 5.1: *Schematic of the operation of co-electrolysis of water and carbon dioxide. CO_2 and water is fed in the cathode in which oxygen travels through the electrolyte, producing syngas. Figure has been taken from [23].*

5.6   Fischer-Tropsch

5.6.1   Introduction to Fischer-Tropsch

Fischer-Tropsch (FT) is a well-known technology, dating back to the early 20th century Germany, and was discovered by Franz Fischer and Hans Tropsch. Today there are several commercial fuel production plants that use FT, of which the largest companies are Sasol and Shell, who operate plants in both Qatar, South Africa and Malaysia. Traditionally, FT has been using coal or natural gas as feedstocks, in which coal is gasified. FT is an essential technology in this study's projection of the future production of liquid fuels since it uses syngas, which, as described earlier, can be produced from methane or electricity, utilizing the strong infrastructure in Denmark.

FT contains a complex collection of chemical processes that converts this syngas to a wax-like crude oil, which in commonly referred to as synthetic crude oil (syncrude), due to its synthetic nature compared to traditional crude oil, and in order to differentiate the sustainable crude oil from traditional crude. The syncrude from FT is, similar to conventional crude oil, only an intermediate product in fuel production since syncrude does not have an immediate use in aviation. It requires refining like conventional crude oil. The syncrude from FT does not refer to one single product, as it can have a wide range of compositions of alkenes, alkanes, alcohols, etc. [89]. The final composition depends on the catalyst and the way the synthesis is conducted. According to [12], low-temperature Fischer-Tropsch (LTFT) is more suited to produce jet fuel compared to high-temperature Fischer-Tropsch (HTFT), the reason for this will be described in Section *5.6.3 Fischer-Tropsch Fuel*, and therefore, only LTFT will be included in this study.

Table 5.1: *Characteristics of syncrude from both HTFT and LTFT compared to conventional crude oil. In many ways, crude oil and synthetic crude from FT are similar. However, in certain aspects, such as the absence of sulphur and nitrogen, the synthetic crude differs from traditional crude oil. Conventional crude oil refining technologies can be used with FT syncrude, but would often require pre-treating [89].*

Compound class	HTFT	LTFT	Crude oil
Alkanes (paraffins)	>10%	Major product	Major product
Cyclo-alkanes (naphtenes)	<1%	<1%	Major product
Alkenes	Major product	>10%	None
Aromatics	5-10%	<1%	Major product
Oxygenates	5-15%	5-15%	<1% O (heavy)
Sulfur compounds	None	None	0.1-5% S
Nitrogen compounds	None	None	<1%N
Organometallics	Carboxylates	Carboxylates	Phorphyrines
Water	Major by-product	Major by-product	0-2%

The syncrude from FT is comparable to conventional crude oil in terms of refining and potential for liquid fuel production. However, there are several differences between them such as the composition of alkanes, alkenes, aromatics and more [89], of which an overview can be seen in Table 5.1. However, these differences will not be further touched upon. The syncrude from FT undergoes a refining process that, in many ways, is similar to that of conventional crude oil. There is an intermediate step between FT synthesis and syncrude refining, called syncrude recovery. An illustration of this intermediate step can be seen in Figure 5.2.

The syncrude from LTFT leaves the reactor in two separate streams. One stream is liquid molten wax which can be collected for refining directly from the reactor. The other stream is in the form of vapor and contains unconverted syngas and light syncrude. Before going to the refining processes, this vapor stream is cooled and fractioned into separate hydrocarbon chains. Therefore, the product of the syncrude recovery process is four separated streams, each containing a range of hydrocarbons, that then go through different refining processes which will be described in the coming sub-section. The four fractions can be roughly categorized as:
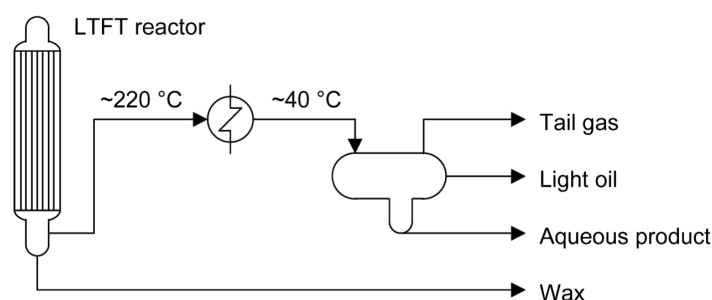
Figure 5.2: *Schematic of the syncrude recovery setup from [12]. The output of the reactor is separated in two streams; one stream with the long-chain syncrude wax that are directly collected for refining, and one with vapor that contains unreacted syngas and lighter syncrude compounds, that are cooled into tail gas, light oil, or condensates, and aqueous products.*

- **Wax**, which should be kept at a temperature above 100 °C, to keep the wax in liquid form. If cooled below 100 °C, the wax starts to congeal making it difficult to circulate in the refining stage. The wax generally consists of heavy hydrocarbons above C_{11}.
- **Tailgas**, which consists of light naphtha and LPG (C_3-C_4).
- **Light oil**, or **condensate**, which is the product of cooling, or condensing, the vapor stream from the LTFT reactor to an oil product containing naphtha (C_6-C_{10}).
- **Aqueous product**, which is also called *reaction water* and is condensed with the condensate from the second syncrude stream.

It has been assumed that the LTFT unit has a constant production for all hours of the year in order to simulate the preferred constant production of jet fuel and by-products from the FT synthesis and thereby forcing it to choose from the economically more feasible syngas feedstock for hybrid configurations.

5.6.2   Refining

Since the output of FT is not the final product, the real value-adding of the product happens during refining. It is during the refining that the long-chain hydrocarbons are converted to valuable liquid fuels. In the LTFT from [12], the refining setup is made to maximize jet fuel output. An illustration of the refining setup can be seen in Figure 5.3.

In the figure, it can be seen that this refining setup uses oligomerisation, hydrogenation, hydrocracking, aromatisation and isomerisation along with purification of ethanol.

Alky- & oligomerization   is used to produce longer chain alkenes from short-chain alkenes. Here short-chain hydrocarbons (C_3-C_5) are sent directly to oligemarisation as well as alkylating benzene (Bz-C_7), producing kerosene.

Naphtha hydrogenation   is used to hydrotreat naphtha, which basically uses hydrogen to remove heteroatoms, which increases the H:C ratio of the feed material. The product is split into kerosene (C_9-C_{10}) for jet fuel production and naphtha (C_6-C_8) for aromatisation.

Hydrocracking   is used to convert the long-chain wax from LTFT to shorter hydrocarbon chains such as jet fuel. The now shorter useful hydrocarbon chain, ranging from C_3-C_{15} is then distributed to the other refining steps in order to produce final products. Hydrocarbons heavier than C_{15} is looped back to the hydrocracker and broken down to lighter hydrocarbons again. The hydrocracker uses hydrogen to saturate the lighter hydrocarbons that have been formed from the heavy hydrocarbon.

Hydroisomerization   is used to increase the octane rating of the produced gasoline. Octane rating is a measure of the fuels ability to compress without igniting. Generally, fuels with high octane rating can be used in high-performance gasoline engines that require high compression ratios.
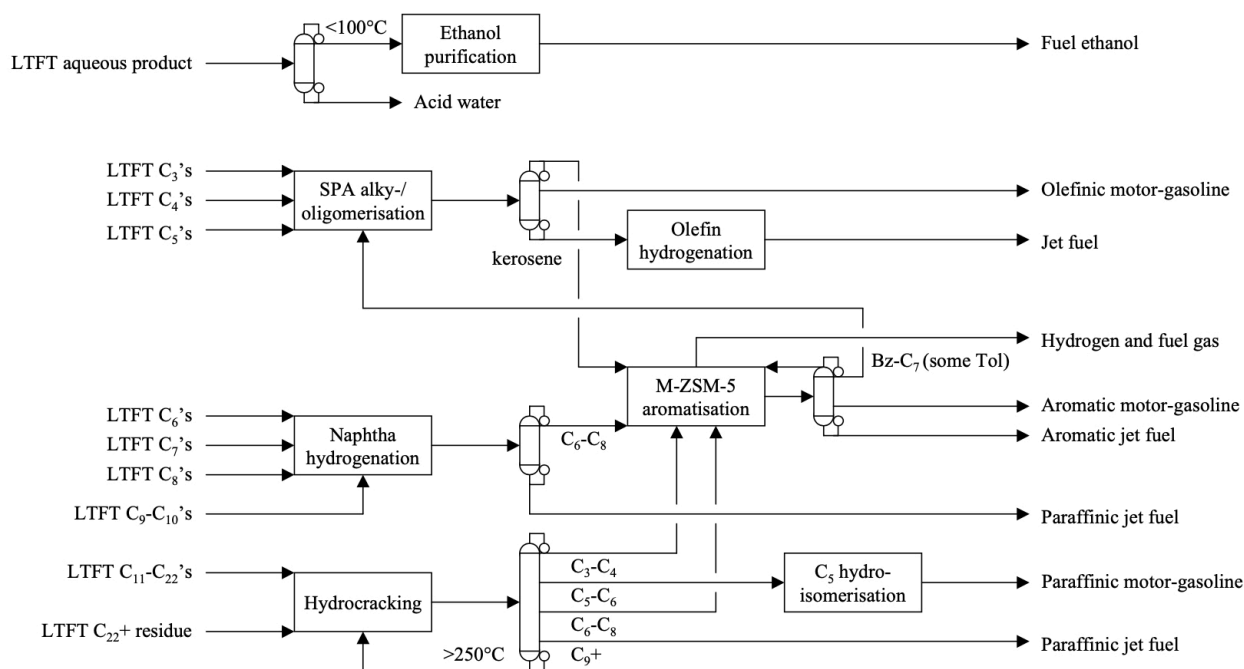
Figure 5.3: *Schematic of the refining process for LTFT from [12]. The LTFT refining process consists of alky- & oligomerisation of the tail gas from the syncrude recovery to produce kerosene, some of which is further refined through olefin hydrogenation to produce jet fuel. The naphtha in the condensate is collected for hydrogenation. The aqueous product is used to produce ethanol through purification. The heavy wax is collected directly for hydrocracking to produce lighter hydrocarbons that can be further refined to motor-gasoline and jet fuel through aromatisation or isomerisation. Some hydrocarbons can be used directly after the hydrocracker.*

5.6.3   Fischer-Tropsch Fuel

As mentioned in the introduction to this section, LTFT is more suited for jet fuel production. Table 5.2 shows the comparison of the fuel from LTFT and HTFT synthesis and refining.

Here, the choice of using LTFT can be justified by the higher share of high-value hydrocarbons in the form of jet fuel and motor-gasoline, constituting 91% of the total mass output of LTFT compared to it constituting 80% for HTFT. The output is based on a refining capacity of 500,000 kg of products per hour from [12].

Table 5.2: *Comparison of the fuel yield from HTFT and LTFT synthesis and refining. It can be seen that LTFT produces more jet fuel and motor-gasoline, which is the primary purpose in this study. Since jet fuel and gasoline are the most valuable products in this process maximizing it will yield better feasibility. Furthermore, there would likely be cheaper ways of producing the by-products from the jet fuel refining. The values are found in [12], and describes the outputs from a refinery facility with an hourly capacity of 500,000 kg of products per hour.*

Product	Refinery production							
	HTFT				LTFT			
	kg/h	m^3/h	bpd	vol%	kg/h	m^3/h	bpd	vol%
Liquid fuels								
Motor-gasoline	98,880	131	19,742	22.4	101,328	137	20,641	23.0
Excess ethanol	17,624	22	3,351	3.8	2272	3	432	0.5
Jet fuel	302,863	389	58,650	66.5	355,912	455	68,720	76.5
Diesel	0	0	0	0	0	0	0	0.0
LPG	23,563	42	6,410	7.3	0	0	0	0.0
Other products								
Fuel gas	32,612				26,781			
Unrecovered organics	14,894				15,634			
Hydrogen	281				-3,242			
Water	9,277				1,315			
Total	**500,000**				**500,000**			

For HTFT jet fuel constitutes 60% of the total output in mass. Motor-gasoline is approximately 20%. The output of an LTFT synthesis and refinery is equal to a facility capacity of 89,361 barrels per day (bpd), which would be equal to almost 45% of the total global capacity of GtL [91] in 2015. The capacity is projected to increase to around 400,000 bpd in 2025 - the majority of this increase in capacity originates from the conversion of a coal-to-liquid (CtL) to GtL in South Africa [91], [92], effectively adding 160,000 bpd to the GtL global capacity. However, regardless of which type of FT is used for syncrude production, they must meet the technical specifications. Jet fuel must meet the specification of Jet A-1, while motor-gasoline must meet the requirements for gasoline set in the European Union [93]. The comparison of the jet fuel and motor-gasoline from the LTFT refining and the requirements for those fuels can be seen in Table 5.3.

It can be seen in the table, that both gasoline and jet fuel meet the technical specifications. However, some specifications are close to the requirements, such as ethanol content in motor-gasoline and aromatics in both jet fuel and motor-gasoline [93]. While the gasoline from the refining meets the requirements for today's motor-gasoline, these requirements can change from now to 2050.

Table 5.3: *Evaluation of the quality of the fuels from LTFT based on for Jet A-1 requirements for jet fuel and Euro 5 requirements for motor-gasoline. Both jet fuel and motor-gasoline from the LTFT satisfies the requirements from their respective standards. It is worth noting that there are some categories in which the fuels are close to the specified requirements such as the vol % of aromatics in jet fuel and the ethanol content in motor-gasoline.*

Fuel properties	Refinery	Fuel specification	
Jet fuel		*Jet A-1*	
Density (kg/m^3)	782	775-840	Range
Aromatics (vol%)	24.8	8-25	Range
Flash point (°C)	52	38	Min
Vapor pressure (kPa)	0.8	-	
Motor-gasoline		*Euro-5 [93]*	
RON	95	95	Min
MON	87	85	Min
Vapor pressure (kPa)	58	60	Max
Density (kg/m^3)	741	720-775	Range
Olefins (vol%)	6.5	18	Max
Aromatics (vol%)	34.9	42	Max
Oxygenates (vol%)	4.6	15	Max
Benzene (vol%)	0.2	1	Max
Ethanol (vol%)	4.6	5	Max

6   Scenario Definition

In the previous section, the individual technologies for the pathway of jet fuel production by LTFT were described. Sustainable liquid fuels, as mentioned earlier, is currently more expensive to produce than fossil fuel. In fact, according to [5], sustainable hydrocarbons will never be produced at the same cost as fossil fuels. This means that it is of even greater importance to explore opportunities to utilize every feasible synergy of by-products and co-production between technologies in order to reduce production costs. This section will provide the reader with key insight to these synergies between the technologies and how they fit together within the plant. Where Section *5 Synthetic Fuel Value Chain* aims to describe *which* technologies are well suited for fuel production, this section aims to answer *why* these technologies are well suited, and how best to utilize mass and energy flows. This is done by evaluating different scenarios for plant configurations along with scenarios for upstream energy pathways. In this study, eight scenarios for plant configurations have been included, each modelled with upstream methane from both biogas upgrading and methanation, to investigate the effect of the methane price.

6.1   Plant Configuration

Eight different plant configurations has been evaluated. Of those eight, two scenarios are limited to being strictly GtL plants, four include the option of producing fuels from both methane and electricity, x-to-liquid (XtL), and two configurations using only electricity, power-to-liquid (PtL). The four plant configurations using both methane and electricity will be referred to as hybrid plants due to their ability to switch between feedstock for syngas production depending on an hourly optimization of the technical and economic feasibility. Since higher-temperature heat is generally more valuable than lower-temperature due to its wider applications, heat has been split up into three categories.

- **District heating (DH)** is categorized as heat below 80 °C.
- **Low-temperature process heat (LTPH)** is categorized as heat from 80-450 °C.
- **High-temperature process heat (HTPH)** is categorized as heat above 450 °C.

In order to make the figures of the plant configurations more simple, the production of LTPH and HTPH have not been illustrated directly in the figures. With that said, this does not mean that the excess heat from intermediate processes within the production plant are necessarily able to supply the entire demand for LTPH and HTPH within the plant, but the streams are merely illustrated to indicate the synergies that exists between the processes in relation to heat. In the Fuel Production Model, four different units for the production of LTPH and HTPH have been modeled. Two different gas boilers are able to produce HTPH - one that can boost the temperature from LTPH to HTPH by combustion of either methane, hydrogen or fuel gas, and one that can produce HTPH without a source of LTPH again by combustion of either methane, hydrogen or fuel gas. Two different units are able to produce LTPH - a heat pump and an electric boiler. The output from the LTPH heat pump has been assumed to only be 150 °C, due to limitations with the

coefficient of performance (COP). Even though the LTPH area generally consists of heat with a temperature between 80-450 °C, the assumption of the heat pump output temperature does not conflict with the LTPH area since no production unit, that has a fuel input of LTPH, uses LTPH with a temperature higher than 150 °C.

For all plant configurations, it has been assumed that the refining of the LTFT syncrude is located at the same site as the actual LTFT synthesis. In the future, the refining process could potentially be located remotely from the synthesis, in which the syncrude would be transported to a larger refining facility. This could potentially mean that some products could not be directly recirculated. However, the analysis of the location of refining has been considered out of the scope of this project. This assumption, however, points out some interesting synergies that arise from locating the refining and syncrude production at the same site such as the ability to recirculate fuel gas, within the production plant, in intermediate processes. Furthermore, locating the refining and synthesis at separate locations would give rise to a need for transportation of the syncrude.

All figures illustrate the technologies and synergies that can be found within the liquid fuel production plant, and the boundary of the plant in shown as a dashed line.

6.1.1   Gas-to-Liquid using Steam-Methane Reforming

This configuration uses SMR to produce syngas, which is then adjusted in a RWGS unit to fit the preferred H_2:CO ratio of 2:1, as mentioned in Section *5.5 Synthesis Gas Production*. Figure 6.1 shows an overview of the mass and energy flows within the fuel production facility. Here, it is assumed that the fuel production plants will be located near waste and biomass incineration plants that are also connected to the largest DH areas in Denmark. Utilizing by-products, from intermediate conversions, and the synergies between technologies help reduce the resulting production cost of liquid fuels, and thereby also the price. It is assumed that waste and biomass incineration plants generate heat at temperatures around 450 °C. While the figure might suggest direct use of LTPH in e.g. SMR, the LTPH is further heated using a gas boiler in order to raise the temperature to those suitable for SMR, RWGS, etc. Furthermore, CO_2 captured in the flue gas from waste and biomass incineration can be used as input to the RWGS reaction.
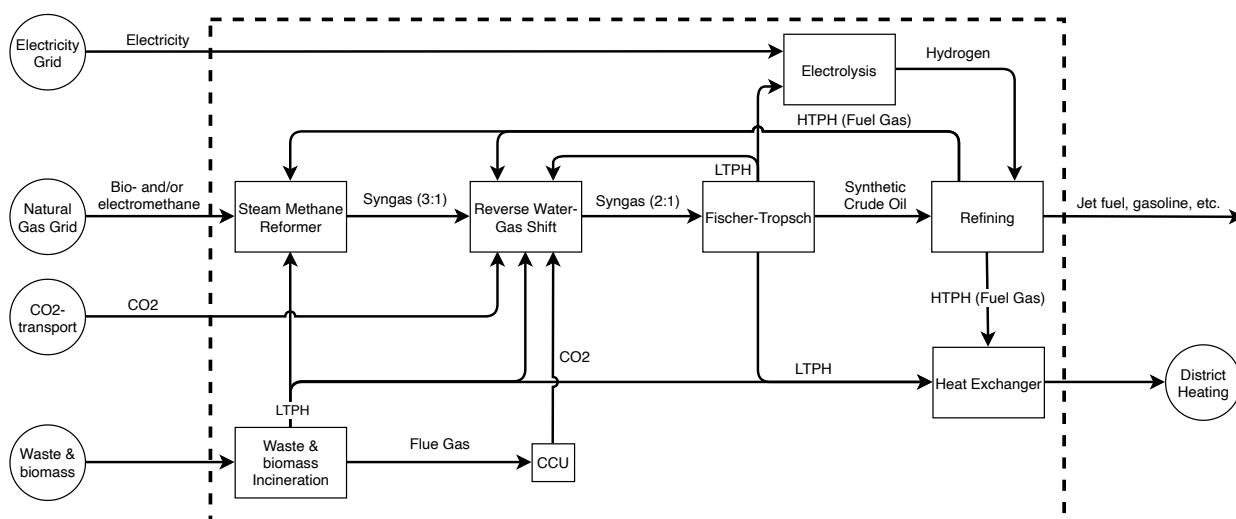
Figure 6.1: *Flow diagram of a GtL plant using SMR to produce syngas. The plant is assumed to be located near a waste and biomass incineration plant to utilize the LTPH and CO_2 from the flue gas. The LTPH from waste and biomass incineration is heated to become HTPH using a gas boiler - if feasible. The by-product of fuel gas from refining can be used in a gas boiler to produce LTPH or HTPH depending on the application. It has been assumed that excess heat from the plant can only be used as DH through a heat exchanger.*

As mentioned in Section *5.5 Synthesis Gas Production*, SMR is a well-known and commercially proven technology. SMR uses HTPH to heat the mixture of steam and methane for it to chemically react into syngas. This creates a synergy between waste incineration and SMR, as this high-value heat can be supplied on-site from the waste or biomass incineration through a gas boiler, as mentioned earlier. Since the LTFT synthesis is an overall exothermic combination of processes, heat is released with a temperature of around 225 °C [30]. This heat can be used to produce steam for electrolysis, boosted in temperature through the gas boiler to produce HTPH for SMR and RWGS, or it can be sold as DH, which can help reduce the overall cost of the liquid fuels.

6.1.2   Gas-to-Liquid using Partial Oxidation

The GtL configuration using POX has fewer flows within the plant. This is mainly due to the fact that POX produces syngas with the desired H_2:CO ratio of 2:1 without the need for adjusting. This eliminates the need for the RWGS unit. In fact, this means that the synergy between waste and biomass incineration and GtL is much less when using POX, since it requires neither HTPH nor CO_2 for adjustment of the syngas. However, using SOEC electrolysis for hydrogen production on-site creates a synergy between the SOEC and POX, since SOEC has an output of oxygen, which is needed in the POX unit. While the oxygen from SOEC can be used, it is likely that an ASU is needed to supply the required amount of oxygen, since the demand for hydrogen on-site, and thereby the production of oxygen, is relatively low. An overview of the configuration can be seen in Figure 6.2.
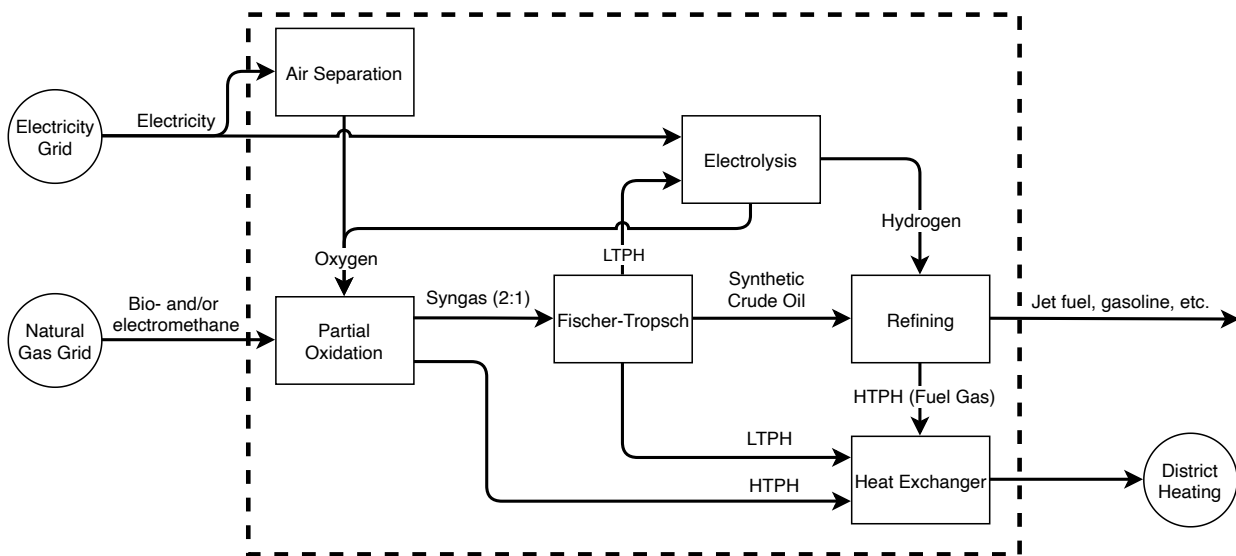
Figure 6.2: *Flow diagram of a GtL plant using POX to produce syngas. Here, the location is less restricted, as there are no obvious synergy between the fuel production and waste incineration. In Sifre, however, the configuration includes waste and biomass incineration, but this has been excluded from the figure to illustrate the lack of synergies. However, locating a plant with this configuration in a large DH area still provide synergies that can reduce jet fuel prices. It has been assumed that excess heat from the plant can only be used as DH through a heat exchanger.*

While the use of POX eliminates the synergy of utilizing heat and CO_2 when placing the plant close to waste incineration, it might still be advantageous to locate the plant at the larger DH areas as there is a high excess heat production - now from both LTFT and from the syngas production. In general, the configuration of the GtL plant using POX to produce syngas has the highest consumption of SNG as this is the only source of carbon. When using SMR this carbon source is divided between consuming SNG and captured CO_2 in RWGS. Using GtL exclusively, especially POX due to the higher consumption, could make the plant more sensitive to fluctuations in the methane price.

6.1.3   Hybrid X-to-Liquid using Steam-Methane Reforming and Co-electrolysis

Synergies between different elements within the plant are arguably more interesting for a hybrid configuration of the liquid fuel production. Here, the producer can decide whether to produce from a methane feedstock, electricity or from both depending on the price of the feedstock or the selling price of heat. This means that the plant is able to always optimize the production according to the lowest possible marginal cost. However, it does require extra investments. This configuration uses SMR with RWGS as well as co-electrolysis for syngas production. The plant configuration is shown in Figure 6.3.
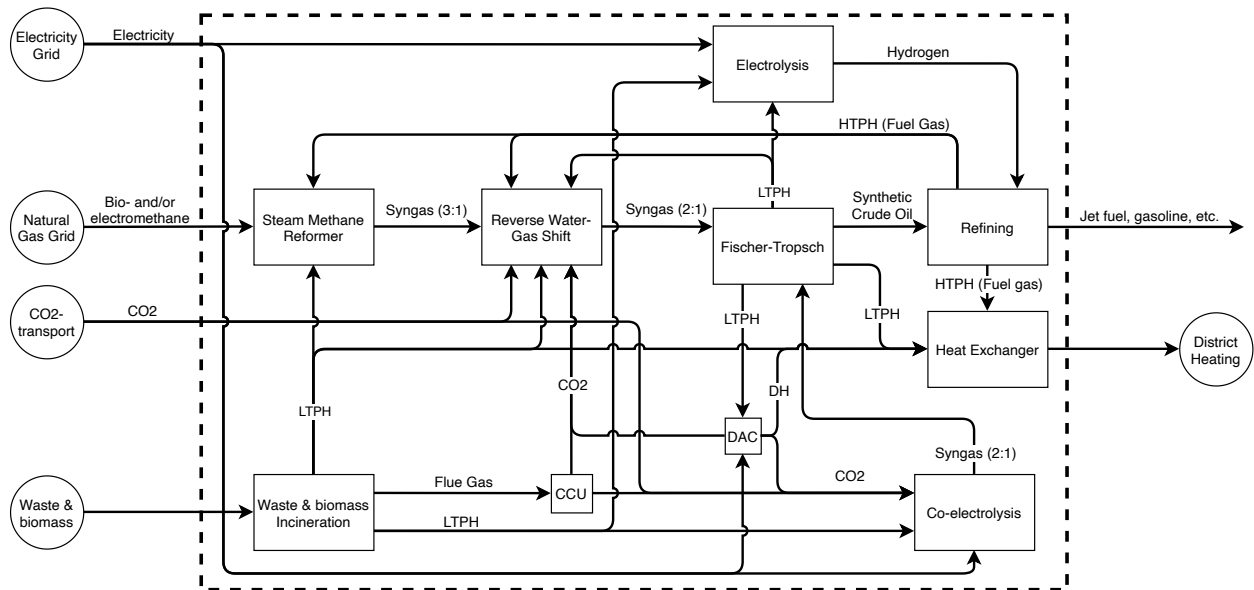
Figure 6.3: *Flow diagram of a hybrid XtL plant using SMR and co-electrolysis to produce syngas. The plant is assumed to be located near waste and biomass incineration to utilize the LTPH and CO_2 from the flue gas. Including a co-electrolysis unit can improve flexibility of the plant by continuously choosing the syngas production option with the lowest marginal cost. However, the potential increased CO_2 requirement for co-electrolysis could lead to the need for a DAC unit. It has been assumed that excess heat from the plant can only be used as DH through a heat exchanger.*

It is evident from the figure that there are significantly more potential synergies within the plant for a hybrid configuration and since both RWGS and co-electrolysis consumes CO_2, locating the plant near waste and biomass incineration is even more advantageous than for the GtL configuration using SMR. However, the CO_2 consumption in co-electrolysis is significantly higher than for adjusting syngas from SMR, which could potentially lead to the need for investing in DAC, if the consumption exceeds the amount contained in the flue gas. CO_2 can also be collected from biogas, which is what *CO2-transport* refers to. Naturally, this CO_2 is only available for upstream methane that has been produced from biogas upgrading.

Collecting CO_2 from the air through DAC requires heat at about 100 °C [45], which is classified as LTPH. This LTPH is used to heat the filter in the DAC unit to release CO_2. Part of this heat can be collected as DH afterwards.

6.1.4   Hybrid X-to-Liquid using Steam-Methane Reforming and Reverse Water-Gas Shift

Hybrid XtL using SMR can be also be accomplished using RWGS for the electricity-only production. Here, the syngas can be produced directly with inputs of hydrogen and CO_2 in the same process that adjusts the H_2:CO ratio of syngas. As with co-electrolysis, this pure electricity pathway for syngas production would result in an increased consumption of CO_2, and would likely mean that a DAC unit would be a necessity. Deciding the best solution between RWGS and co-electrolysis depends on many factors in the system, such as electricity prices, transmission capacity, CO_2 sources and more. This will be further investigated in Section *8 Simulation Results*. The plant configuration with RWGS seems more simple than co-electrolysis as the RWGS unit is already present when using SMR, and producing PtL would depend only on the choice of feed to the RWGS unit. Furthermore, the technology is more mature, and would likely be ready for deployment much earlier than 2050. However, the electricity consumption for RWGS is higher than for co-electrolysis, which could potentially prove challenging in the power system. A schematic of the plant configuration is shown in Figure 6.4.
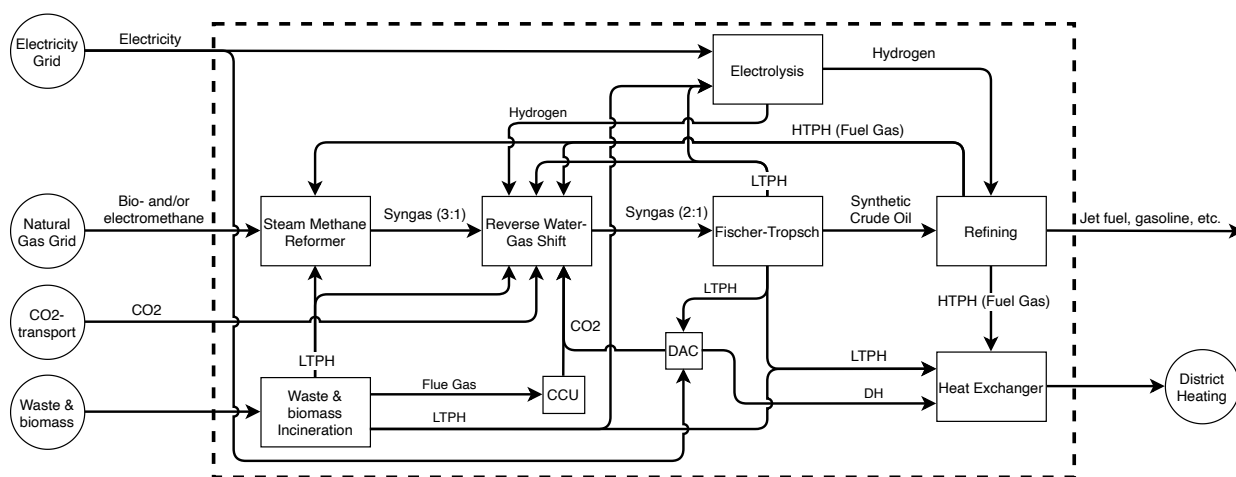
Figure 6.4: *Flow diagram of a XtL plant using SMR and co-electrolysis to produce syngas. The plant is assumed to be located near a waste incineration plant to utilize the LTPH and CO_2 from the flue gas. Using RWGS for direct syngas production can improve flexibility of the plant by continuously choosing the syngas production option with the lowest marginal cost, and might be a more simple solution than installing a separate unit in the form of co-electrolysis. However, the potential increased CO_2 requirement for RWGS could lead to the need for a DAC unit. It has been assumed that excess heat from the plant can only be used as DH through a heat exchanger.*

Many of the same synergies as the configuration described in Section *6.1.3 Hybrid X-to-Liquid using Steam-Methane Reforming and Co-electrolysis* can be found when using RWGS. The electrolysis unit would be significantly larger when using RWGS rather than co-electrolysis for PtL as it would be a primary input to the RWGS unit. It is worth considering that using this configuration would mean that RWGS would be the only unit requiring CO_2, increasing the simplicity in the plant configuration.

6.1.5   Hybrid X-to-Liquid using Partial Oxidation and Co-electrolysis

While locating GtL using POX near waste incineration proved to be only marginally advantageous, for the configuration using POX and co-electrolysis it will likely prove more desirable. Using CO_2 from the waste and biomass incineration plant, given that the waste is biogenic, is a suitable way of disposing CO_2 from the flue gas while putting the greenhouse gas to good use. A schematic of the plant configuration is shown in Figure 6.5.
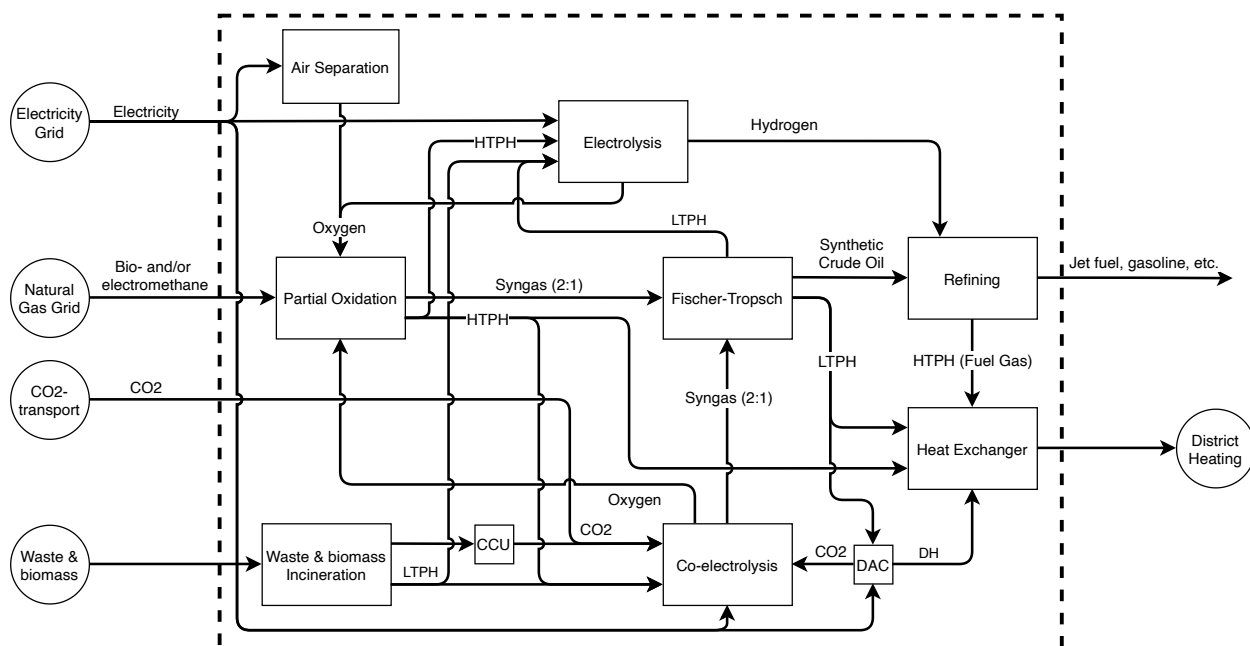
Figure 6.5: *Flow diagram of a XtL plant using POX and co-electrolysis to produce syngas. While GtL using POX was did not seem to provide any synergies with waste incineration, combining it with co-electrolysis unit will again provide an incentive to place it near existing waste incineration plants. The schematic for the hybrid plant using POX and co-electrolysis seems more simple than those using SMR. However, the required size of the ASU could prove challenging as the electrolysis unit would not produce significant amounts of oxygen due to the low demand for hydrogen.*

It is clear from the figure that, as with GtL in the configuration in Section *6.1.2 Gas-to-Liquid using Partial Oxidation*, using POX is schematically more simple. Using POX in a hybrid configuration with co-electrolysis could potentially reduce the need for an ASU since oxygen is a by-product to syngas in the co-electrolysis unit. Therefore, the ASU would likely be dependent on the syngas production from co-electrolysis. In general, the amount of excess heat produced in configurations with POX is significantly higher due to the fact that POX is an exothermic process and not endothermic as the SMR.

6.1.6   Hybrid X-to-Liquid using Partial Oxidation and Reverse Water-Gas Shift

This configuration is very similar to the one in Section *6.1.5 Hybrid X-to-Liquid using Partial Oxidation and Co-electrolysis*. However, in this configuration electrolysis is a more central technology to the liquid fuel production - as with *6.1.4 Hybrid X-to-Liquid using Steam-Methane Reforming and Reverse Water-Gas Shift* - since RWGS uses hydrogen as the primary input. A schematic of the plant configuration is shown in Figure 6.6.
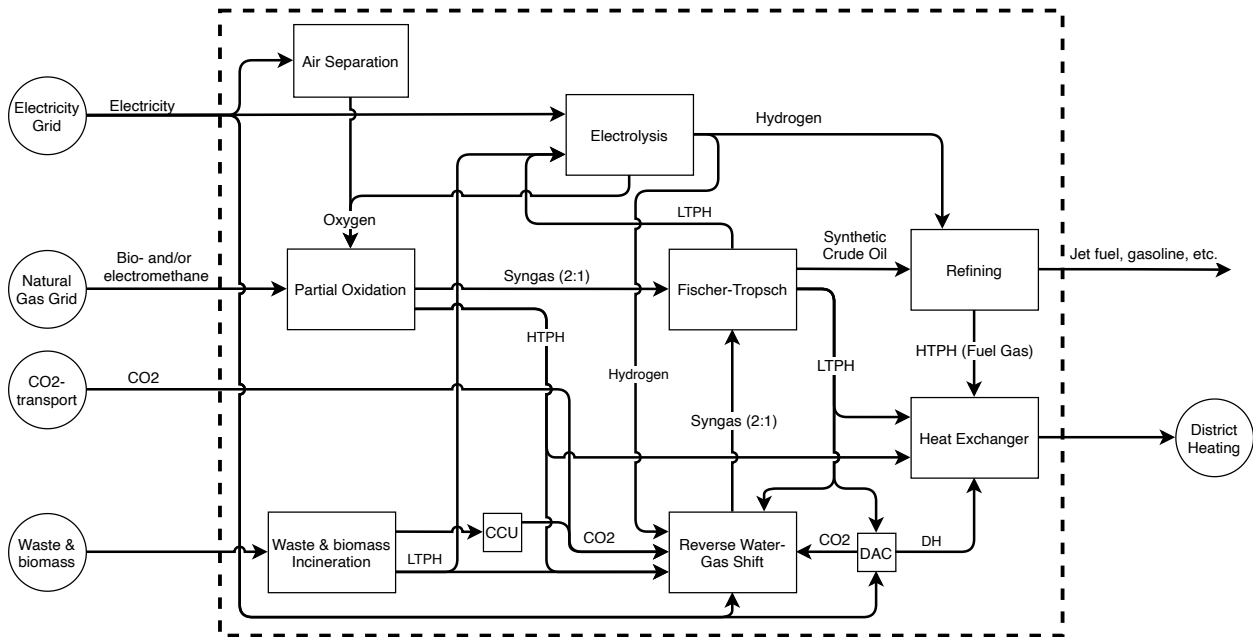
Figure 6.6: *Flow diagram of a XtL plant using POX and RWGS to produce syngas. Combining POX with RWGS instead of co-electrolysis could prove desirable, as the need for an ASU would be reduced due to the larger production of hydrogen, and thereby also the oxygen by-product from SOEC. Similar to the configuration with co-electrolysis, locating the fuel production near waste and biomass incineration would provide some synergies as the CO_2 would be required for PtL through RWGS.*

Combining POX, instead of SMR, with RWGS could prove to be the preferred PtL addition, since the SOEC unit produces oxygen as a by-product to hydrogen, as evident on Figure 6.6. This means that given the higher demand for hydrogen, due to the feed to RWGS, more excess oxygen would be produced, and the capacity of the potentially limiting unit, ASU, would be less required, and therefore, the investment might be difficult to justify. From the schematic, this configuration seems more desirable than that in Section *6.1.5 Hybrid X-to-Liquid using Partial Oxidation and Co-electrolysis* since the heat from POX could also be used in the RWGS.

6.1.7   Power-to-Liquid using Co-electrolysis

As GtL uses only gas, electricity-only production can be used isolated for fuel production, PtL. The fuels produced this way would be classified as pure electrofuels. Similar to GtL, using electricity as the only feed for syngas production could prove challenging in the energy system. Using only electricity would also mean that at times with very high electricity prices, the plant would be forced to purchase a feed that could potentially increase the price of jet fuel significantly if the production is not combined with storages. However, as described in Section *4.3 Market Prices*, the electricity price is relatively constant in most hours of the year. However, as with the hybrid configurations, the PtL would be able to produce at significantly lower costs in approximately 1500 hours during the year due to the low electricity prices. A schematic of the plant configuration is shown in Figure 6.7.
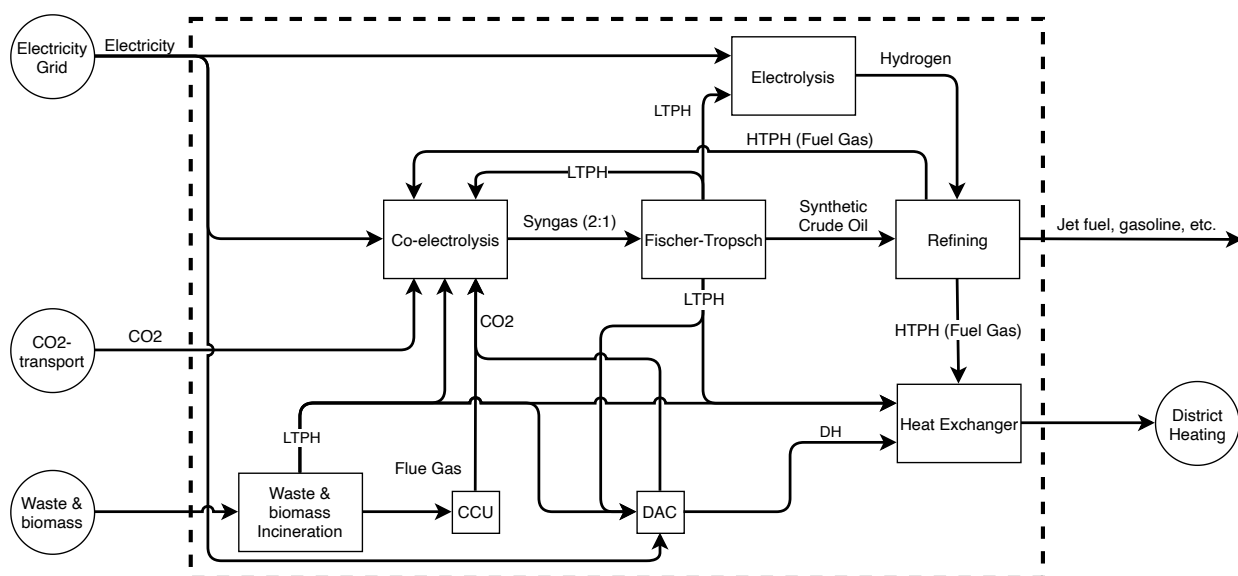
Figure 6.7: *Flow diagram of a PtL plant using co-electrolysis to produce syngas. It can be seen, that pure electrofuel provides a synergy with waste and biomass incineration, as co-electrolysis uses a significant amount of CO_2 and has an input of steam, which can be produced by using LTPH. As producing syngas only from co-electrolysis requires a significant amount of CO_2, a DAC unit will likely be required if the methane is produced from methanation, driving up the price of CO_2 and thereby the price of jet fuel as well.*

Producing pure electrofuels can be seen to still offer synergies when located near waste and biomass incineration, as shown on Figure 6.7. This is especially due to the feed of CO_2 that is required in co-electrolysis to produce syngas. Co-electrolysis requires a high amount of CO_2 and a DAC unit would likely be required as CO_2 from waste incineration is limited. Only the minimum capacity of electrolysis, used to close hydrocarbon chains from LTFT, is needed in this configuration as co-electrolysis produces syngas directly from CO_2 and electricity. Compared to using RWGS, co-electrolysis requires more CO_2 and process heat, but less electricity, due to the extra conversion step in electrolysis for RWGS.

6.1.8   Power-to-Liquid using Reverse Water-Gas Shift

As mentioned, RWGS is a more mature technology and evaluating the feasibility of RWGS compared to co-electrolysis is interesting. As mentioned in the previous section, RWGS requires more electricity due to the intermediate conversion step from electricity to hydrogen, in which there are losses that is not present when using co-electrolysis. However, the amount of CO_2 used is less. Similar to the pure electrofuel configuration with co-electrolysis, using RWGS provide synergies with waste and biomass incineration that are desirable to exploit.
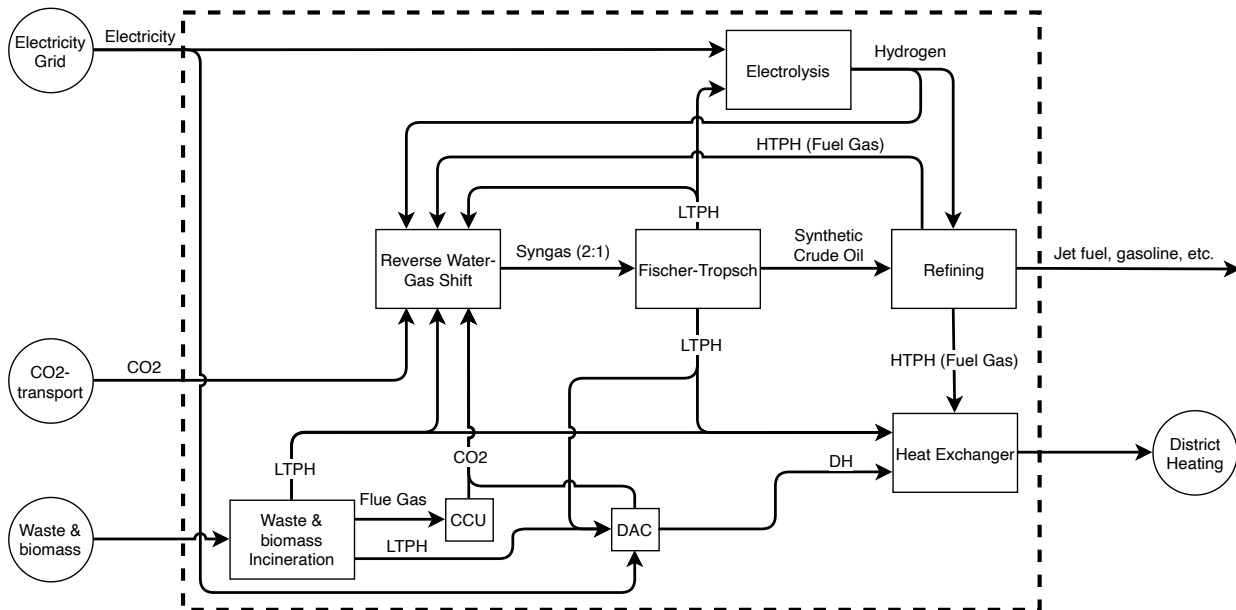
Figure 6.8: *Flow diagram of a PtL plant using RWGS to produce syngas. It can be seen, that pure electrofuel provides a synergy with waste incineration, as RWGS uses a significant amount of CO_2 and has an input of HTPH, which can be produced by boosting the temperature of the LTPH from incineration in a gas boiler. As producing syngas only from RWGS requires a significant amount of CO_2, a DAC unit will likely be required if the methane is produced from methanation, driving up the price of CO_2 - and thereby the price of jet fuel as well.*

While it might seem like the heat from waste incineration is used directly in the RWGS unit, the LTPH must be further heated in a gas boiler in order to reach the required temperature of approximately 700 °C, as mentioned in Section *5.5.3 Reverse Water-Gas Shift*. This gas boiler is relatively feasible as long as the gas used is the by-product of fuel gas from refining - when this is not available, either hydrogen or methane must be used, and that is generally significantly more expensive than fuel gas.

7   Modelling

This section will provide the reader with insights on how the scenarios for production of liquid fuels, presented in Section *6 Scenario Definition*, has been modelled in Sifre. The section will begin with a short description of the methodology behind the Sifre and ADAPT tools, followed by an overview of techniques used for modelling complex energy systems such as the ones in this study. Finally, the model is validated by a short analysis of its dynamics.

Appendix *C Sifre and ADAPT Input Data* contains technical data inputs for every conversion unit, storage and interconnection lines modelled in Sifre including economical data inputs modelled in ADAPT.

Appendix *D Sifre Modelling* contains figures illustrating the design of the model in Sifre.

7.1   Sifre and ADAPT Methodology

The modeling of the different pathways related to liquid fuel production by GtL and PtL, used in this study, and the investments required for them, are performed in Sifre and ADAPT. The tools Simulation of Flexible and Renewable Energy sources (Sifre) and Adaptive Planning Tool (ADAPT) are developed and used by Energinet [94] - both in relation to modeling and analysing the characteristics of the current energy system but also for developing system perspectives for the future.

7.1.1   Sifre

The goal of Sifre it to simulate the spot market behaviour of energy systems with a high degree of flexibility and integration. Sifre is based on the unit commitment (UC) problem. In short terms the UC problem provides a solution to the optimal production schedule for a set of generators so that the energy demands are met by minimization of the production costs or maximization of the production revenue. In Sifre the goal is to meet all demands by a minimization of the productions costs [95].

Originally, UC problems consider only the production side of electricity generation without considering the fuel consumption used for the production. The only goal is to match some energy demand by the generation of said energy. This is not ideal since some generators in the energy system use energy, produced by other generators, as fuel input. E.g. heat pumps use electricity to generate heat and electrolysis uses electricity to generate hydrogen. However, fuel consumption is an important result when simulating and analysing energy systems, and therefore the UC problem in Sifre is extended to account for fuel consumption [95]. An example of this is electricity production from wind power. A unit of electricity produced by a wind turbine is not necessarily used to satisfy some demand of electricity, but it can also be used as fuel input in e.g. an electrolysis unit, which is what differentiates the original UC problem with the extended version hardcoded in Sifre. Even though Sifre was originally developed for simulating heat and power production in Denmark, the formulation is not limited to handling energy types such as heat and electricity. Furthermore, it is not hardcoded to any specific energy system but is as generic simulation tool for energy systems.

Energy systems are modeled in Sifre using a set of building blocks: *areas*, *conversion units*, *storages* and *interconnection lines* [95].

Areas represent a geographical area and an energy type. E.g. an area might be syngas produced on a liquid fuel production site, which conversion units such as SMR or co-electrolysis produces to and which FT uses as a fuel input.

Conversion units convert energy by using fuel from one area and producing energy to another area. Conversion units can use an infinite number of fuel types but are limited to producing only two different energy types.

Storages are connected to areas and can store energy from those areas.

Interconnection lines can connect two areas of the same energy type. E.g. DK1 and DK2 can be connected by an interconnection line since they are two electricity areas, but DK1 can not be connected to the district heating area in Odense since they are different energy types.

One of the main results derived from a simulation in Sifre is the resulting area prices. The area price reflects the marginal cost of production without taking into account the operation cost per hour or the start-up cost. This means that if one more unit of energy is demanded in a given area the area price is set to the marginal cost of producing that unit of energy i.e. the marginal production cost of the marginal producer [95]. For electricity areas the derived area price corresponds to the clearing price of the electricity spot market.

7.1.2   ADAPT

ADAPT is a tool integrated as a module in Sifre, and can be used to evaluate socioeconomic investments in an energy system. ADAPT is used by setting an interval of investment opportunities with associated capital expenditure (CAPEX), operational expenditure (OPEX), socioeconomic discount rate and investment lifetime. The tool then evaluates the different investment opportunities by comparing the total socioeconomic net system cost resulting from making the different investments. ADAPT then selects the optimum investment capacity of every technology, that is inserted into the ADAPT module, based on a minimization of the total socioeconomic net system cost, thereby maximizing the socioeconomic surplus, defined as the sum of the consumer surplus, producer surplus and congestion revenue [96]. In ADAPT the change in total socioeconomic net system cost by a given change in the energy system is calculated as the change in socioeconomic surplus with an opposite sign.

In this way ADAPT can be used to determine specific investment capacities of conversion units, storages and interconnection lines etc., which it is also used for in this study.

7.2   Modelling of Liquid Fuel Production

In this study, all the different plant configurations for the production of liquid fuels, presented in Section *6 Scenario Definition*, have been modelled, including different variations of the pathways, with the purpose of answering the research questions stated in Section *2.1 Research Questions*. Furthermore, every plant configuration has been modelled with two different upstream systems for methane production. Both an

upstream system where methane is produced through methanation of CO_2 in the biogas, and an upstream system where methane is produced through conventional biogas upgrading is modelled. This gives 16 different simulations since are eight different liquid fuel production plant configurations. It should be mentioned, that even though the two PtL configurations described in Section *6.1.7 Power-to-Liquid using Co-electrolysis* and *6.1.8 Power-to-Liquid using Reverse Water-Gas Shift* seemingly does not depend on the upstream system for methane production, some methane might still be consumed downstream for the production of LTPH, which could affect the resulting jet fuel price. Therefore, those two plant configurations have also been modelled into the two different upstream systems for methane production. A list of these 16 main scenarios modelled and simulated in this study can be seen in Table 7.1. As can be seen, the main elements that differentiate the scenarios are the syngas production units on the liquid fuel production site, and the method for upstream methane production. The table does not include every scenario simulated in Sifre, but only the main scenarios. The scenarios related to each sub-analyses or sensitivity analysis will be described together with a presentation of their respective results in Section *8 Simulation Results* and *9 Sensitivity Analysis.*

Table 7.1: *This table lists the main differences between all main scenarios modelled and simulated in this study. The table does not include every scenario modelled.*

Code	Syngas prod. unit 1	Syngas prod. unit 2	Upstream methane prod.
1.1	SMR	-	Methanation
1.2	POX	-	Methanation
1.3	SMR	Co-electrolysis	Methanation
1.4	SMR	RWGS	Methanation
1.5	POX	Co-electrolysis	Methanation
1.6	POX	RWGS	Methanation
1.7	Co-electrolysis	-	Methanation
1.8	RWGS	-	Methanation
2.1	SMR	-	Biogas Upgrading
2.2	POX	-	Biogas Upgrading
2.3	SMR	Co-electrolysis	Biogas Upgrading
2.4	SMR	RWGS	Biogas Upgrading
2.5	POX	Co-electrolysis	Biogas Upgrading
2.6	POX	RWGS	Biogas Upgrading
2.7	Co-electrolysis	-	Biogas Upgrading
2.8	RWGS	-	Biogas Upgrading

Appendix *C Sifre and ADAPT Input Data* contains technical data inputs for every conversion unit, storage and interconnection lines modelled in Sifre including economical data inputs modelled in ADAPT, while Appendix *D Sifre Modelling* contains figures illustrating the design of the Sifre model. A brief overview containing energy inputs and outputs, total efficiencies, CAPEX and OPEX of some of the conversion units can be seen in Table 7.2. All economical data are given per primary output since Sifre and ADAPT are

hardcoded for this input. General for every investment opportunity modelled in ADAPT is a socioeconomic discount rate of 4% [97]. All prices have been adjusted for inflation by an average inflation rate of 2% and is given in a 2020 price level. All prices are converted to EUR by using the exchange rates 7.5 DKK/EUR and 0.91 USD/EUR.

Table 7.2: *The table gives an overview of the input and output energies, total efficiencies, CAPEX and OPEX of the different conversion units used in Sifre and ADAPT. The mass streams of CO_2 and Oxygen have been converted to energy by their arbitrary heat heating value as explained in Section 7.2.1 Mass Streams. Energy balances and economical data for all technologies can be seen in Appendix B Technology Data including relevant references.*

	Inputs [% energy of total input]	Outputs [% energy of total input]	Total efficiency [total output /total input]	CAPEX [M€/MW]	OPEX [€/MW/y]
Biogas Upgrading	Biogas = 95.93% Electricity = 4.07%	Methane = 95.45% CO2 = 1.89%	97.35%	0.487	12,255
Methanation	Biogas = 53.79% Hydrogen = 46.21%	Methane = 89.80% LTPH = 9.20%	99.00%	0.713	25,394
Electrolysis (SOEC)	Electricity = 85.00% LTPH = 15.00%	Hydrogen = 93.00% Oxygen = 5.21% LTPH = 1.50%	99.71%	0.475	14,246
Co-electrolysis (SOEC)	Electricity = 73.93% LTPH = 21.71% CO2 = 4.36%	Syngas (2:1) = 80.46% Oxygen = 4.52%	84.98%	0.475	14,246
Steam Methane Reforming (SMR)	Methane = 81.28% HTPH = 18.72%	Syngas (3:1) = 85.45%	85.45%	0.064	3,210
Partial Oxidation (POX)	Methane = 99.05% Oxygen = 0.95%	Syngas (2:1) = 90.23% HTPH = 3.78%	94.01%	0.039	1,926
Air Separation Unit (ASU)	Electricity = 100.00%	Oxygen = 19.00%	19.00%	3.449	103,465
Reverse Water-Gas Shift 1 (RWGS 1)	Syngas (3:1) = 97.57% HTPH = 1.18% CO2 = 1.26%	Syngas (2:1) = 97.50%	97.50%	0.006	298
Reverse Water-Gas Shift 2 (RWGS 2)	Hydrogen = 91.77% HTPH = 3.98% CO2 = 4.24%	Syngas (2:1) = 82.36%	82.36%	0.006	298
Low-temperature Fischer Tropsch + Refining (LTFT + Refining)	Syngas (2:1) = 95.98% Hydrogen = 4.02%	Jet fuel = 53.07% Gasoline = 15.35% Fuel gas = 4.51% Ethanol = 0.21% LTPH = 22.04%	95.20%	0.309	15,475
Direct Air Capture (DAC)	LTPH = 87.50% Electricity = 12.50%	CO2 = 13.89% DH = 25.00%	38.89%	2.859	57,185
Biomass Boiler	Wood chips = 100%	LTPH = 88.00% CO2 = 7.08%	95.08%	0.346	26,056
Waste Boiler	Waste = 100%	LTPH = 88.00% CO2 = 7.14%	95.14%	1.358	54,542

Modelling of complex energy systems can lead to a series of complexities which are typically a result of limitations in the modelling tool used. Sifre also has limitations which have been worked around in some way or another. The following of this section will explain how these limitations have been handled and give insight to general modelling techniques used in the Fuel Production Model.

7.2.1   Mass Streams

Since Sifre is a tool used for simulating energy systems it naturally deals with energy streams. However, when modelling the production of liquid fuels, mass streams are essential. This is because CO_2 and oxygen, which act as fuel inputs and products from several conversion units, do not contain energy. Therefore, these substances have been given an arbitrary heating value in order to be able to model them. The arbitrary heating value have been assumed to be 1 GJ/tonne (0.001 PJ/kt) for both CO_2 and oxygen. A consequence of the this is the fact that economical figures for units that deals with CO_2 and oxygen might appear significantly higher or lower compared to other units. They will, however, reflect the real costs associated with units.

7.2.2   Splitting Conversion Units

Another element in the Fuel Production Model in Sifre is a consequence of the limitation that conversion units can only handle two production outputs. This limitation is explained by the original purpose of the tool i.e. modelling of heat and power systems where a conversion unit would not have more than two production outputs such as a CHP producing electricity and heat. This creates a challenge for two of the conversion units modelled in this study: *LTFT + Refining* and *Electrolysis (SOEC)*. LTFT + Refining has five different outputs: Jet fuel, gasoline, fuel gas, ethanol and LTPH, where Electrolysis (SOEC) has three: Hydrogen, oxygen and LTPH. This challenge has been handled by creating areas which are mixtures of products and conversion units that splits these mixtures. These splitting units are merely conversion units used as a modeling technique and there are no costs or production limitations associated with them. An overview of the series of splitting processes applied for the conversion units LTFT + Refining and Electrolysis (SOEC) can be seen in Figure 7.1 and 7.2.
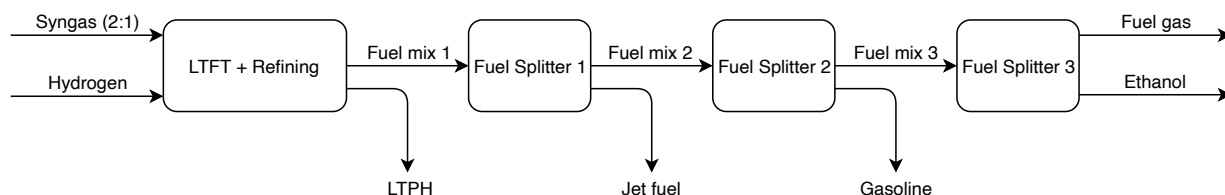
Figure 7.1: *The figure shows how the primary output of the LTFT + Refining conversion unit is split into jet fuel, gasoline, fuel gas and ethanol in a series of fuel splitting processes. Syngas (2:1) refers to syngas with an* H_2*:CO ratio of 2:1.*

As can be seen in Figure 7.1, the primary output from LTFT + Refining is Fuel mix 1, which is a mixture of jet fuel, gasoline, fuel gas and ethanol. The secondary ouput is LTPH. Fuel mix 1 is split to jet fuel and fuel mix 2 in Fuel Splitter 1, which primary output is Fuel mix 2 and secondary output is jet fuel. Fuel mix 2 is

then split in Fuel Splitter 2 and so on. As can be seen in Figure 7.2, the same modelling technique is used for splitting Gas mix 1, which is a mixture of hydrogen and oxygen and is the primary output of Electrolysis (SOEC). However, only one splitting unit is required for this process.
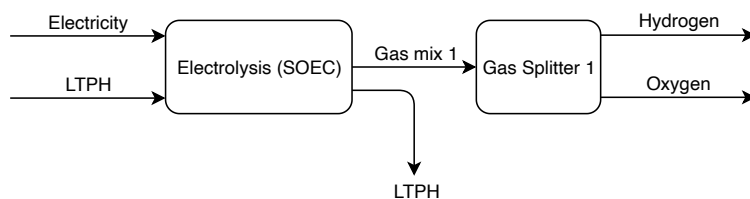
Figure 7.2: *The figure shows how the primary output of the electrolysis (SOEC) conversion unit is split into hydrogen and oxygen in a gas splitter.*

7.2.3   Under- and Overproduction

As mentioned in Section *7.1.1 Sifre* the goal of the UC problem, which Sifre is based on, is to meet all demands of all areas in any given hour at the lowest possible production cost. If Sifre is not able to exactly meet the demand, creating either under- or overproduction, it is penalized by a cost per MWh of under- or overproduction. The cost of underproduction is set to 3000 EUR/MWh while the cost of overproduction is set to 500 EUR/MWh. These costs represent the price caps on the day-ahead market at Nord Pool [98].

7.2.4   Markets and Sinks

Since several of the secondary outputs from the conversion units modelled are not demanded or used as a fuel input in other conversion units, sinks and markets have been modelled. A market is essentially an area with a market price > 0 EUR/GJ whereas a sink is an area with a market price = 0 EUR/GJ. Sinks and markets can absorb as much energy or mass as required. E.g. gasoline, which is an indirect secondary output from the LTFT + Refining conversion unit, is transferred, by an interconnection line, to the Gasoline market where the market price is 37.7 EUR/GJ, recalling from Section *4.3 Market Prices*. Oxygen, which is an indirect secondary output from the Electrolysis (SOEC) conversion unit is transferred to the Oxygen sink where the price is 0.0 EUR/GJ.

7.2.5   Reverse Water-Gas Shift Units

Recalling from Section *5.5.3 Reverse Water-Gas Shift*, the RWGS can be operated both for adjusting the syngas ratio and for producing syngas where it is operated with an excess of hydrogen. When studying the hybrid XtL plant configurations where the plant has the two options for producing syngas - either by SMR followed by RWGS for adjustment of the syngas ratio, and producing syngas purely by the RWGS unit, it is essential to know in which hours the syngas it produced by which units. Therefore, the RWGS reaction have been modelled in two different units, where the stoichiometric relationship between the inputs and outputs are the exact same, but the fuel inputs are different. The difference between the two conversion units can be seen in Figure 7.3.
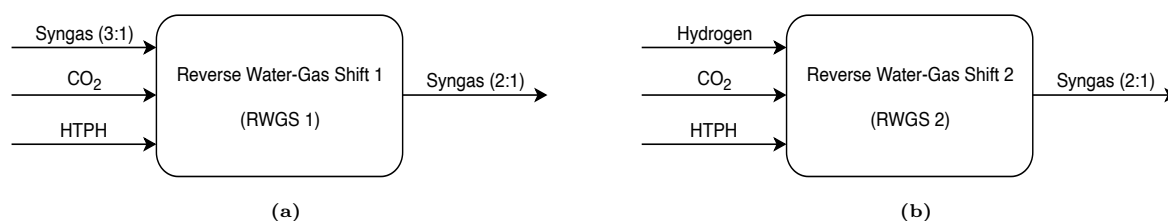
Figure 7.3: *The figure shows the two different types of RWGS units modelled in the Fuel Production Model. The RWGS 1 conversion unit, seen in (a), converts syngas with a H_2:CO ratio of 3:1, CO_2 and HTPH to syngas with a H_2:CO ratio of 2:1. The RWGS 2 conversion unit, seen in (b), also has CO_2 and HTPH as fuel inputs, but uses pure hydrogen in an excessive amount to produce syngas with a H_2:CO ratio of 2:1.*

It can be seen that the RWGS 1 conversion unit is used for adjusting the syngas' H_2:CO ratio from 3:1 to 2:1. In the RWGS 2 conversion unit syngas with a H_2:CO ratio of 2:1 is produced by excess of hydrogen input.

7.2.6 The Hierarchy of Heat

In the Fuel Production Model a hierarchy of heat has been modelled. This means, that within the same production site heat with a higher temperature level can always be transferred to heat with a lower temperature level but not the other way around. The underlying assumption is, that the production site contains heat exchangers with a 100% efficiency which can be used for this purpose. Figure 7.4 shows how the hierarchy of heat works within the Fuel Production Model.
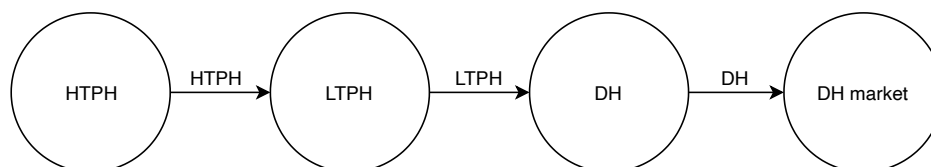
Figure 7.4: *The figure shows the hierarchy of heat modelled within each production site. Heat can always be transferred to a heating area where the temperature is lower, but not the other way around.*

It can be seen how heat in the HTPH heating area can be transferred, by an interconnection line, to the LTPH heating area and so on. The arrows indicate the direction of the hierarchy of heat. The final heating area is the DH market, which is an external market representing DH networks in Denmark, where excess heat from liquid fuel production can be sold at the price levels stated in Section *4.3.2 Excess Heat*.

7.2.7 Production Sites

As indicated in the explanation of the hierarchy of heat the Fuel Production Model contains different production sites. With the purpose of keeping the model somewhat simplistic only two different production sites have been modelled - *onsite* and *offsite*. Generally speaking, offsite resembles all decentral production sites. These sites include conversion units such as Biogas Upgrading, Electrolysis (SOEC), Gas Splitter 1, Methanation.

Onsite resembles all central production sites with some liquid fuel production plant. These sites include conversion units such as SMR, Co-electrolysis (SOEC), ASU, DAC etc. Some units might appear both offsite and onsite, such as the LTPH Electric Boiler. The technical specifications and economical figures are, however, the exact same at both sites.

Among other reasons, onsite and offsite have been split up in the Fuel Production Model in order to keep track of investments in the conversion units that appear on either sites. Furthermore, its purpose is to underline the differences appearing from designing the decentral offsite part of the synthetic fuel value chain in different ways. E.g. the methane price which the central liquid fuel production, located onsite in the model, is highly dependent on has different price levels depending on which production method is used offsite. The resulting methane price from methanation is somewhat different from that of conventional biogas upgrading. Also, in order to model some transport of energy or mass between a decentral and central location, two different sites that can be connected by an interconnection line must be modeled.

7.2.8 CO_2 Production and Consumption

One part of the Fuel Production Model has been modelled in greater detail than the rest of the model i.e. the production and consumption of CO_2. This has been done in order to keep track of exactly how much CO_2 that are produced from each CO_2 producing unit in any given hour, and to keep track of how much each CO_2 producing unit contribute to supplying the different CO_2 demands.

There are four different sources of CO_2 and two general demands. The first general demand of CO_2 is related to liquid fuel production. Specific conversion units related to this general demand is Co-electrolysis (SOEC), RWGS 1 and RWGS 2. All these units consume CO_2 in order to produce Syngas (2:1), which is needed for the production of liquid fuels. The other general demand is the demand for CO_2 reduction which essentially is a demand for a negative CO_2 emission as a consequence of the sectors that can not lower their CO_2 emission to a net zero emission level e.g. the agricultural sector. This demand can be satisfied by capturing and storing biogenic CO_2 as described in Section *4.2 Demands and Constraints*. However, since some methods have a limited potential for capturing biogenic CO_2, DAC will likely have a role in the future Danish energy system, and can potentially be one of the measures utilized in order to reach a net zero emission energy system by 2050. The demand for CO_2 reduction will be further investigated in Section *9.3 Demand for Negative CO_2 Emission*.

In Figure 7.5 it can be seen how the production and consumption of CO_2 have been modelled in the Fuel Production Model. The production side of CO_2 consists of Biogas Upgrading, DAC and CC of either waste and biomass incineration. In order to utilize CO_2 from waste and biomass incineration it must be captured from the flue gas. As mentioned in Section *4.2.5 Carbon Capture* the cost of CC is assumed to be 45.3 EUR/tonne CO_2 as estimated by the Global CCS Institute.

However, as can be seen in the figure, three of the CO_2 production methods also have the possibility of emitting the biogenic CO_2 produced, which is modelled by transferring the CO_2 to the CO_2 sink with an associated price of 0.0 EUR/tonne. This might be relevant since the production of CO_2 is secondary productions for all three methods. Biogas upgrading primarily produces methane while the waste and
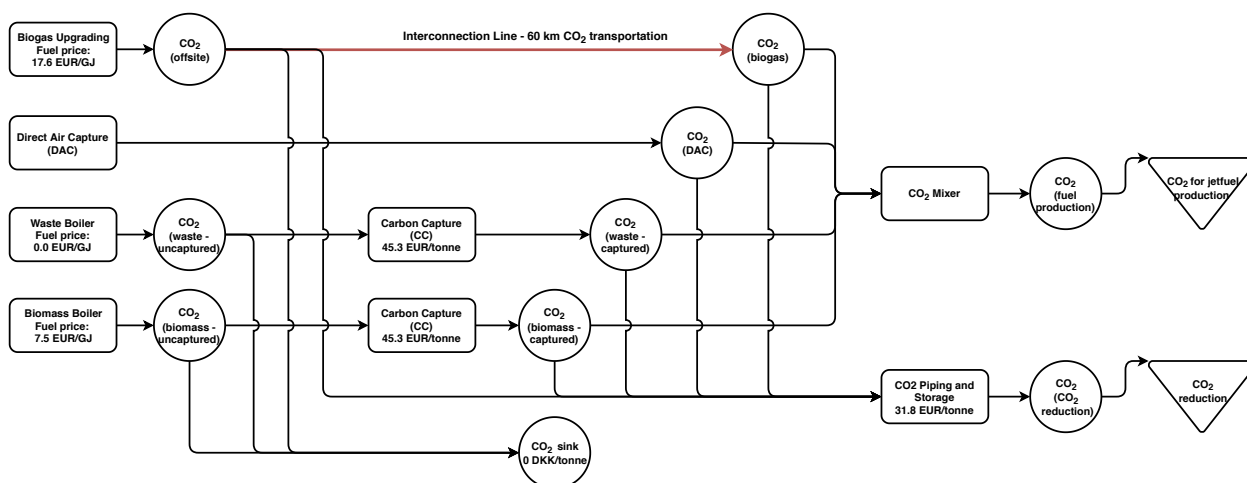
Figure 7.5: *The figure shows how the production and consumption of CO_2 have been modelled in the Fuel Production Model. Rectangles = Conversion units, Circles = Areas, Red lines = Interconnection lines, Triangles = Demands.*

biomass boilers produces LTPH as a primary production. In some cases it might be feasible to produce the primary product, i.e. biogas or LTPH, but not utilize the secondary product, i.e. CO_2, since the secondary product requires further costs in order to finally be sold to some CO_2 demanding unit. Biogas Upgrading requires an interconnection line for CO_2 between the decentral biogas production site and the central liquid fuel production site, and the waste and biomass boilers require the cost of capturing the carbon in a CC unit. As can be seen in Figure 7.5, the resulting CO_2 areas from biogas, DAC or CC of either waste or biomass boilers have the two aforementioned demands to satisfy. CO_2 used for liquid fuel production needs no further processing costs in order to satisfy the demand, but in order to satisfy the demand negative CO_2 emission, the biogenic CO_2 must be piped away from the production site to the storage site and then be stored, which has a combined cost of 31.8 EUR/tonne CO_2.

7.3 Model Validation and Dynamics

The final part of this section provides a brief insight into some dynamics of the model, and how these dynamics can be used to validate the model behaviour.

The first model behaviour that has been evaluated is the operation behaviour of the XtL plant configurations. More specifically it is the fuel production configuration explained in Section *6.1.5 Hybrid X-to-Liquid using Partial Oxidation and Co-electrolysis.* This plant configuration has two possible methods for syngas production. It can either produce syngas in a POX unit or in a co-electrolysis unit. The whole idea behind the hybrid plant configuration is the ability to optimize the production according to external prices such as the electricity price. This means that one should expect the co-electrolysis unit to produce the syngas required for LTFT in hours where the electricity price is below a certain point, and the POX unit to produce when the electricity price is above a certain point, since the methane price is less hourly dependent than the electricity price. Figure 7.6 shows the production of syngas from the POX and co-electrolysis units, described in the liquid fuel production plant configuration in Section *6.1.5 Hybrid X-to-Liquid using Partial Oxidation and Co-electrolysis* during a randomly chosen week.
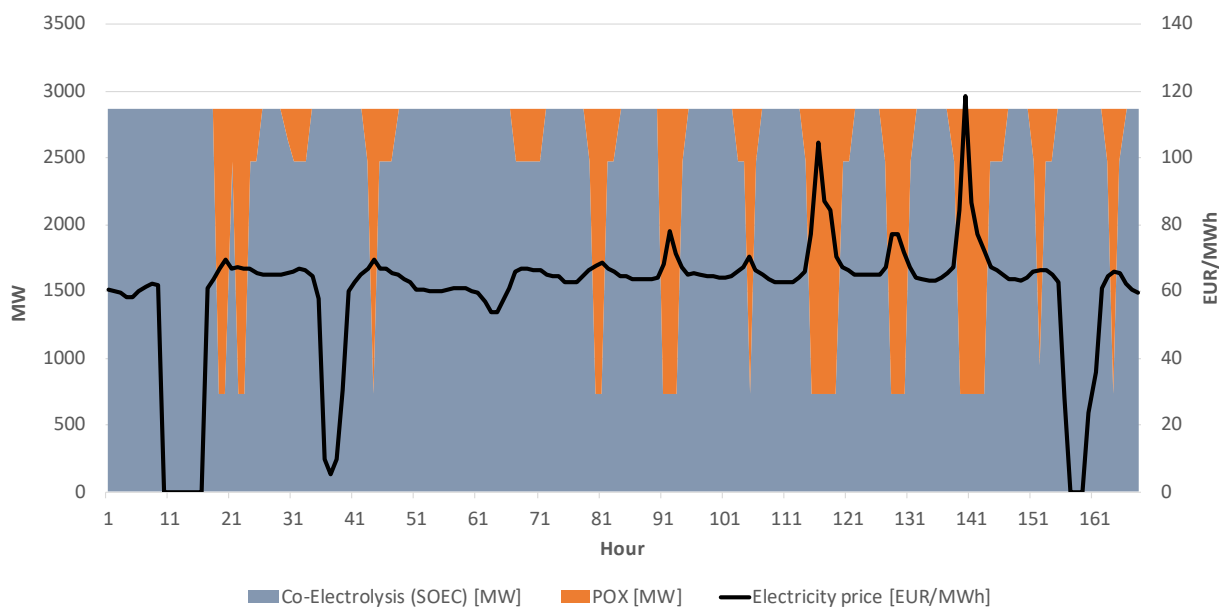
Figure 7.6: *The figure shows how the production of syngas from the POX and co-electrolysis (SOEC) units, described in the liquid fuel production plant configuration in Section 6.1.5 Hybrid X-to-Liquid using Partial Oxidation and Co-electrolysis, depends on the electricity price.*

As can be seen, the total production of syngas is constant at 2865 MW throughout the week, but the conversion unit supplying the demand for syngas changes. The main producer is the co-electrolysis unit but it can clearly be seen, that in hours where the electricity price peaks, or only tends to be somewhat higher than normal, the POX unit starts producing syngas. However, at no point does the POX unit supply the entire demand of syngas. Its maximum production during an hour is 2138 MW in which the co-electrolysis produces the remaining 727 MW. Furthermore, it can be seen that in no hour where the electricity price is lower than normal does the POX unit produce syngas. This example of model dynamics confirms that the hybrid fuel production plant configuration works as intended.

Another element of the Fuel Production Model is storages. The general intention of storages is to inject into them in hours where the cost of production is at such a level that it is economically feasible to produce more than what is demanded for the purpose of storage injection. Then in other hours where the cost of production is higher, energy or mass can be extracted in order to still supply the demand. Figure 7.7 shows how the operation of the DAC conversion unit and the CO_2 storage is dependent on the electricity price during the same week as in Figure 7.6. As can be seen, the DAC unit produces CO_2 at 15.8 MW, equivalent to 56.9 tonne CO_2 per hour, for several hours during the week. The production of 15.8 MW is a result of the arbitrary heating value of CO_2 of 1 MJ/kg.

At this production of 15.8 MW the DAC unit only produces CO_2 with the purpose of supplying to either the co-electrolysis or RWGS 2 unit. However, in some hours where the electricity price tends to be lower, the DAC unit increases the production to 21.2 MW, equivalent to 76.3 tonne CO_2 per hour, and injects CO_2 into the CO_2 storage. It can also be seen, that in hours where the electricity price tends to be higher than

normal, the DAC unit shuts down the production all together and in these hours the entire demand of CO_2 is supplied by the CO_2 storage.

From these examples of dependencies in the model and many other validation tests, the Fuel Production Model has been proved to function as intended. All simulation results will therefore we presented and discussed in the following sections.
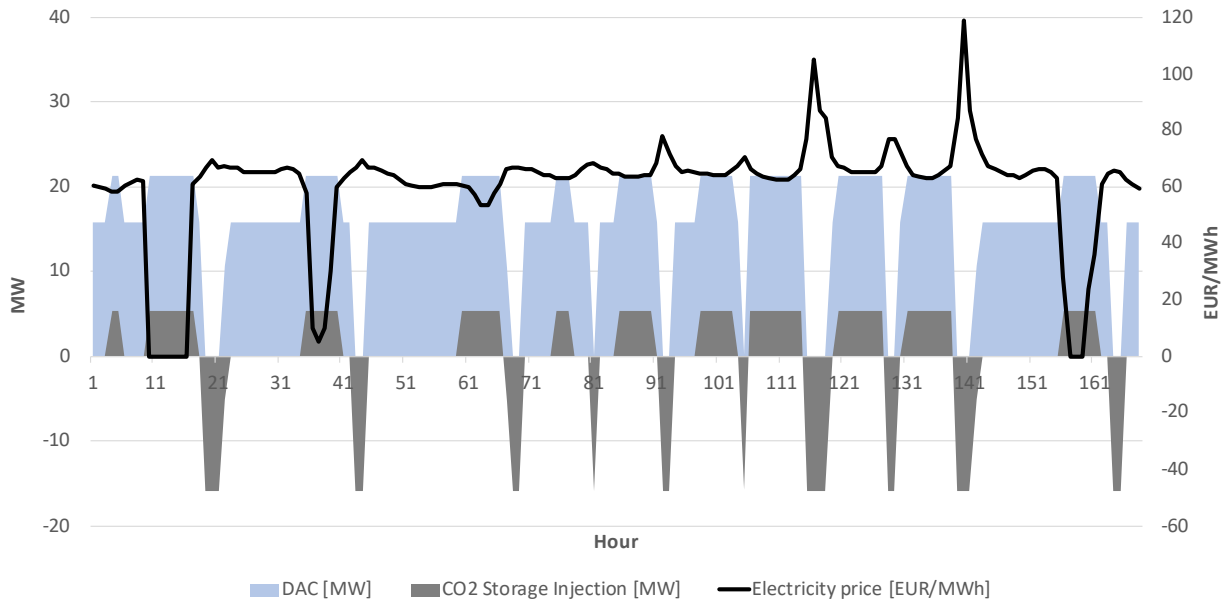
Figure 7.7: *The figure shows how the production of CO_2 from DAC and the injection of the CO_2 storage is dependent on the electricity price. The production of the DAC unit and the injection of the CO_2 storage are products of the arbitrary heating value of CO_2. Negative values for injection of the CO_2 storage indicates extraction.*

8   Simulation Results

In this section, the results for the 16 main scenarios that was described in the previous section, will be presented and analyzed. Recalling from Section *6 Scenario Definition*, the eight different plant configurations are modelled with each of the two different upstream methane production; methanation and biogas upgrading. The analysis will cover some of the main results from the simulations that provide key insight in the prospects of the future Danish jet fuel production, as the total amount of information from such a model is massive and is not suitable to present in full. Furthermore, the simulation of the case study of Funen will be analyzed in order to investigate potential pitfalls regarding electricity network limitations. Some results from the main analysis has given rise to sub-analyses in which the influence of changing key parameters has been analyzed, and these will be further described and analyzed in Section *9 Sensitivity Analysis*.

As mentioned in Section *7.1.1 Sifre* the goal of Sifre is to find the optimal production schedule, for all conversion units, that meets all demands by a minimization of the production costs. A consequence of this form of optimization is that, when making of change in the system, that change affects the jet fuel price in way that would not be expected. The reason for this is because it is not a minimization of the jet fuel that is the overall optimization objective. However, optimization with the objective of minimizing the production cost of a single conversion unit, e.g. the production cost of the LTFT unit and thereby minimizing the jet fuel price, in a vast energy system containing several conversion units, is not a viable method for a socioeconomic optimization. By doing this, several pitfalls might be evident for some of the conversion unit that are part of the total energy system. This risk of pitfalls for some conversion units are not nearly as severe when optimizing the operation schedule with the objective of minimizing the operation cost, of every conversion unit in the entire energy system all at once, in order to find the most socioeconomic optimal solution.

8.1   Main Scenarios

The significant results to analyze in this section has been found to be; resulting jet fuel prices, aggregated required production capacities, influence of upstream methane production on the methane price, and lastly, an in-depth analysis of the production patterns that make some configurations more attractive than others.

Recalling from *4.2.3 Biogas Potential*, the total potential biogas resource that is available for jet fuel production has been estimated to be around 50 PJ. However, producing 50 PJ of jet fuel exclusively from a methane feedstock would result in a consumption of a minimum of 51 PJ when methane is produced by methanation and 86 PJ when it is produced from biogas upgrading, meaning that the demand for jet fuel can not exclusively be produced from GtL. While the total demand can not be produced from GtL, some can, and therefore, in order to investigate the possible jet fuel price from GtL plants, the demand has been lowered to 25 PJ for scenarios with only GtL.

8.1.1   Jet Fuel Prices

As described in Section *7.1 Sifre and ADAPT Methodology*, the jet fuel price that is reported by Sifre is calculated based on the true marginal production cost, ignoring operation and startup costs. This means that the jet fuel price that is being calculated refers to the output from Fuel Splitter 1, in which the mixture of products from LTFT is being split into jet fuel and Fuel Mix 2, containing gasoline, ethanol, etc., as shown in Figure 7.1. The jet fuel price therefore becomes the result of the economic balance of "purchasing" Fuel Mix 1 and "selling" Fuel Mix 2 divided by the amount of jet fuel that is produced. This calculation is shown in Equation 8.1.

$$C_{\text{Jet Fuel}} = \frac{E_{\text{Fuel Mix 1}} \cdot C_{\text{Fuel Mix 1}} - E_{\text{Fuel Mix 2}} \cdot C_{\text{Fuel Mix 2}}}{E_{\text{Jet Fuel}}} \tag{8.1}$$

Here, *E* refers to the amount of energy of input that is "purchased" in MWh and *C* is the cost per MWh. This calculation is then done for every hour of 2050, after which the average of all hours are reported as the jet fuel price.

Figure 8.1 shows the average jet fuel prices for all main scenarios described in Section *7.2 Modelling of Liquid Fuel Production*. Here, at every plant configuration for upstream methane from methanation is shown next to the the same configuration with upstream methane from biogas upgrading.

	SMR	POX	SMR / Co-electrolysis	SMR / RWGS	POX / Co-electrolysis	POX / RWGS	Co-electrolysis	RWGS
	GTL		Hybrid				Electrofuel	
Methanation	32,7	33,3	32,5	34,0	32,1	33,6	31,8	33,9
Biogas Upgrading	26,9	25,2	29,9	33,5	30,2	33,7	31,9	33,7
Low Jet Fuel Price	10,0	10,0	10,0	10,0	10,0	10,0	10,0	10,0
High Jet Fuel Price	20,0	20,0	20,0	20,0	20,0	20,0	20,0	20,0
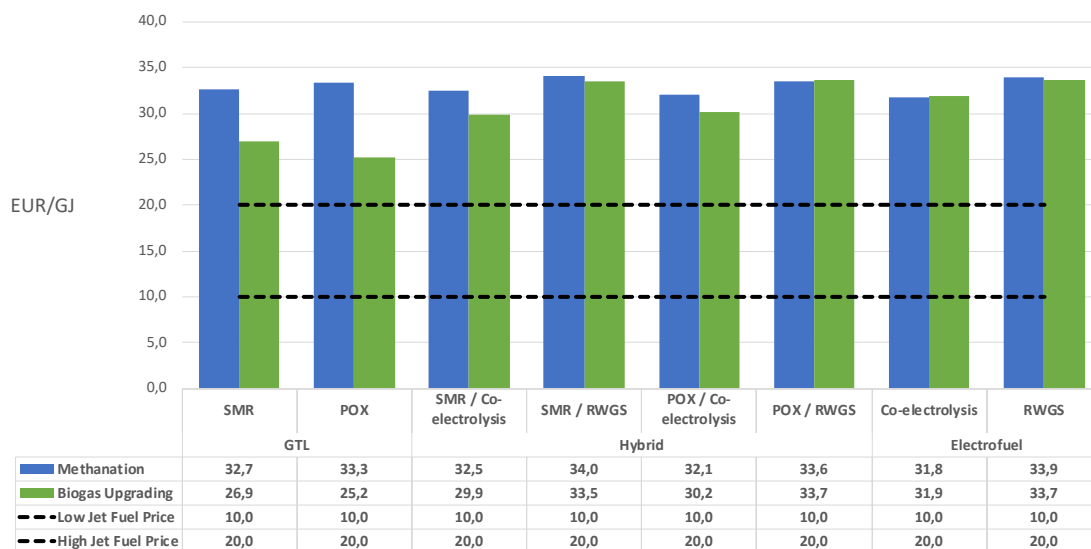
Figure 8.1: *Illustration of the resulting jet fuel prices from scenarios 1.1 to 2.8. The blue columns depict the jet fuel prices of all configurations with upstream methane from methanation, while the green columns show for upstream methane from biogas upgrading. It is clear that the jet fuel prices using methane from biogas upgrading results in generally lower prices. The scenario yielding the lowest jet fuel price is 2.2, which is POX using methane from biogas upgrading at a price of 25.2 EUR/GJ. The highest price can be seen for scenario 1.4, which is the hybrid configuration with SMR and RWGS at a price of 34 EUR/GJ. The dashed lines illustrate an estimate of the lower and higher fossil jet fuel prices of 2019, similar to [9].*

From the figure, it is clear that the lowest jet fuel prices are obtained when methane is produced from biogas upgrading. The tendency is naturally more notable in the GtL configurations as the jet fuel production is forced to consume methane regardless of the cost, while hybrid configurations can shift towards PtL if the production cost is favorable, which it inevitably will become sometimes when the methane is produced from methanation.

It can be seen that the plant configuration that yields the lowest jet fuel price is the one in scenario *2.2 POX*, which is exclusively GtL from POX, at 25.2 EUR/GJ, while the configuration yielding the highest is the one in scenario *1.4 SMR / RWGS* that use a combination of SMR and RWGS, resulting in a jet fuel price at 34 EUR/GJ. While it might seem sub-optimal for the hybrid scenarios to actually invest in both GtL and PtL, Sifre optimizes for the lowest possible production cost, as described in the introduction to this section, and therefore, while the jet fuel price might be slightly higher, the overall production cost is lower.

The tendencies in the resulting jet fuel prices generally follow those from *Nordic GTL* [9]. Here, it was found that the lowest jet fuel price would result from a biomethane feedstock, the highest price from a bio- and electromethane feedstock and pure electrofuel in between, while more similar to that of bio- and electromethane feedstock. Figure 8.2 shows a selection of the jet fuel prices from Figure 8.1.
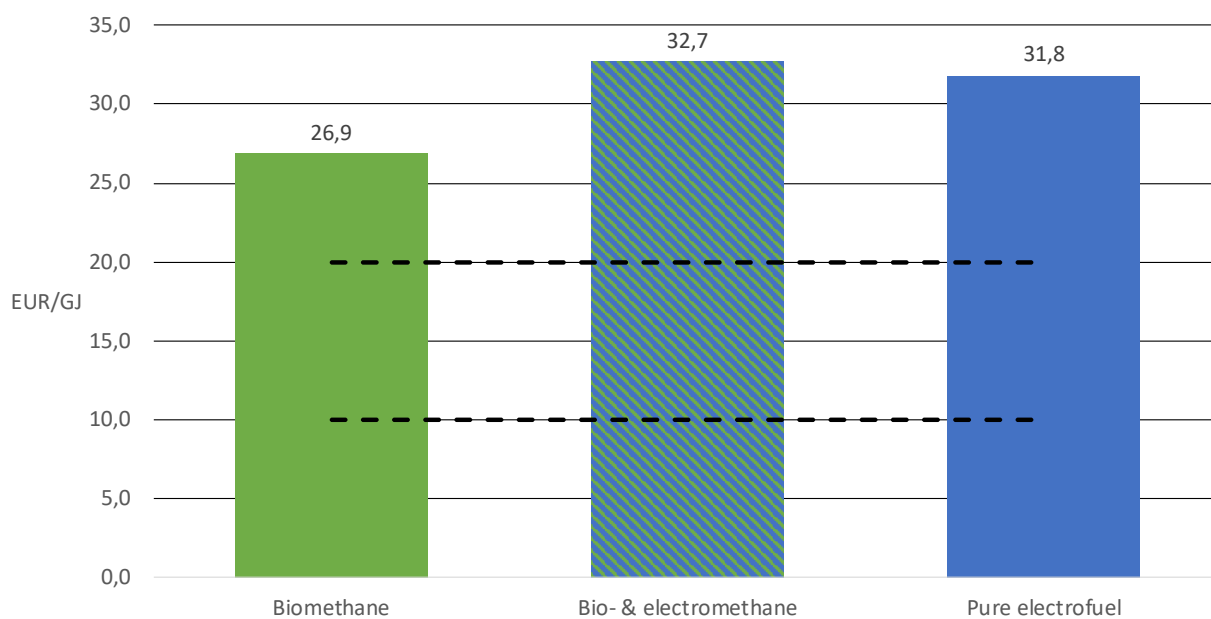
Figure 8.2: *Comparison of the jet fuel prices from feedstock of biogas upgrading (biomethane), methanation (bio- and electromethane) and pure electrofuel. This shows that the tendency of the feedstock's influence on the jet fuel price in this study fits with the discoveries of [9].*

In the figure, biomethane depicts methane feedstock from biogas upgrading in scenario *1.1 SMR* with a plant configuration of exclusively SMR, bio- and electromethane in scenario *1.2 SMR* too exclusively with SMR, while pure electrofuel in scenario *1.7 Co-electrolysis* is exclusively from co-electrolysis. What constitute the prices are similar to the breakdown from [9] in which it was found that the majority of the cost

originates from the purchase of methane or electricity, and naturally, much of the added cost for bio- and electromethane is due to an increased consumption of electricity from producing hydrogen for methanation. The results also showed that the investment costs are relatively insignificant compared to especially the cost of electricity and methane. The cost breakdown will not be of further focus as the results show the same tendencies as [9].

Lastly, based on the resulting jet fuel prices, the same conclusion as [9] and [5] can be made - the sustainable jet fuel price are likely to be higher than that of fossil jet fuel, given the framework conditions for the main scenarios used in this study. Similar to [9], the sustainable jet fuel prices are around double those of their fossil counterparts, as evident from the black dashed lines that depict an estimate of the lower and higher jet fuel prices of 2019.

8.1.2   Hybrid Configurations

As described earlier, producing jet fuel from only GtL or PtL inherently give rise to some potential challenges regarding grid constraints or access to resources, and therefore, the hybrid configurations could prove more viable overall, despite the slightly higher resulting jet fuel prices compared to jet fuel prices from GtL from biogas upgrading. However, recalling from the introduction of the results for the main scenarios, GtL using methane from biogas upgrading can not exclusively satisfy the entire Danish demand and therefore, it is not a possible solution. In this sub-section, it will be investigated how the plant would operate in a hybrid configuration and to which extent the flexibility of having two separate feedstock is utilized. Figure 8.3 shows the yearly distribution between syngas production from GtL and PtL out of the total fixed syngas production.
The figure shows that the flexibility of optimizing between GtL and PtL is significantly more notable with methane from biogas upgrading, naturally due to the lower price of methane. When methane is produced from biogas upgrading, it can be seen that the production of syngas is split almost equally between GtL and PtL, ranging from 50% when using POX to 55-60% when using SMR. However, when upstream methane originates from methanation, for most scenarios, PtL outperforms in terms of production cost in majority of the year. This tendency can be seen for all configurations except those in scenarios *1.6* and *2.6 POX / RWGS*, in which GtL has a higher production proportion with upstream methane from methanation than from biogas upgrading.

The thing that makes synergies very cost-effective, also makes the price mechanisms more difficult to investigate as many different elements are intertwined and co-dependent. The reason why scenarios *1.6* and *2.6 POX / RWGS* do not follow the same tendency as the other scenarios can likely be found by a combination of several aspects that combined lead to RWGS becoming the most feasible production unit in fewer hours in scenario *1.6 POX / RWGS* even though methane is produced by methanation. It can be seen by both the POX and RWGS being close to producing half of the total syngas that their average hourly costs are very close - more so than either of the two GtL technologies is to co-electrolysis. Therefore, since the costs are
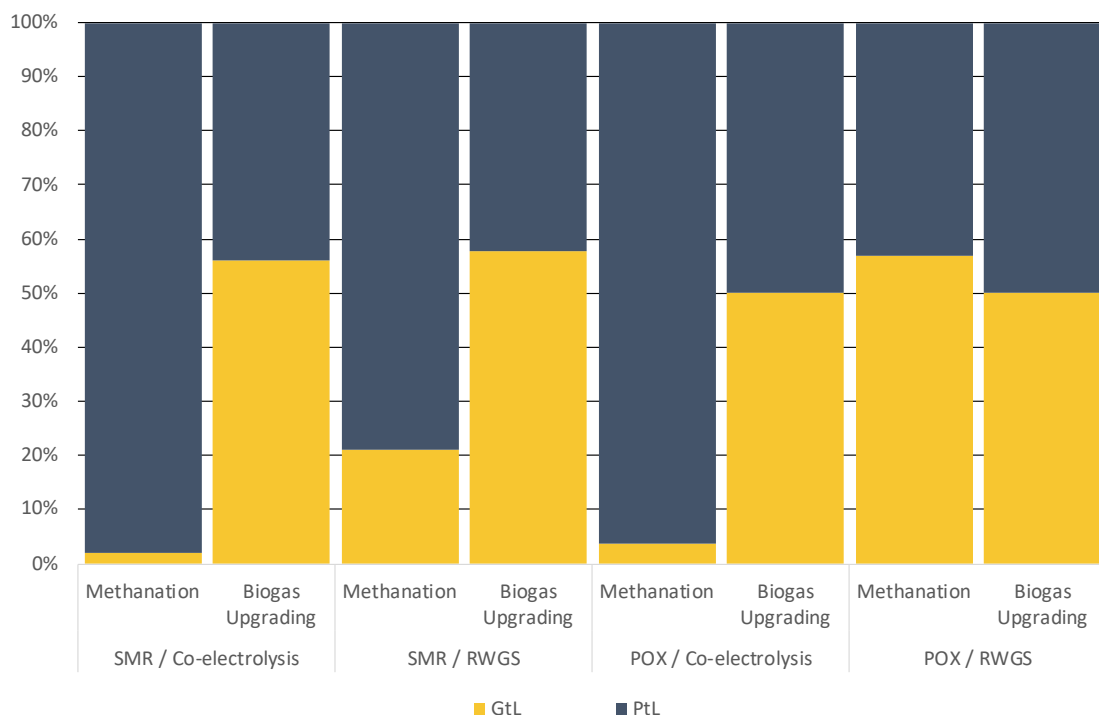
Figure 8.3: *Yearly proportion of the total syngas produced from GtL and PtL for all hybrid scenarios. Common for most configurations is that GtL is outperformed economically most of the time when methane is produced from methanation, as can especially be seen in scenarios 1.1 SMR, 2.1 SMR and 1.2 POX.*

very close, small changes can have larger effects on the production curve of the syngas units. Within these two scenarios, the reason why RWGS produces more syngas, in the scenario with biogas upgrading compared to the scenario with methanation, even though the average cost of methane is lower, is likely because of the less costly CO_2 that is produced as a by-product in biogas upgrading. This means that the RWGS becomes less costly by a larger margin than POX do when methane becomes less costly. In other words, the cost of purchasing CO_2 is reduced more than the cost for the resulting methane. In scenario *1.6*, the average yearly methane price is 23.59 EUR/GJ while it is 22.58 EUR/GJ in scenario *2.6 POX / RWGS*. For CO_2, the price gap is significantly more notable, with the average price in scenario *1.6 POX / RWGS* being 54.16 EUR/tonne while it is only 49.26 EUR/tonne in scenario *2.6 POX / RWGS*.

While Figure 8.3 shows the aggregated proportions for a whole year, it is interesting to investigate the mechanism that makes the production shift between GtL and PtL on an hourly resolution. Similar to Figure 7.7, Figure 8.4 shows the hourly production of syngas between GtL and PtL for a randomly selected week. Here, scenario *2.3 SMR / Co-electrolysis* is shown with the electricity price, and it is clear that the co-electrolysis unit reacts to fluctuations in the electricity price within a margin of approximately 1000 MW. In the figure, it can be seen that there is a clear threshold electricity price, at 59.60 EUR/MWh, to which the co-electrolysis reacts. This can especially be seen in hours 38 and 168 in which the electricity price just falls below this threshold, and therefore, the co-electrolysis increases its production, albeit slightly. Furthermore, in the period from hour 18-22 and again in the period from 60-64, the electricity price is just above the threshold,

meaning that it does not increase its production in which syngas production from co-electrolysis starts to increase.

Interestingly, it can be seen that neither unit ever produces the entire syngas demand. This is due to the fact that when methane is produced for SMR, CO_2 is produced as well, and the most cost-efficient way of utilizing this CO_2 is to produce syngas by co-electrolysis. This means that the two units are co-dependent to some extent, in which the hourly proportion is a result of the optimization in Sifre.
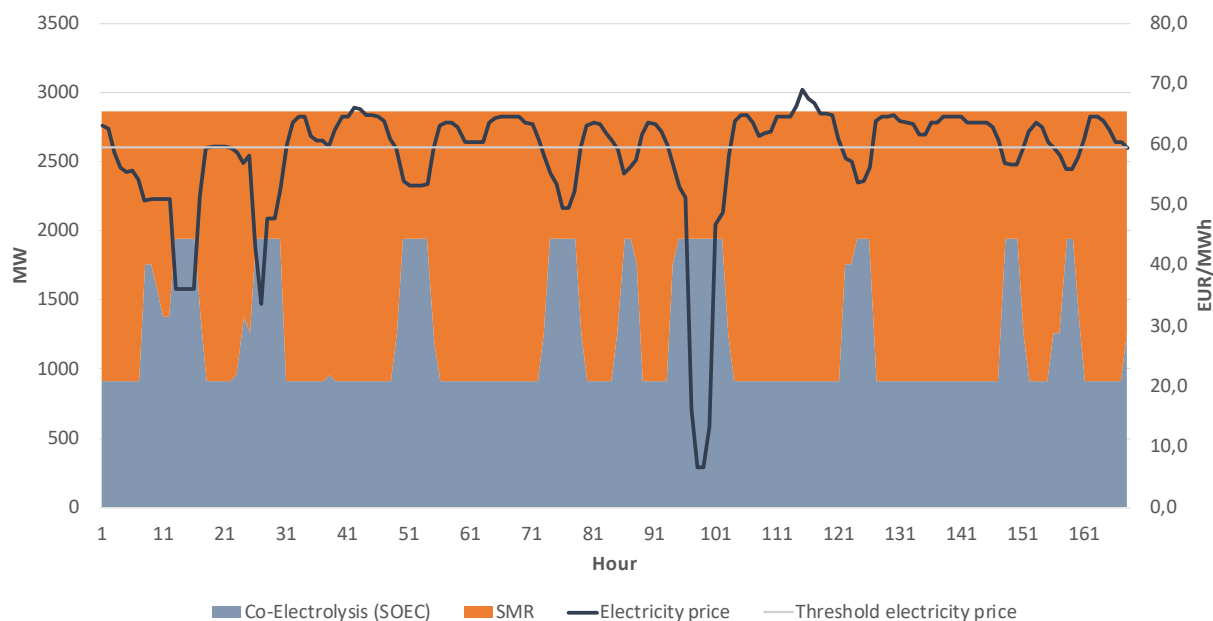
Figure 8.4: *Production of syngas from co-electrolysis and SMR in scenario 2.3 SMR / Co-electrolysis during a randomly selected week. The black line shows the electricity price. It can be seen that the syngas production from co-electrolysis is directly dependent on the electricity price.*

8.1.3   Upstream Methane Production

The future of methane is, as many aspects within the field of liquid fuel production, still uncertain. The source of methane in the future is difficult to fully and accurately predict, and therefore, as mentioned in Section *7.2 Modelling of Liquid Fuel Production*, all plant configurations have been simulated with upstream methane production from both biogas upgrading and methanation, which is meant to represent a lower and higher estimate of the resulting methane price, respectively. The price of methane is relevant to investigate as it can be a determining factor for the value of hybrid configurations and therefore, the resulting jet fuel price. Figure 8.5 shows the average hourly methane and jet fuel price across all scenarios, split into scenarios with upstream methane from biogas upgrading and methanation. The figure shows, to some extent, a dependency of the the jet fuel price to the methane price. Naturally, this dependency is more notable in some scenarios than others, e.g. scenarios with only PtL. As mentioned, simulating all scenarios with methane from both biogas upgrading and methanation is done in order to provide a range of methane prices that are likely to be seen in 2050. It is close to impossible to accurately predict the specific price of an element that is

dependent on many different factors, and methane is no different. Instead of trying to figure out the exact price of methane in the future, it is usually very helpful to provide a likely lower and higher limit. In 2050, the methane price is likely produced from both methanation and biogas, and therefore, will fall somewhere within the price of methane from biogas upgrading and methanation.
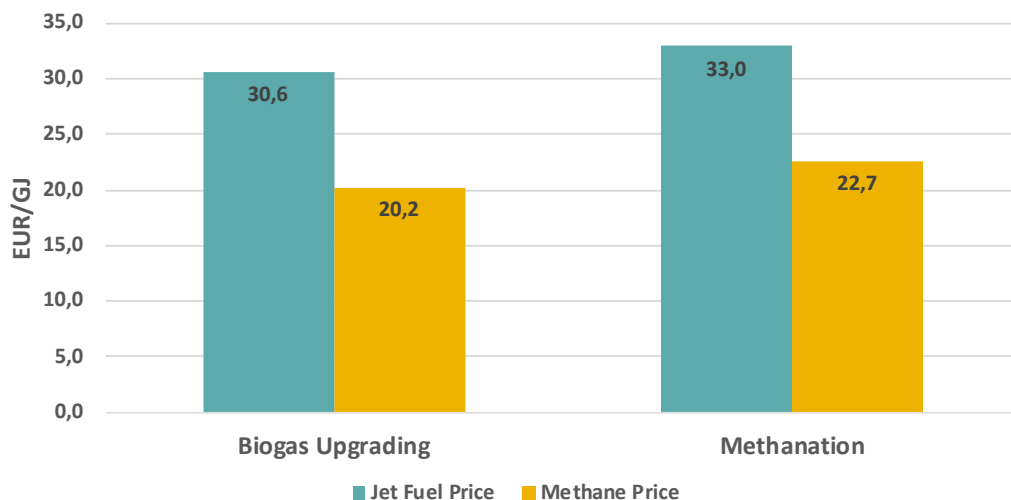
Figure 8.5: *Average price of methane for all hours across every scenario for both upstream methane from biogas upgrading and methanation. Next to the methane price, the corresponding jet fuel price are shown, and it can be seen that the jet fuel price and the methane price is to some extent dependent.*

8.1.4 CO_2 as a Commodity

The cost of acquiring CO_2 can change from source to source. The production cost of CO_2 from different sources is an interesting analysis, albeit difficult, that can help understand the variations in jet fuel prices based on the required output from LTFT. This study has included three different viable sources of CO_2 for fuel production; CO_2 from biogas upgrading, CC of waste and biomass incineration and DAC. Some methods have been further investigated with changing parameters such as the method and distance of transportation and cost of heat, in order to provide clearer insight in how they compare. This analysis has resulted in a merit order curve showing the cost of "producing" and acquiring CO_2 along with the potential amount from that source with the mentioned parameters - much like a merit supply curve for electricity production. The merit curve for CO_2 production can be seen in Figure 8.6. In order to investigate all production methods of CO_2, each method has been isolated in the same scenario, meaning that the framework parameters are constant, but only one method is used at a time, forcing sources to satisfy the demand individually.

The figure shows that by some margin, CO_2 from biogas upgrading has the lowest acquisition cost for the fuel production plant, due to the fact that CO_2 has been assumed to be a by-product of methane production and therefore, methane would fully cover the expenses for electricity and biogas. This means that the production of CO_2 would not be imposed any of the production costs, and the price of this CO_2 for the fuel production plant would be equal to the cost of transporting it from the biogas plant to the fuel production plant. Here, it can be seen that, while the costs are all relatively low, piping seems to be the favorable option between
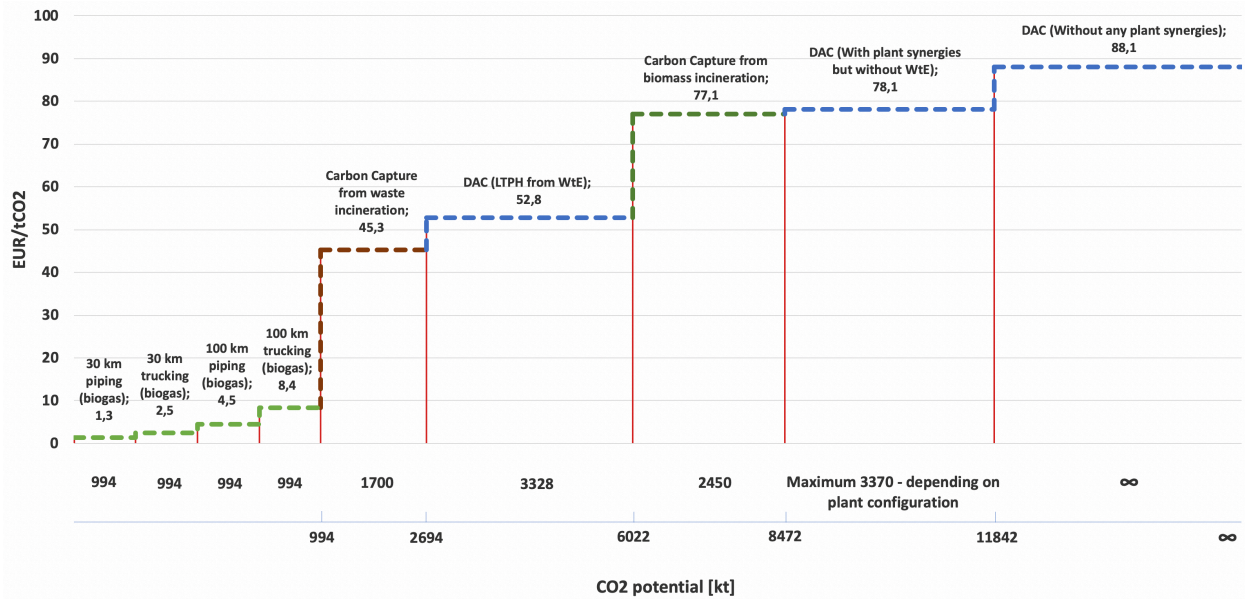
Figure 8.6: *Merit order of the cost of "producing" and acquiring CO_2 a the fuel production plant. The y-axis shows the cost in EUR per tonne, while the top x-axis shows the amount of CO_2 that can be acquired from each measure, and the bottom x-axis shows the accumulated amount of CO_2 that can be acquired. Since some CO_2, e.g. from biogas, refers to the same amount, this can naturally only be acquired once. The lowest costs with a significant margin can be seen to be CO_2 from biogas upgrading. The cost of producing this CO_2 has been assumed to be zero, and the total cost of the CO_2 then becomes equal to the transportation cost from the biogas plant to the fuel production plant. Values are given for yearly averages, and could paint a different picture in specific hours.*

that and trucking. CO_2 pipes does require an initial capital cost, as most infrastructure does, but the long life time of 50 years helps lower the CAPEX due to the long depreciation period. The cost of CO_2 piping has been based on [69], [70], [99]. The amount of CO_2 that could potentially come from biogas upgrading has been identified as 994 kt, given that all biogas is upgraded rather than methanated.

Capturing CO_2 from waste incineration results in a lower cost per tonne of CO_2 than from biomass incineration even though the actual capture cost has been assumed the same at a rate of 45.3 EUR/tonne. This can be explained by the fact that waste does not have a fuel cost, meaning that it can produce LTPH at a cost that is always lower than what can be sold for DH, and therefore, it will always be price-taker. As the DH price is always higher than the cost of producing LTPH, the production costs of waste incineration are always covered by the revenue from heat, and the plant would have no expenses to be covered by the revenue from CO_2, resulting in a CO_2 price equal to the capture costs.

Contrary to waste, biomass has a fuel cost, which means that it is far more dependent on the price of DH. For biomass incineration, considerably higher costs are connected to the production of heat

Due to the price of biomass, the production cost of biomass incineration is considerably higher than for waste incineration, and therefore, more dependent on the price of DH. The production cost of biomass incineration can not be covered only from revenue of heat, and therefore, some expenses must be covered by a revenue from CO_2, increasing the price of CO_2. This means that the price of CO_2 from biomass incineration is

highest in the summer period, since less costs are covered by the sale of heat during that period.

Interestingly, the cost of DAC can actually be lowered to such a degree that it can compete with capturing CO_2 from biomass incineration. DAC uses a significant amount of heat, and most of its production cost is due to this heat. If heat at a lower cost can be used, which is the case with excess heat from either waste incineration or fuel production processes, the production costs can be reduced significantly. Furthermore, while much heat is consumed when heating the filter to release CO_2, some heat can be sold if the unit is located near DH areas. This means that locating DAC at fuel production plants, provides a sum of synergies that could potentially lower the cost per produced tonne CO_2 from 88.1 to 52.8 EUR/tonne, which is fairly close to the capture cost from waste incineration. It should be noted that the values in Figure 8.6 are given for the yearly average, which means that some hours could show a different merit order, e.g. if the electricity price is very high, every form of DAC would be more costly than either form of carbon capture from flue gas. While the low cost of LTPH helps reduce the general cost of the DAC unit, it can be seen in Figure 7.7 that it is quite dependent on the electricity price as well.

8.1.5   Required Production Capacities

In the following, the resulting invested capacities from the ADAPT optimization will be presented. The capacities presented are of the key units that are required to produce 50 PJ of jet fuel. As mentioned in Section *5.6 Fischer-Tropsch*, it has been assumed that the LTFT unit has a constant production all hours of the year. Since the LTFT unit does not have any options for flexible production, ADAPT invests in the same capacity of LTFT in every scenario, except the GtL scenarios, in order to deliver the demand of 50 PJ jet fuel. The total output capacity of the LTFT and refining is approximately 2200 MW, of which approximately 1600 MW is jet fuel production. In the GtL scenarios these respective capacities are half since the jet fuel demand is set to 25 PJ.

Table 8.1 shows a part of the collection of the economically optimized invested capacities from ADAPT for all main scenarios, while Appendix *E Collection of ADAPT results* contains the extended collection of all invested capacities in ADAPT for all main scenarios. It can be seen that there is a significant difference in what ADAPT finds economically feasible for each scenario. Naturally, methanation and biogas upgrading are both a direct result of the invested capacities in either SMR or POX, which can be seen by almost no capacity being invested in, in scenarios *1.7 Co-electrolysis*, *1.8 RWGS*, *2.7 Co-electrolysis* and *2.8 RWGS* - except for a small capacity that produces methane for a HTPH boiler. Recalling from the previous section, it was found that in scenarios *1.3 SMR / Co-electrolysis*, *1.4 SMR / RWGS* and *1.5 POX / Co-electrolysis*, a very little proportion of the syngas during a year was produced from a methane feedstock, with the highest being in scenario *1.3 SMR / RWGS* at approximately 20%. This can also be seen in invested capacities in methanation for these scenarios, in which a maximum of only 119 MW was found feasible for all jet fuel production. This further underlines the favorable economics of PtL when methane is produced from methanation.

In general, it can be seen that the investments in electrolysis is directly dependent on methanation and RWGS in scenarios that contain this as well, evident in the capacities in scenarios *1.3 SMR / Co-electrolysis* and *1.4 SMR / RWGS*. Electrolysis can be found in every scenario, since it is used in the refining stage of the LTFT synthesis to close hydrocarbon chains. The capacity needed for this can be seen to be 127-128 MW of electrolysis - small differences can be explained by utilization of storages. While large capacities of methanation demands a higher capacity of electrolysis, it can be seen that it is scenarios with RWGS that ramp up the investments in electrolysis.

In the table, it can be seen that, in order to continuously produce syngas for 50 PJ of jet fuel production, a total of 2865 MW capacity is needed. Interestingly, in most hybrid configurations, investing in both GtL and PtL does not substitute capacity - rather, in these scenarios, the total syngas production capacities reach a maximum of 5400 MW, which can be seen in scenario *2.6 POX / RWGS*. This suggests that savings in the flexibility of the hybrid configuration largely outweigh the total investment costs. Therefore, over-investing does not seem to be a significant issue with fuel production facilities, and providing the flexibility between GtL and PtL is generally feasible. This also makes the plants more versatile to fluctuations in the surrounding prices.

For all scenarios, 665 MW of waste incineration is invested in, which is corresponding to the total amount of waste in 2050. The reason why this capacity is invested in regardless of the scenario and configuration is due to the production of LTPH at a very low cost, since the fuel has been assumed to be 0 EUR/GJ. Therefore, even if the scenario does not require LTPH, this heat can be used for DH. In scenarios with PtL and GtL from SMR, waste would also be the least costly method of acquiring CO_2, after biogas, which proved significantly less costly than any other source, as described in Section *8.1.4 CO₂ as a Commodity*. Furthermore, it can be seen that the investment decisions in CO_2 production for all scenarios follow what was found in the aforementioned section, in which DAC could outperform CO_2 capture from biomass, given that the LTPH can be provided at a low cost and the DH output can be sold. DAC outperforming CCU from biomass is evident as there is only capacity for biomass incineration in scenarios that have a capacity of approximately 95 MW for DAC.

95 MW of DAC corresponds to an hourly capture capacity of just under 350 tonne of CO_2, totalling almost 3000 kt per year, given constant maximum production. In Figure 8.6, it can be seen that the maximum capture from DAC using low-cost LTPH is around 3300 kt - however, some of the low-cost LTPH is used in processes producing syngas.

Table 8.1: *Collection of invested capacities for all main scenarios in MW. Capacity for LTFT has not been included since it constant for all scenarios (except for scenarios with GtL exclusively. This capacity is 2200 MW, in which 1600 MW is jet fuel.*

Scenario	Biogas Upgrading	Methanation	Electrolysis	SMR	POX	RWGS	Co-electrolysis	DAC	Waste Incine.	Biomass Incine.
#					[MW]					
1.1 (25 PJ jet fuel)	-	1370	920	1432	-	-	-	-	665	-
1.2 (25 PJ jet fuel)	-	1580	921		1432	-	-	-	665	-
1.3	-	57	160	139	-	-	2864	95	665	56
1.4	-	57	3577	900	-	2667	-	75	665	-
1.5	-	119	191	-	409	-	2865	94	665	40
1.6	-	1807	4342	-	2544	2749	-	23	665	-
1.7	-	2	128	-	-	-	2865	95	665	69
1.8	-	2	3497	-	-	2865	-	94	665	-
2.1 (25 PJ jet fuel)	1420	-	176	1433	-	-	-	-	665	-
2.2 (25 PJ jet fuel)	1576	-	63	-	1433	-	-	-	665	-
2.3	1590	-	127	1957	-	-	1939	8	665	-
2.4	1590	-	2935	2421	-	2389	-	4	665	-
2.5	1590	-	127	-	2514	-	2865	-	665	-
2.6	1590	-	3496	-	2544	2865	-		665	-
2.7	2	-	127	-	-	-	2865	96	665	69
2.8	2	-	3496	-	-	2866	-	94	665	-

8.2   Case Study of Funen

Key results from the case study of Funen will include an analysis of the strain that is posed on the electricity network as a result of producing 5 PJ of jet fuel in Odense. Different configurations for liquid fuel production will be analyzed in the case study, but first the framework for the case study will be presented.

8.2.1   Case Study Framework

Most of the framework regarding the Funen Case Study remains the same as for the main scenarios. There are, however, some deviations. The framework conditions of the main results do not contain production and consumption of electricity. When analysing the network strain, that the production of liquid fuels pose, it is important to include this since some strain might be mitigated through local production of electricity, where a local demand of electricity would only increase potential strain. Therefore, both the electricity production from renewable energy, wind and solar, and the consumption of electricity will be simulated as a framework for the Funen Case Study.

The demand of electricity on Funen in 2050 is based on the LUP framework as explained in Section *4.1 LUP Framework*. The demand is divided into five sectors: *Classic*, *Transport*, *Large data centers*, *Individual heat* and *Process heat*. The transport category includes electrification of both rail and light transportation. The consumption of electricity for light transportation is based on an assumption of approximately 300,000 electric vehicles on Funen in the LUP framework. The classic electricity consumption includes consumption for electric appliances, lighting etc. in both households, service and industry. Both the consumptions for individual heat and process heat are results of electrification in households and the industry respectively. Here, the gas consumption for heat is displaced by a consumption of electricity for heat pumps and electric boilers. The hourly electricity consumption of the five sectors on Funen in 2050 can be seen in Figure 8.7, and the yearly consumptions can be seen in Table 8.2.

Table 8.2: *The table shows the yearly electricity consumption on Funen in 2050 divided into Classic, Transport, Large data centers, Individual heat and Process heat.*

Yearly electricity consumption on Funen in 2050 [PJ]					
Classic	*Transport*	*Large data centers*	*Individual heat*	*Process heat*	*Total*
11.06	5.64	3.68	0.96	0.49	21.83
51%	26%	17%	4%	2%	100%

As can be seen, the largest share of electricity consumption is the classic electricity consumption followed by the consumption for transportation. Since these two demands also have a seasonal dependency the total electricity consumption also has a clear seasonal dependency with a smaller consumption of electricity during the summer months. This dependency can also clearly be spotted in the consumption of electricity for individual heating. It is not only a seasonal dependency that can be found but also a daily and weekly dependency. Figure 8.8 shows the total hourly electricity consumption during a random week in may. It can
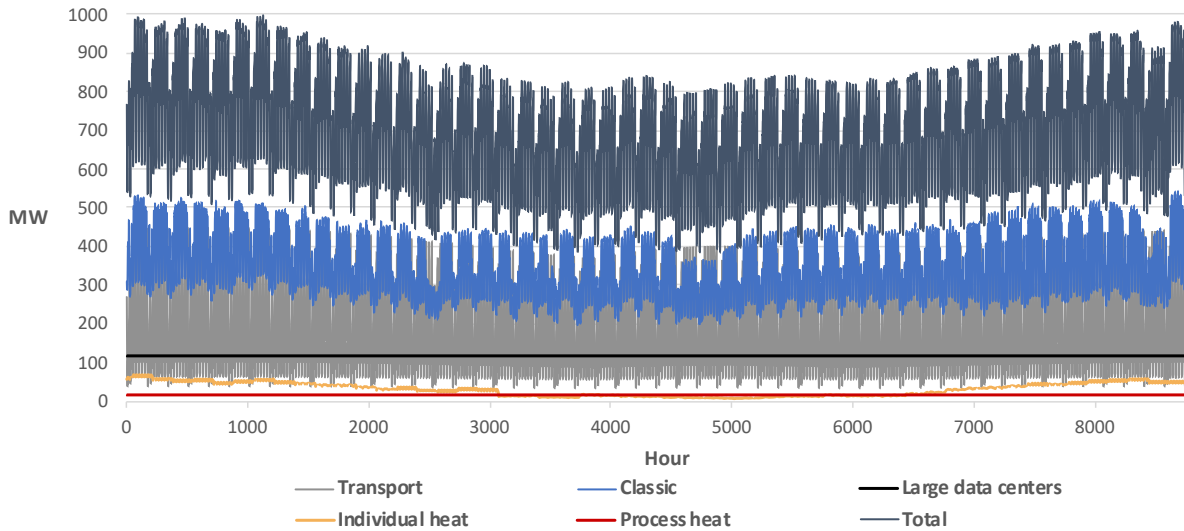
Figure 8.7: *The figure shows the hourly electricity consumption of Funen in 2050 based on the LUP framework. The consumption is divided into the five sectors: Classic, Transport, Large data centers, Individual heat and Process heat.*

clearly be seen that the consumption of electricity is dependent on the time of the day and week day and weekends. It should however be noticed, that the total electricity consumption peaks rather late during the day compared to the classic demand, which normally peaks around 5 pm. This is due to the fact that the electricity consumption for transport peaks around 0 am where all the electric vehicles charge at maximum capacity. Since the electricity consumption for transport has a significant share in the total electricity consumption this results in the total consumption peaking around 0 am.
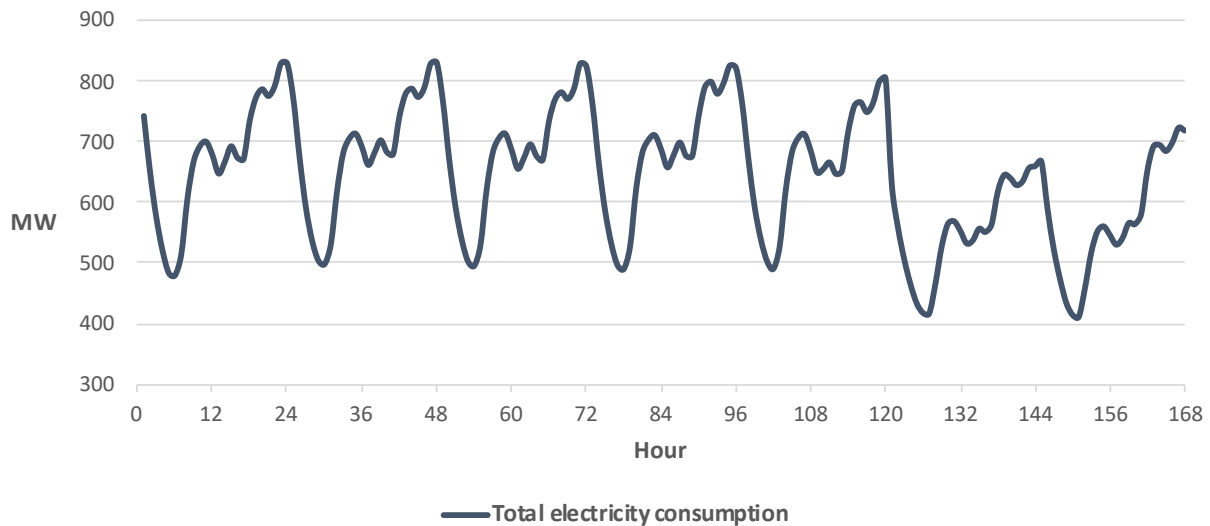
Figure 8.8: *The figure shows the total hourly electricity consumption of Funen in 2050 during a random week in May.*

The hourly electricity production for both solar and onshore wind power on Funen in 2050 can be seen in Figure 8.9, while the yearly productions can be seen in Table 8.3. It is clear that solar power has the highest impact in the electricity production during the summer, whereas onshore wind power produces more

or less stable within a margin of 200 MW throughout the year. The production from solar power has clear fluctuations between night and day. This can also be seen in Figure 8.10 where the production from onshore wind is rather constant around 200 MW and the clear fluctuation in the total electricity production is a result of the production from solar power. The production from solar power is 0 MW during the night and peaks during the day to 773 MW at the highest point during the week.

Table 8.3: *The table shows the yearly electricity production from solar and onshore wind power on Funen in 2050.*

Yearly electricity production on Funen in 2050 [PJ]		
Solar	*Onshore wind*	*Total*
5.82	2.69	8.51
32%	68%	100%

The final framework condition relevant to the Funen Case Study is the interconnection line capacity from both Southern Jutland to Funen and Western Zealand to Funen. Recalling from Section *4.2.8 Network Constraint*, the capacity of the interconnection line between Southern Jutland to Funen is 1116 MW (import and export) and the capacity of the interconnection line across the Great Belt connecting Funen to Western Zealand is 600 MW import and 590 MW export. This gives an import capacity of 1716 MW and an export capacity of 1706 MW which is initially used as the capacity of the interconnection line connecting the local electricity area with the external electricity area i Sifre. The local electricity area represents Funen meaning that electricity can be imported to Funen at a maximum of 1716 MW and exported from Funen at a maximum of 1706 MW.
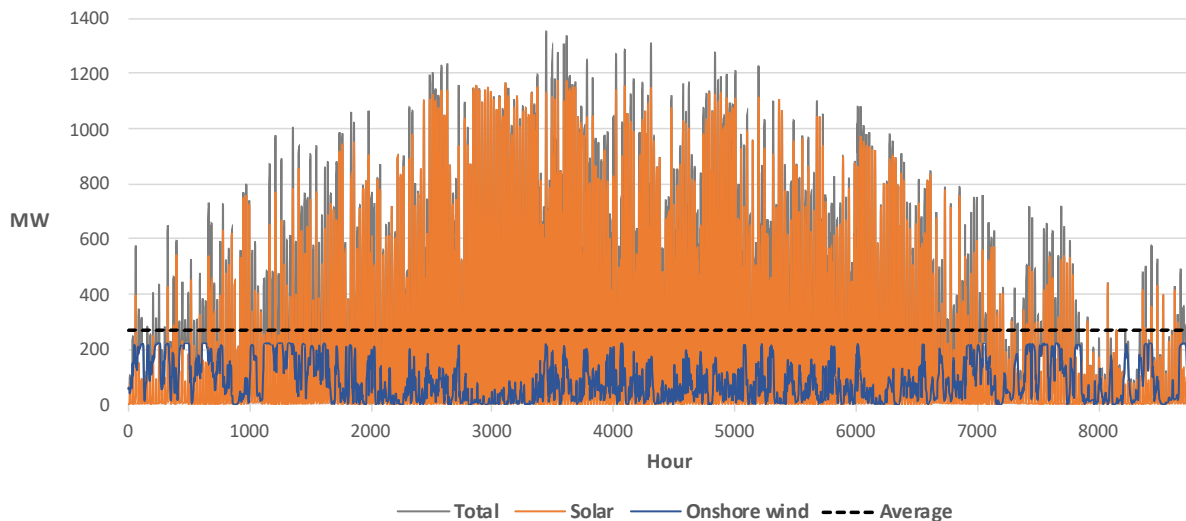
Figure 8.9: *The figure shows the electricity production from renewable energy sources on Funen in 2050 based on the LUP framework. The production is divided into Solar and Onshore wind.*
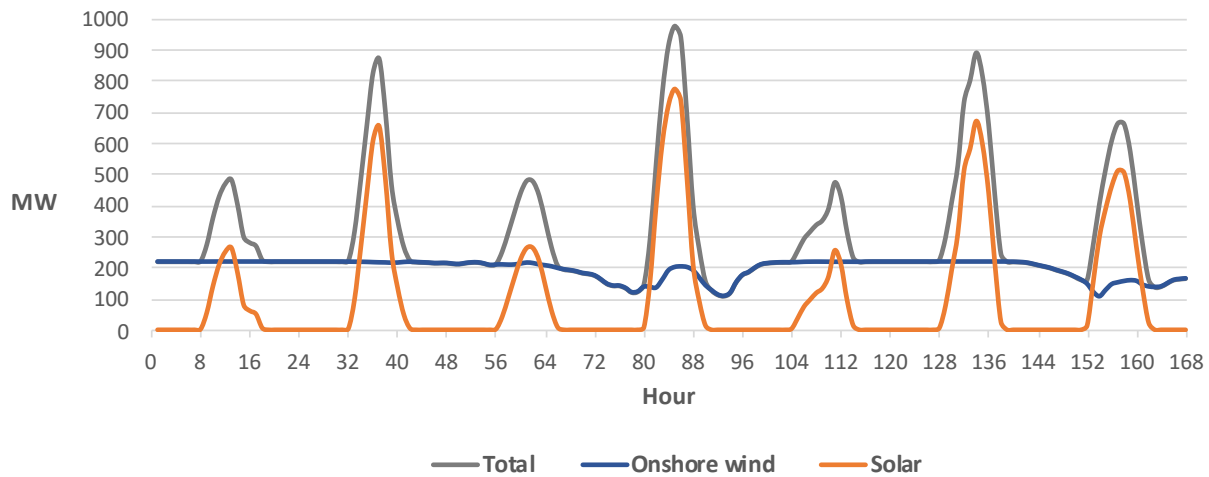
Figure 8.10: *The figure shows the hourly electricity production from renewable energy sources on Funen in 2050 during a random week in February. The production is divided into Solar and Onshore wind.*

8.2.2   Resulting Strain on the Electricity Network

Initially, the Funen Case Study has been set out to determine strain on the electricity interconnection lines, connecting Funen with its surrounding areas, in the pure PtL scenarios *1.7 Co-electrolysis* and *1.8 RWGS* since these are overall the most electricity-intensive configurations for liquid fuel production. Import strain on the interconnection lines in any given hour is effectively a result of local electricity consumption minus the local electricity production exceeding the import capacity in that hour. Export strain is a result of the local electricity production minus the local electricity consumption exceeding the export capacity. The resulting import on the interconnection line connecting Funen with its surrounding areas can be seen in Figure 8.11. As can be seen, no strain occurs in any hour during the year and the production of liquid fuels is unaffected by the interconnection line capacity. However, it is clear that electricity is being imported to Funen in a majority of hours during the year - approximately 8400 hours. The average net import in scenario *1.7 Co-electrolysis* is 784 MW whereas this import is 807 MW in scenario *1.8 RWGS*. In these two cases ADAPT does not find it socioeconomically feasible to invest in any other storages than LTPH and CO_2 storages. In scenario *1.7 Co-electrolysis* it invests in 1318 MWh and 1094 tonne LTPH and CO_2 storages respectively. In scenario *1.8 RWGS* it invests in 1234 MWh and 720 tonne LTPH and CO_2 storages respectively. This is because the LTPH and CO_2 storages have relatively low investment costs so the economic surplus from storing LTPH and CO_2 produced in hours with low electricity prices and utilizing the stored energy/mass in times with higher electricity prices can easily outweigh the investment cost. Even though hydrogen is also an essential fuel for the production of syngas through RWGS, no hydrogen storage is invested in in scenario *1.8 RWGS*. This can be explained by the investment cost of the hydrogen storage which is more than eight times higher than the cost of a LTPH storage. The fluctuations in the electricity price has to be significant or strain on the interconnection lines has to be present in order for the hydrogen storage to find an economic surplus and invest. The electricity price and the resulting jet fuel prices throughout the year can be seen in Figure 8.12.
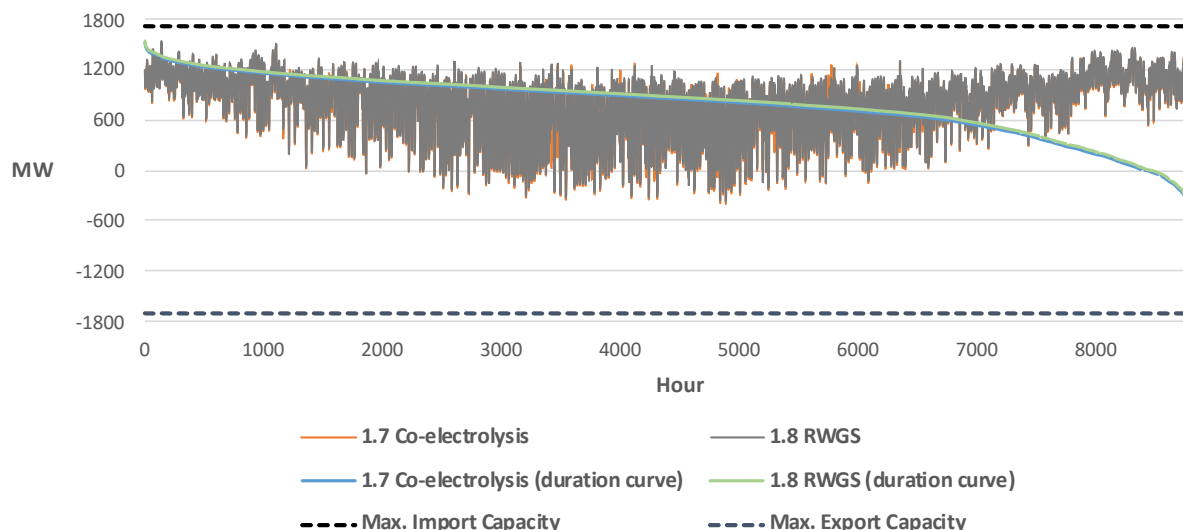
Figure 8.11: *The figure shows the hourly import on the interconnection line connecting Funen with its surrounding areas for both scenario 1.7 Co-electrolysis and 1.8 RWGS.*

It can clearly be seen that the resulting jet fuel price in either scenario is highly dependent on the electricity price. The resulting average jet fuel prices during the year are 32.7 EUR/GJ and 34.4 EUR/GJ for scenario *1.7 Co-electrolysis* and *1.8 RWGS* respectively. These jet fuel prices are slightly higher than the jet fuel prices found in the main scenarios for *1.7 Co-electrolysis* and *1.8 RWGS* (see Figure 8.1).
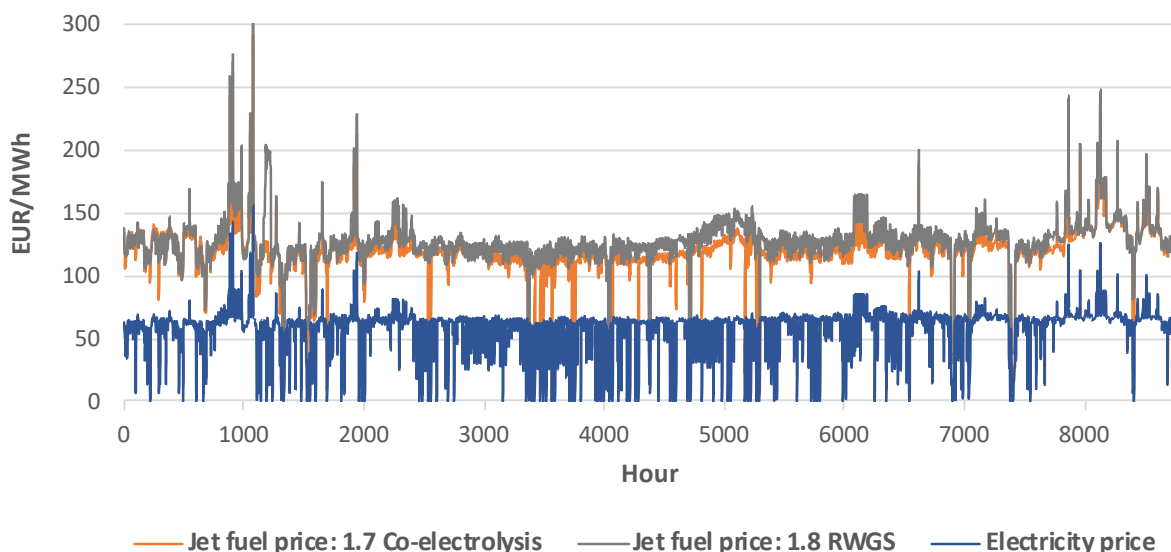
Figure 8.12: *The figure shows the hourly electricity price and resulting jet fuel prices for both scenario 1.7 Co-electrolysis and 1.8 RWGS.*

8.2.3   Resulting Strain on the Electricity Network with Reduced Capacity

Section *8.2.2 Resulting Strain on the Electricity Network* showed the initial results from the Funen Case Study with a import capacity of 1716 MW on the interconnection line and a production of 5 PJ jet fuel.

Here it was evident, that the interconnection line was not subject to strain in any hour during the year, but electricity was however imported in the majority of hours. Only in approximately 350 hours, for both *1.7 Co-electrolysis* and *1.8 RWGS*, was electricity exported away from Funen. Having an island in the middle of Denmark being so dependent on import of electricity from both Southern Jutland and Western Zealand might not be a viable solution, since Funen would only be able to function as a transit of electricity between DK1 and DK2 at a very limited capacity during the year. Therefore, it has been chosen to investigate the consequence of reducing the import capacity of the interconnection line. The import capacity of the interconnection line connecting the local electricity area with the external electricity area has been reduced by a capacity equivalent to the capacity on the interconnection line connecting Funen with Western Zealand i.e. 600 MW. In this analysis the export capacity has been kept constant at 1706 MW. This gives a resulting electricity import capacity to Funen of 1116 MW. Since the electricity consumptions of both scenario *1.7 Co-electrolysis* and *1.8 RWGS* are rather close, with scenario *1.8 RWGS* being slightly higher, it has been chosen to only include scenario *1.8 RWGS* in this analysis. Furthermore, in order to compare the result from reducing the interconnection line capacity with the previous result, it is chosen to only allow investment opportunities in the LTPH and CO_2 storage. In this way, consequences from reducing the capacity can only be traced back to the reduction itself.

Figure 8.13 shows the resulting import on the interconnection line with reduced import capacity. As can be seen, electricity is imported at the maximum of 1116 MW in 2000 hours of the year.
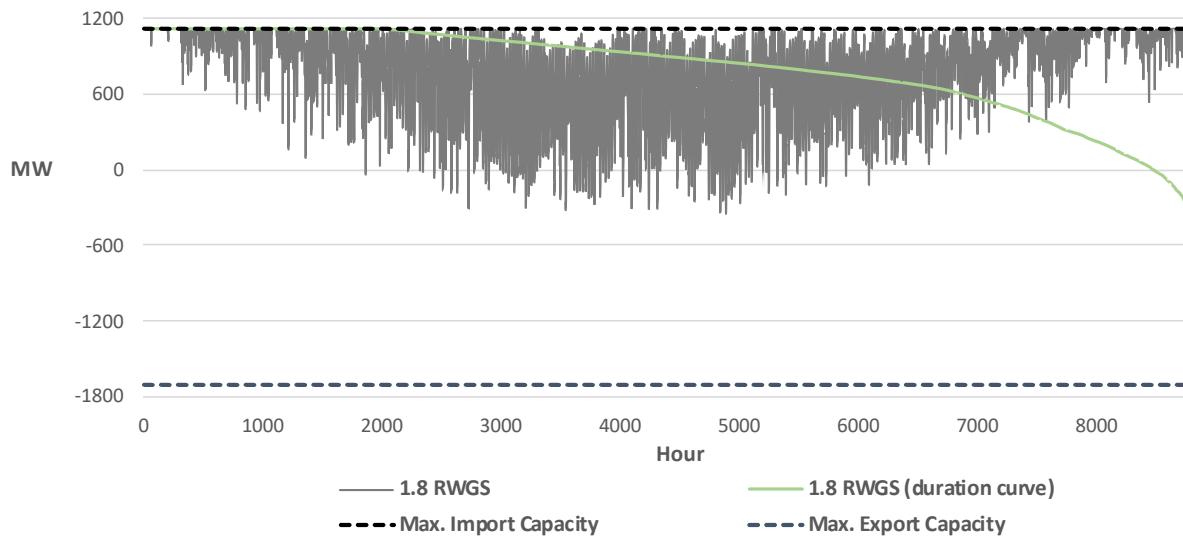
Figure 8.13: *The figure shows the hourly import on the interconnection line connecting Funen with its surrounding areas for scenario 1.8 RWGS with reduced capacity on the interconnection line.*

Because the production of liquid fuels is not given the necessary measures for more flexible production in order to accommodate the reduced import capacity, the jet fuel experiences an underproduction of jet fuel in 506 hours during the year. These hours are primarily in the winter months where the production of local electricity from solar power is limited and the local consumption of electricity is generally high. As mentioned in Section *7.2.3 Under- and Overproduction*, underproduction in any given area results in a cost

of underproduction of 3000 EUR/MWh. Therefore, the resulting average jet fuel price during the year in this scenario is significantly higher than usual, with a price of 94.5 EUR/GJ, due to the many hours with a resulting jet fuel price of 3000 EUR/MWh. ADAPT does invest in a LTPH storage twice the size (2241 MWh) as in the previous two analyses in order to accommodate the reduced import capacity. In this way LTPH used for hydrogen production, which is used in the RWGS unit, can be produced by the heat pump or electric boiler in hours with available capacity on the interconnection line and then stored for later use in hours with strain on the interconnection line. However, this measure is not nearly enough to mitigate strain on the interconnection line.

8.2.4   Resulting Strain from Implementation of Mitigation Measures

To the transmission grid operator, it is of obvious focus that an increasingly larger part of the energy consumption is based on electricity, and as the previous analyses have shown this may very likely lead to strain on interconnection lines. Therefore, different measures associated with liquid fuel production, that can be utilized for mitigation of electricity network strain, is investigated. The analysis is conducted with the same scenario *1.8 RWGS* and with the same yearly demand of jet fuel of 5 PJ.

Hydrogen Storage   The first measure investigated is the possibility to store hydrogen. Hydrogen is the primary fuel input of the RWGS unit and electrolysis is an electricity intensive process. Therefore, a hydrogen storage might be one of the obvious solutions for mitigation of strain on the electricity network. As shown in Figure 8.8 the daily pattern for electricity consumption clearly follows a curve with minimum electricity consumption during the night and early morning after which it experiences its first peak of the day around 11-12 am. The idea with a hydrogen storage follows the same logic as the LTPH and CO_2 storages mentioned in Section *8.2.3 Resulting Strain on the Electricity Network with Reduced Capacity*. During the period in the night where the consumption is less than normal and there is a higher amount of available capacity on the interconnection line, hydrogen can be produced in higher amounts than in a system without a hydrogen storage, and be stored for use in periods where the are no available capacity on the interconnection line. In this way the production of syngas in the RWGS unit, and thereby the production of jet fuel in the LTFT unit, is less dependent from the amount of available capacity on the interconnection line. The difference between utilizing a hydrogen storage compared to LTPH and CO_2 storages is, as mentioned earlier, hydrogen is the primary fuel input of the RWGS unit and the production of hydrogen is therefore a more electricity intensive process then the production of LTPH and CO_2.

In order to produce syngas in a RWGS unit steadily throughout the year, to supply 5 PJ of jet fuel, the RWGS must have a supply of approximately 320 MWh hydrogen per hour and around 7680 MWh per day. Therefore, it has been chosen to invest in a hydrogen storage with a pre-defined capacity of 4000 MWh, using the ADAPT module, in order to fully utilize the hours with available capacity on the interconnection line. However, initial simulations have shown a complication with this method. Since a startup inventory level of the hydrogen storage can not be defined when using the ADAPT module, the first week during the simulation year is still influenced by strain on the interconnection line resulting in underproduction in some

of the areas which then results in significantly high area prices. Therefore, it has been chosen to remove the investment opportunity from ADAPT, and then force it to install of 4000 MWh hydrogen storage in Sifre with a startup inventory level of 4000 MWh. In this way the investment cost of the hydrogen storage is not accounted for which might influence the resulting jet fuel price. However, it is not expected that this can alter the jet fuel price significantly although it should be expected that the actual jet fuel price will be higher than the results of this analysis. An investment in a 4000 MWh hydrogen storage would result in a yearly investment cost of 7.1 MEUR per year.

The results from implementing a hydrogen storage show that strain on the interconnection line can in fact be mitigated and no area experiences underproduction in any hour. With that said the interconnection line is still used at the maximum of 1116 MW in approximately 2000 hours during the year, and the electricity import looks very similar to the profile shown in Figure 8.13. However, the capacity of the interconnection line is used more efficiently than in the previous scenario without hydrogen storage. ADAPT chooses to increase the investment of the onsite electrolysis unit from 350 MW, which is the invested capacity with the high interconnection line import capacity of 1716 MW, to 530 MW in order to utilize the hydrogen storage for hydrogen production in hours with available capacity on the interconnection line. The operation of the hydrogen storage is very dependent on the electricity price as can be seen in Figure 8.14. In the first part of the week the electricity price is quite high due to a high local consumption of electricity and low local production of electricity. This creates strain on the interconnection line inducing a congestion rent which is imposed on the electricity price. In the final part of the week the general consumption of electricity seem to decrease which lowers the electricity prices. However, it can clearly be seen that the injection and extraction of hydrogen follows the electricity price and general consumption of electricity. Hydrogen is injected into the storage in hours with lower electricity prices, and extracted in hours where the electricity price is high.
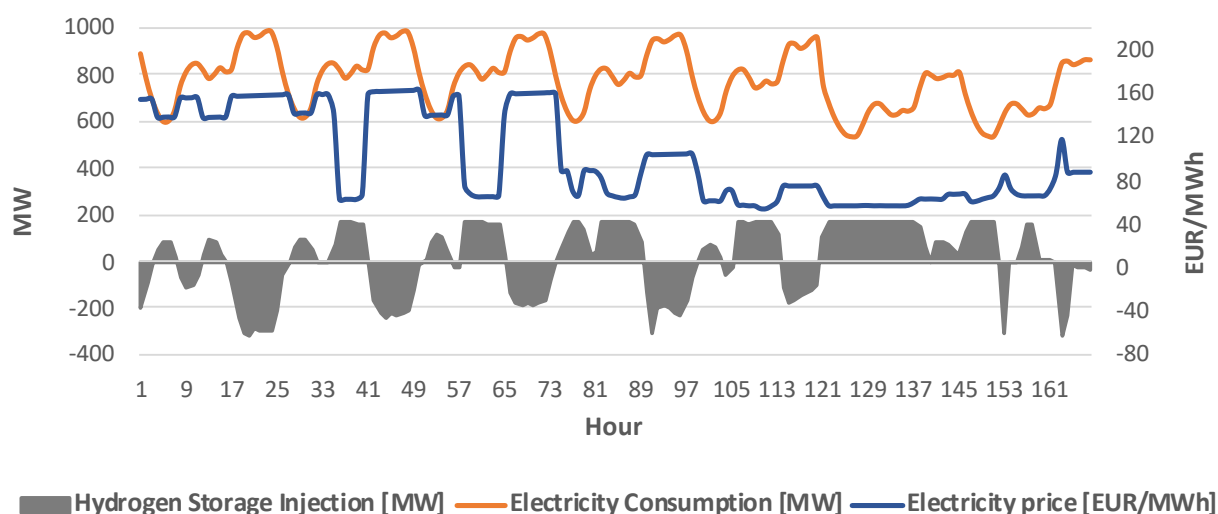
Figure 8.14: *The figure shows the hourly import on the interconnection line, the hourly electricity price and the hourly injection into the hydrogen storage during a week in March. Negative injection values indicates extraction of the hydrogen.*

Even though the hydrogen storage operates efficiently in order to accommodate the reduced interconnection line capacity, there are still around 2000 hours where the import of the interconnection line is at its maximum of 1116 MW. As mentioned earlier this induces a congestion rent which is imposed on the electricity price. This means that during these 2000 hours the electricity price is significantly higher than normal with prices all the way up to 336 EUR/MWh. This results in a higher price of hydrogen which finally results in a higher jet fuel price, through an increased cost of syngas, in those hours. The peak price of jet fuel is 181.4 EUR/GJ while the average jet fuel price during the year is 43.7 EUR/GJ. This jet fuel price is significantly higher than any jet fuel price in the main scenarios and around 9 EUR/GJ higher than the corresponding scenario without a reduced capacity on the interconnection line. Since the investment of the hydrogen storage is not included in the jet fuel price of 43.7 EUR/GJ it can only be expected to be higher.

Hydrogen Piping   The next measure investigated is hydrogen piping. Obviously, as with the hydrogen storage, hydrogen piping is only relevant for hydrogen intensive processes such as the RWGS and methanation. In this analysis, hydrogen piping will serve as an alternative to producing the hydrogen used for RWGS, and to a smaller degree LTFT, on the liquid fuel production site. The idea of hydrogen piping relates to the NSWPH consortium where the goal is to install large amounts of offshore wind power in the North Sea supplying the surrounding countries, including Denmark, with renewable electricity in order to reach the goals of the Paris-agreement. The capacity of offshore wind power in the North Sea can potentially reach 180 GW in 2045. A result of massive amounts of fluctuating electricity is the need for balancing the production and demand. Electrolysis is a measure for this challenge and therefore, a part of the NSWPH is to install large-scale electrolysis at the western coast of Jutland where the electricity goes ashore [6]. This hydrogen can be utilized in liquid fuel production but this requires a method for transporting the hydrogen around to central production sites such as Odense. Therefore, it is investigated how central production of hydrogen at the western coast of Jutland, and piping of hydrogen to Odense, affects liquid fuel production in Odense. This has been investigated using the same scenario, *1.8 RWGS*, with the same yearly demand of jet fuel of 5 PJ and with the reduced electricity import capacity for Funen of 1116 MW.

A set of other assumptions is underlying for this analysis. First, the hydrogen pipe is assumed to be 150 km. The investment cost of the pipe has been provided by Energinet, which gives an indicative investment cost, excluding cost of compression, of 0.37 EUR/MW/m [17]. Since this cost is excluding the cost of compression, which is a significant part of the total cost for hydrogen piping, it has been assumed that this cost is equivalent to the cost of compressing upgraded biogas to gas transmission pressure i.e. approximately 0.2 MEUR/MW [64]. This gives total cost of the hydrogen pipe of 0.25 MEUR/MW.

Some assumptions have also been made regarding the central production of hydrogen at the western coast of Jutland. Since the electricity input to the electrolysis process does not make use of the electricity network in Denmark, no electricity tariffs have been added to the electricity price, and the cost of electricity for hydrogen production is therefore the true electricity price. Furthermore, it is likely that the production of hydrogen might reap benefits from economies of scale. However, an investigation of the economies of scale of hydrogen production have been outside the scope of this project. Therefore, it has been assumed that

the investment and O&M costs of hydrogen production at the western coast of Jutland is 25% lower than normal. Finally, it is assumed that the excess heat from hydrogen production can not be utilized in any DH network and therefore can not serve as a revenue from the hydrogen production.

The resulting hourly import capacities to Funen of both electricity and hydrogen can be seen in Figure 8.15. As can be seen, the electricity import is less than the capacity of 1116 MW in almost every hour during the year. The average net import rate is 327 MW in this scenario. Furthermore, as can be seen, hydrogen is imported from the western coast of Jutland almost constantly at a rate of 332 MW during the year, which is also the capacity that ADAPT chooses to invest in. Hydrogen is imported almost constantly since the production of hydrogen is now independent from the capacity of the interconnection line connecting Funen with Southern Jutland. The specific yearly investment cost in this hydrogen pipe is 11,689 EUR/MW which amounts to a total yearly investment cost of 3.88 MEUR.
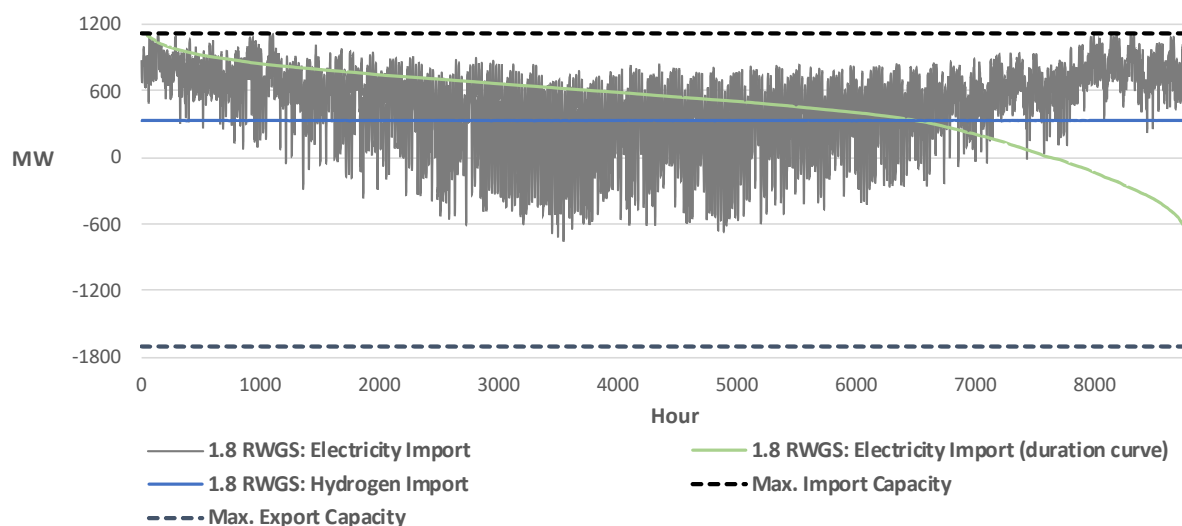
Figure 8.15: *The figure shows the hourly import capacities for Funen of both electricity the electricity interconnection line and hydrogen pipe.*

Figure 8.16 shows the resulting area price of hydrogen on the liquid fuel production site i.e. after it has been piped from the western coast of Jutland to Odense. The area price of onsite hydrogen from the previous scenario, with hydrogen production on the liquid fuel production site and a hydrogen storage as a measure for strain mitigation, has also been included in order to compare the prices. The figure shows a clear difference in hydrogen price. As earlier mentioned in the scenario with onsite electrolysis and a hydrogen storage, the electricity price increases significantly in some of the hours during the winter months due to strain on the interconnection line. The consequence of this is a significant increase in the price of hydrogen. Since electrolysis located on the western coast of Jutland is unaffected by strain in the electricity network, the resulting hydrogen price is only affected by the pure electricity price and does not suffer from higher electricity prices due to strain in the electricity network. Excluding the hours (0-1100 and 7800-8760) with significantly higher hydrogen prices due to network constraints the average hydrogen price is approximately 20.5 EUR/GJ, while the average hydrogen price in the corresponding hours in the scenario

with hydrogen piping is 16.8 EUR/GJ. Generally the hydrogen price difference between the two scenarios, during unconstrained hours, is between 2.8-4.2 EUR/GJ, which is the result of hydrogen production that is not subject to electricity transmission tariffs and can benefit from economies of scale. Naturally, this low-priced hydrogen also has an impact in the resulting jet fuel prices. The resulting average jet fuel price during the year is 27.2 EUR/GJ, which is only slightly higher than the lowest jet fuel prices resulting from the main scenarios.
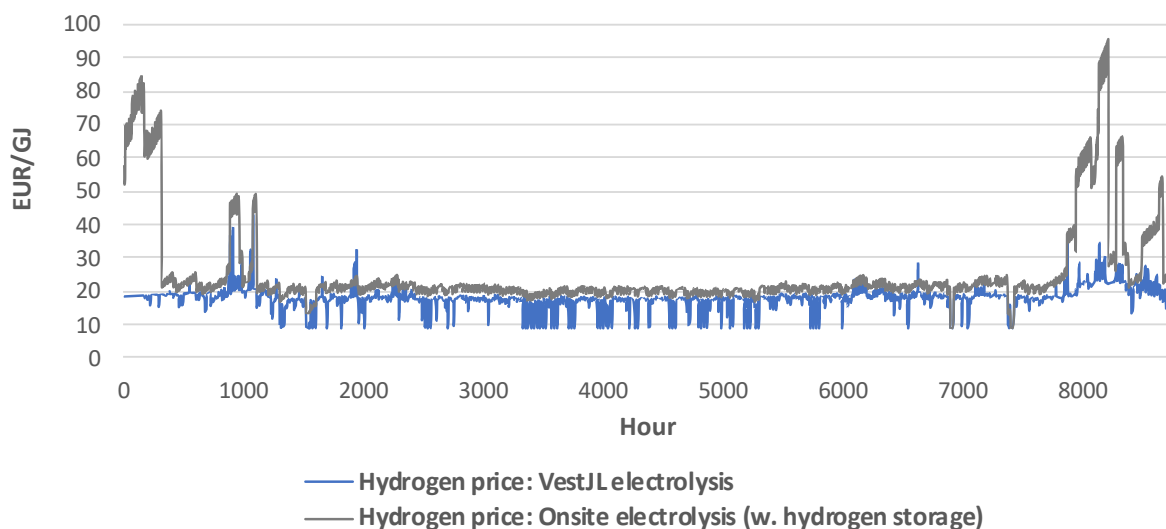
Figure 8.16: *The figure shows the hourly area price of hydrogen on the liquid fuel production site for both the scenario with onsite hydrogen production and a hydrogen storage as a mitigation measure, and the scenario with hydrogen production on the western coast of Jutland and hydrogen piping to the liquid fuel production site in Odense, Funen.*

Hybrid Production Configuration The last measure for mitigation of strain in the electricity network is not so much a measure as it is a general way of designing the liquid fuel production plant i.e. the hybrid production configuration. The idea behind the hybrid production configuration in relation to network strain is, that the plant is able to optimize its production of syngas based on the available capacity in the electricity network. When there is available capacity in the network the plant can produce syngas by both co-electrolysis and RWGS if other conditions are desirable for PtL. When the network is strained due to a high local consumption of electricity or a low local production of electricity, the plant can produce syngas through POX or SMR in order to accommodate the strain in the electricity network.

The Funen Case Study has been applied to every hybrid liquid fuel production configuration with the same demand of jet fuel of 5 PJ, and with the reduced electricity import capacity of 1116 MW, in order to investigate how the hybrid configurations perform compared to piping of hydrogen. The results show, that in none of the hybrid scenarios does any area suffer from underproduction. This is because of the flexibility of the plant configuration. As an example, Figure 8.17 shows the production of syngas from both the POX and co-electrolysis unit in scenario *1.5 POX / Co-electrolysis*. These syngas productions have been plotted together with the import of electricity where the consumption for co-electrolysis have been subtracted and with the actual import in the same scenario during a random week in February. Although it can be difficult,

a pattern of syngas production in relation to the import of electricity can be found. The pattern shows that in hours where the import without the consumption for co-electrolysis seems to drop, the production from co-electrolysis increases, and in hours where that import seems to increase the production from POX increases. Furthermore, when the production of syngas from co-electrolysis increases, the actual import of electricity increases accordingly. In this way the hybrid liquid fuel production configuration is able to efficiently adapt to changes in the available capacity in the electricity network.
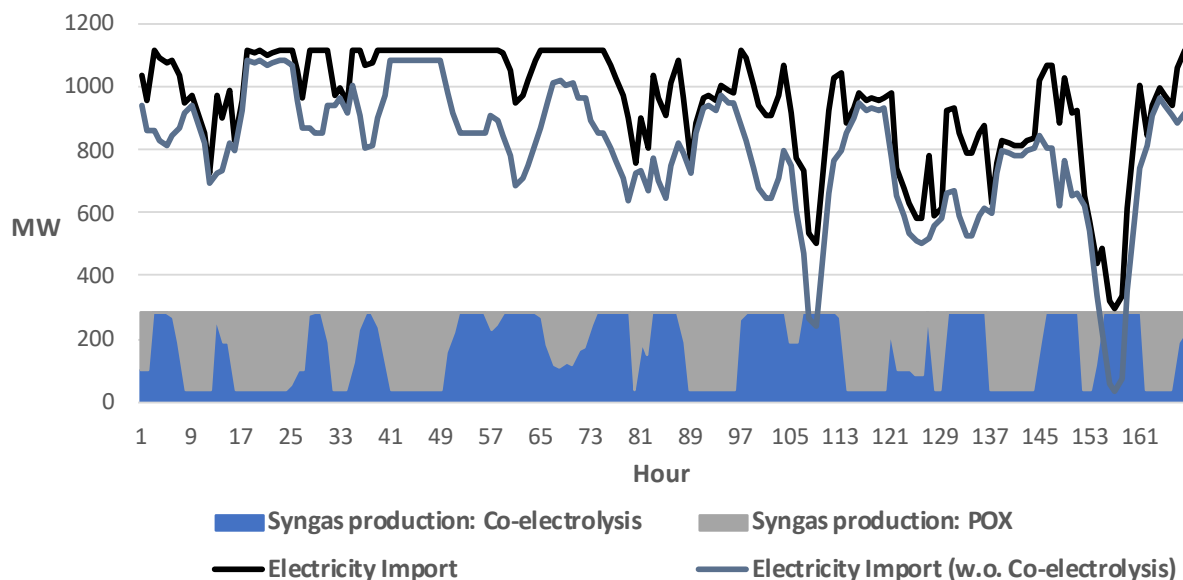
Figure 8.17: *The figure shows the hourly production of syngas from both the POX and Co-electrolysis unit in scenario 1.5 POX + Co-electrolysis together with the import of electricity in the same scenario during a random week in February.*

As mentioned earlier, the Funen Case Study has been simulated on all hybrid production configurations. Furthermore, the hydrogen piping solution has been implemented for the Funen Case Study on all hybrid scenarios that includes a RWGS unit for syngas production. The purpose of this is to compare the resulting jet fuel prices for these two methods of mitigating strain in the electricity network. Throughout the hybrid scenarios, ADAPT has been given the possibility of investing in hydrogen storages. However, this is only found desirable to a small degree given that the largest investment is a 24 MWh hydrogen storage. Generally the investment in a hydrogen storage is between 0-6 MWh, which is significantly smaller than the LTPH, HTPH and CO_2 storages that are generally being invested in by ADAPT. This indicates that the hybrid syngas production configuration is more socioeconomically feasible to invest in compared to the hydrogen storage as a measure of mitigating strain in the electricity network. The resulting jet fuel prices of the hybrid and hydrogen piping scenarios for the Funen Case Study can be seen in Figure 8.18. It can be seen that the measure of producing hydrogen at the western coast of Jutland, and piping the hydrogen to Odense, seems to be the more feasible solution. The figure shows, that for the four scenarios, in which both mitigation measures are compared, the piping of hydrogen outperforms the hybrid production configuration in resulting jet fuel price. However, it seems that the hybrid configurations that use POX with methane from biogas upgrading is able to economically compete with all scenarios with hydrogen piping. This is because the POX

unit can produce jet fuel at a low price due to the low-priced methane, and because the demand of jet fuel has been set to 5 PJ there are no restrictions in relation to the input of biogas in the system. Therefore, the resulting jet fuel prices resemble those from the pure GtL in the main scenarios, where the jet fuel demand has been set to 25 PJ since the pure GtL pathway can not supply the full Danish demand of jet fuel of 50 PJ. As with the main scenarios, this price is therefore not scalable to the entire jet fuel production in Denmark.

| | **Methanation** | | | | **Biogas Upgrading** | | | |
	SMR / Co-electrolysis	SMR / RWGS	POX / Co-electrolysis	POX / RWGS	SMR / Co-electrolysis	SMR / RWGS	POX / Co-electrolysis	POX / RWGS
Hybrid	32,5	34,3	32,5	32,5	32,1	32,9	27,8	25,7
Hydrogen Piping		27,5		28,1		26,0		25,4
Low Jet Fuel Price	10,0	10,0	10,0	10,0	10,0	10,0	10,0	10,0
High Jet Fuel Price	20,0	20,0	20,0	20,0	20,0	20,0	20,0	20,0
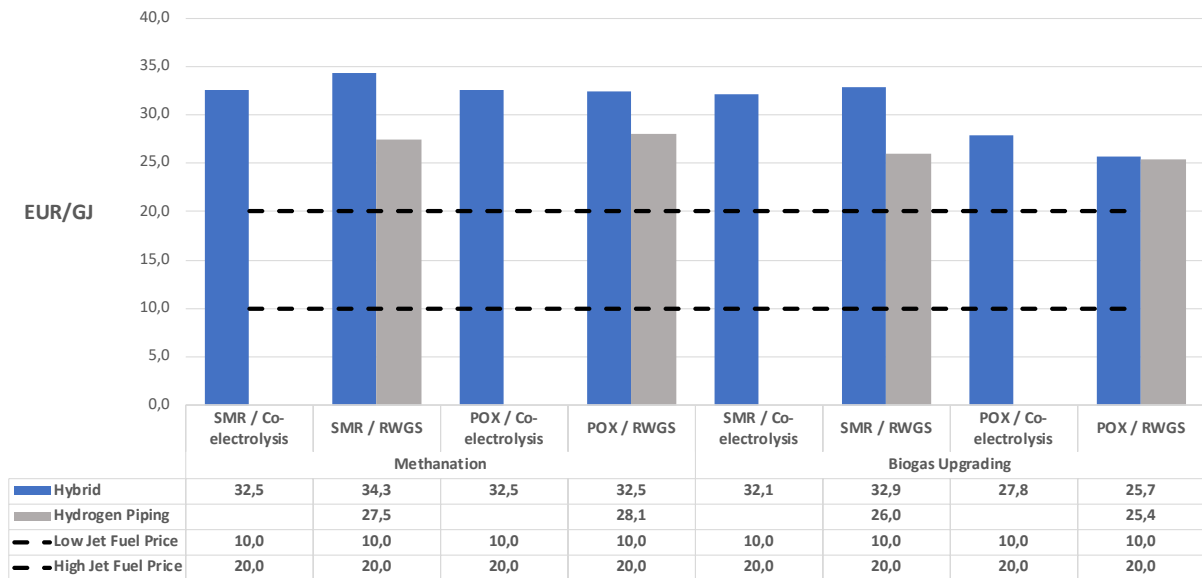
Figure 8.18: *The figure shows the yearly average jet fuel prices for the scenarios with a hybrid syngas production configuration and for the hybrid scenarios with a RWGS unit where hydrogen is supplied to the production site through a hydrogen piping from the western coast of Jutland where hydrogen production is located.*

9   Sensitivity Analysis

In this project, assumptions, approximations and projections, have been made - many of which are very uncertain due to the temporal scope of 2050. While qualified estimates are provided based on the literature study made prior to modelling, they remain qualified estimates and their influence on the final results should be investigated to determine if single parameters or assumptions can greatly impact the results of the simulations.

9.1   Effect of CO_2 and LTPH from waste and biomass incineration

The purpose of the first sensitivity analysis is to investigate the consequence of not being able to utilize the CO_2 and LTPH sources from waste and biomass incineration. The general framework until now has been that the production of liquid fuels are located on the same production site as both waste and biomass incineration. It is, however, rather difficult to predict how influential waste and biomass incineration are going to be in the future energy system. It is therefore interesting to investigate how robust the jet fuel price is to a change in the framework i.e. the availability of CO_2 and LTPH from both waste and biomass incineration. As can be seen in Table 8.1, ADAPT invests 665 MW in the waste incineration boiler in every main scenario, and the biomass incineration boiler in four scenarios. Therefore, the presence of the incineration boilers might affect the CO_2 and LTPH prices and thereby the jet fuel price.

Another factor in relation to waste and biomass incineration that can affect the CO_2 price from these two sources is the cost of capturing the CO_2. Recalling from Section *4.2.5 Carbon Capture* the cost of CC in the main scenarios has been based on economic figures from the Global CCS Institute, which estimates that the cost of CC will fall to between 31.7-45.3 EUR/tonne CO_2 as a result of current development in solvent innovation and process integration and intensification [44]. The upper limit of this price interval has been assumed for the cost of CC in the main scenarios. However, a recent report from NIRAS states that the current price of CC is somewhat different. Here it is stated that the current cost of capture to liquid CO_2 is between 66.7-120 EUR/tonne CO_2, and that a cost of 93.3 EUR/tonne can be expected [47]. Therefore, it has been chosen to investigate the consequence of increasing the capture cost to the 93.3 EUR/tonne stated by NIRAS, which is about double the value of 45.3 EUR/tonne used in the main scenarios.

Both the sensitivity analysis of removing the production of CO_2 and LTPH from waste and biomass inciner-ation, and the increase of the CC cost have been investigated for scenario *1.7 Co-electrolysis.* This is because scenario *1.7 Co-electrolysis* is the liquid fuel production configuration which has the highest consumption of CO_2 and a relatively high consumption of LTPH. It is therefore expected, that the consequences of these changes would have the highest impact in scenario *1.7 Co-electrolysis.* The resulting yearly average area prices of LTPH, CO_2 and syngas produced on the liquid fuel production site can be seen in Figure 9.1 together with the resulting yearly average jet fuel prices. As can be seen, the CO_2 area experiences a rather significant price increase in both sensitivity analyses. The impact is however most significant when

removing the waste and biomass incineration where the CO_2 area price increases from 67.9 EUR/tonne to 91.3 EUR/tonne. This is because the DAC unit has to increase its production and produce CO_2 in hours with higher electricity prices, and because it does not have a low-priced heat source from the waste and biomass incineration. Generally, the LTPH area price does not increase significantly by either changes. Nor does the jet fuel price, which only increases 1.9 EUR/GJ in both sensitivity scenarios. One of the reasons that the jet fuel price does not increase more with increasing LTPH and CO_2 prices is, that the cost of electricity constitutes the majority of fuel cost for the co-electrolysis unit. Generally the cost of CO_2 only contributes with approximately 20% of the fuel cost for the co-electrolysis unit, while the cost of electricity is the majority of the fuel cost with around 70%. Therefore, the price of syngas produced in the co-electrolysis unit does not increase more than 2.1 EUR/GJ, which finally affects the jet fuel price with an increase of only 1.9 EUR/GJ.

	Main Scenario	No waste and biomass incineration	Increased CC cost
LTPH	8,8	12,6	9,6
CO2 (EUR/tonne)	67,9	91,3	85,9
Syngas	25,3	27,4	26,5
Jet fuel	31,8	33,7	33,7
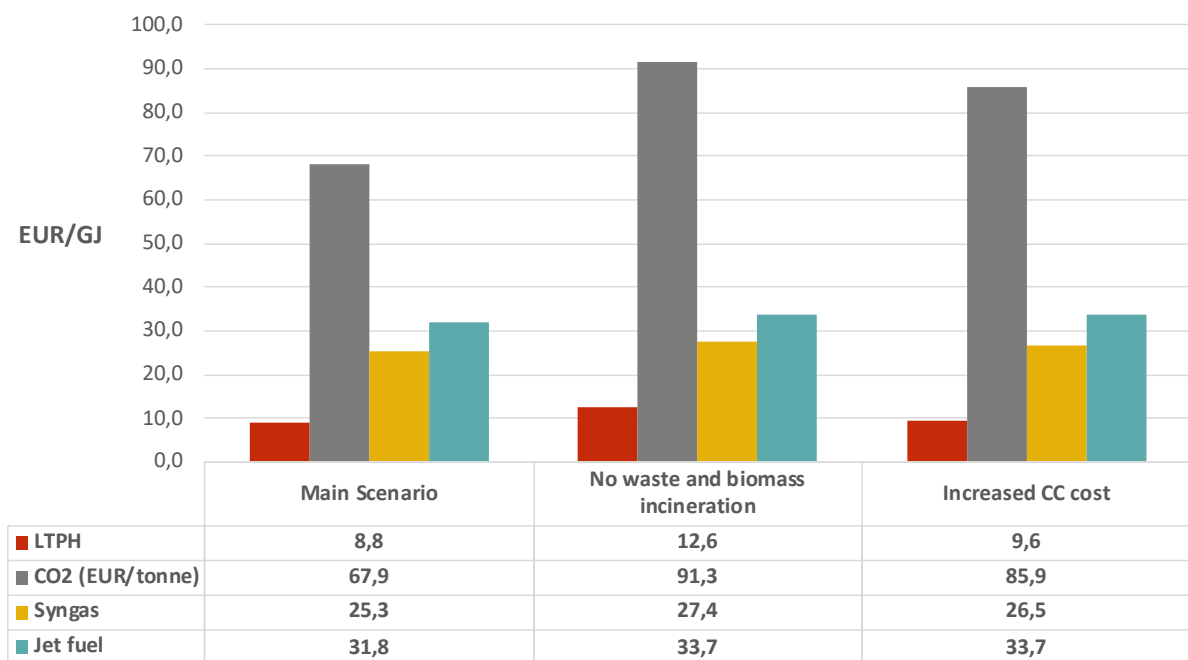
Figure 9.1: *The figure shows the yearly average LTPH, CO_2 and jet fuel prices the sensitivity analysis without onsite waste and biomass incineration and with a high cost of CC. As can be seen, the price of CO_2 is given in EUR/tonne and not EUR/GJ.*

The reason why the LTPH price changes from scenario to scenario is effectively a result of the production from waste incineration and the consumption from processes within the plant. In many cases, the waste incineration produces more LTPH than is consumed, but in cases with e.g. only co-electrolysis, more LTPH is consumed than is produced from waste incineration and other production units are forced to produce. Figure 9.2 shows the hourly LTPH price for scenarios *1.4 SMR / RWGS*, *1.7 Co-electrolysis* and *1.7 Co-electrolysis excluding waste and biomass incineration.*

In the figure, three different cases of marginal suppliers can be seen. In scenario *1.4 SMR / RWGS*, the hourly consumption of LTPH is never higher than the production from waste incineration, which results in the price being equal to the selling price of DH, since the production costs of LTPH will always be lower than
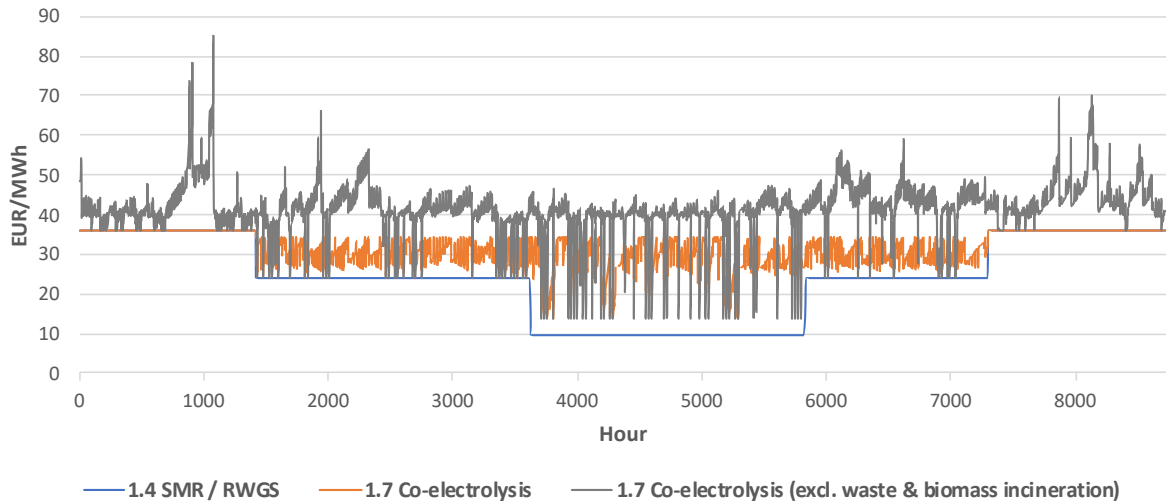
Figure 9.2: *Comparison of the hourly LTPH price in three different cases of the marginal supplier. Scenario 1.7 Co-electrolysis has been simulated both with and without LTPH and CO$_2$ from waste and biomass incineration to show the effect of not having a source of low-priced LTPH. Scenario 1.4 SMR / RWGS is shown alongside in order to show a price curve of LTPH that is always equal to the price of DH.*

the willingness to pay for LTPH to supply the DH demand. In scenario *1.7 Co-electrolysis*, the consumption within the plant is generally higher than what is produced from waste incineration, and the marginal supplier therefore becomes a weighting between excess heat from other processes, biomass incineration and electricity-based LTPH. The price curve for this scenario can be seen to be fluctuating during the months from March through October, while it is equal to the price of DH during November through February. This can be explained by the fact that the price of DH in the winter months at 36 EUR/MWh is higher than the marginal production costs from either of the alternative suppliers of LTPH, and there would therefore always be a willingness to pay what is equal to the price of DH for LTPH. This means that order to consume LTPH for fuel production, units have to "pay" the same for the LTPH as it can be sold for as DH. In the summer months where the price of DH is significantly lower, at 9.6-24 EUR/MWh, the production costs from any of the alternative suppliers of LTPH is always higher. In fact, the production cost can be seen to fluctuate from around 26 to 35 EUR/MWh, which is effectively what the price of LTPH becomes. Therefore, when the value of DH drops below these production costs, the marginal producer will be setting the price on LTPH according to its production cost.

The effect of not having LTPH from waste incineration and biomass incineration can be seen in the price curve from scenario *1.7 Co-electrolysis excl. waste & biomass incineration*. Here, it can be seen to be much more fluctuating than the prices from either scenario *1.4 SMR / RWGS* and *1.7 Co-electrolysis*, and it can be seen to be directly dependent on the electricity price during the entire year, since only electricity-based production units are used to produce LTPH. Furthermore, it can be seen that the price of LTPH never drops below the price of DH, since the area of DH is always willing to pay this price for the LTPH. When the production cost of LTPH is higher than the price of DH, it is the marginal production cost of the marginal

supplier that is setting the price on the market, while it is the price of DH that is setting the price on LTPH when the production cost is lower.

9.2   Volatile Electricity Prices from Global Climate Action

Another element of the simulations that could potentially greatly affect the results is the electricity price, as the results show that PtL is likely to be a significant part of the production of jet fuel in 2050. Therefore, investigating the sensitivity of changing this electricity price is essential to validate the results of the study. This sensitivity originates from the energy system development taking another path than the one described in Section *4.1 LUP Framework*. Here, a future in which renewables are even more dominant in the market clearing of the electricity price is interesting to evaluate as the electricity price in such a case becomes more volatile.

9.2.1   Background of the Electricity Price

Recalling from Section *4.3.1 Electricity*, the electricity prices for the main results have been based on the data from ENTSO-E's European TYNDP scenario *Sustainable Transition* (ST). ST is described as an on-target scenario that reach the target through national regulation, emission trading schemes and utilization of existing infrastructure [100], which fit well with the focus of this study. However, in Denmark, the focus on fast, and early decarbonization is increasing as quick action are to be taken in order to keep with the goal of the European 2030 and 2050 ambitions, and the Paris Agreement. The European 2030 ambition includes a reduction target of GHG emissions of 40%, while the 2050 target is climate neutrality [101], [102]. Therefore, a more aggressive decarbonization scenario exists in TYNDP called *Global Climate Action* (GCA). GCA is described as a full speed decarbonization with large-scale renewable development in both electricity and gas sectors. In case this scenario would be closer to the reality in 2050, which is not necessarily unlikely, the resulting electricity prices would behave significantly different than in the ST scenario. The electricity prices in such a scenario would be more volatile and fluctuate significantly more - but also have more hours with prices that are extremely low, or even zero.

Figure 9.3 shows the hourly electricity prices from the GCA scenario in 2040 along with the duration curve to show the more volatile nature than that of the ST seen in Figure 4.7. Compared to the electricity price used in the main scenarios, the prices from GCA are, on average, lower. While both time series has hours with prices of zero, the number of those hours are significantly higher in GCA with approximately 2500, compared to only approximately 350 in ST. On average the GCA price is more than 15 EUR/MWh lower than for ST with an average yearly price of 42.6 EUR/MWh. The significantly more volatile electricity price can also be seen by the higher standard deviation, which is 47.8 EUR/MWh for GCA compared to 18.0 EUR/MWh for ST.

This sensitivity has been simulated for all plant configurations with upstream methane production from methanation, i.e. scenarios *1.1 SMR* through *1.8 RWGS*. The is due to the fact that a change in the electricity

price would have a greater effect on scenarios with a larger production and consumption of hydrogen, as well as PtL producing a larger proportion of the total syngas in most scenarios. This means that the results shown in this sensitivity would also be observed in scenarios with biogas upgrading - however, to a smaller degree.
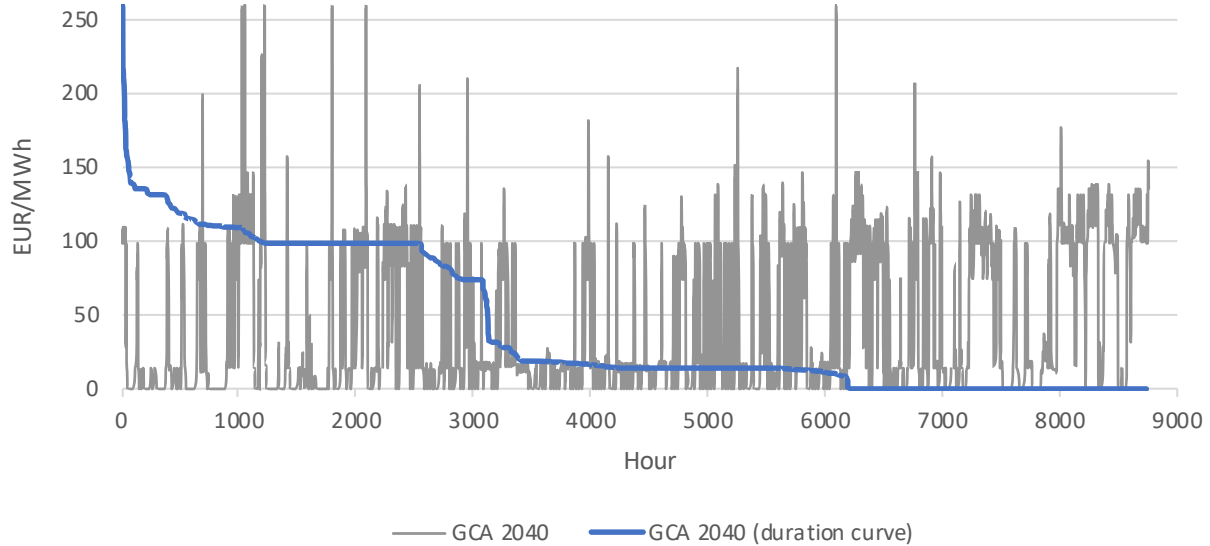
Figure 9.3: *Hourly electricity prices from the ENTSO-E and ENTSO-G TYNDP 2018 scenario Global Climate Action. The prices can be seen to more volatile and fluctuating than those seen for Sustainable Transition. The duration curve shows that there are almost 2500 hours in which the electricity price is zero. The more volatile nature of the electricity prices could prove hybrid solutions more attractive as they can utilize the low-price hours while shifting towards GtL in high-price hours.*

9.2.2   Resulting Jet Fuel Prices

While the results of not having CO_2 or LTPH from waste or biomass incineration showed to have little effect on the resulting jet fuel prices, the opposite goes for the GCA electricity price. The electricity price can be seen to significantly affect the resulting average jet fuel prices, which are shown in Figure 9.4.

It is clear that these electricity prices reduce the jet fuel price for all plant configurations. However, it is interesting to see that the configurations that can be seen to benefit most from the fluctuating electricity price is the hybrid configurations. This is due to the fact that the plants can utilize hours with zero-prices better than pure GtL or PtL. It can be seen that the resulting jet fuel prices from using the GCA electricity price are almost half for the hybrid scenarios, with a reduction from more than 32 EUR/GJ to as low as 16.2 EUR/GJ. What is worth noting about this result is that this price lies within the interval of the estimated lower and higher jet fuel price of 2019, i.e. the cost of the fuel would almost equal that of the jet fuel price of today. While the difference in jet fuel price between the different hybrid configurations in the main results show little variation, the variation with the GCA prices are even smaller, as can be seen in the figure, with the highest jet fuel price being 16.9 and the lowest being 16.2. This can most likely be explained by the fact that many of these hours of production happens when the electricity price is zero. When the cost of one central input is removed one potential gap is removed as well, moving the results closer to each other.

	SMR	POX	SMR / Co-electrolysis	SMR / RWGS	POX / Co-electrolysis	POX / RWGS	Co-electrolysis	RWGS
	GTL		Hybrid				Electrofuel	
Main results	32,7	33,3	32,5	34,0	32,1	33,6	31,8	33,9
With GCA electricity prices	24,2	25,1	16,4	16,8	16,2	16,9	23,6	26,0
Low Jet Fuel Price	10,0	10,0	10,0	10,0	10,0	10,0	10,0	10,0
High Jet Fuel Price	20,0	20,0	20,0	20,0	20,0	20,0	20,0	20,0
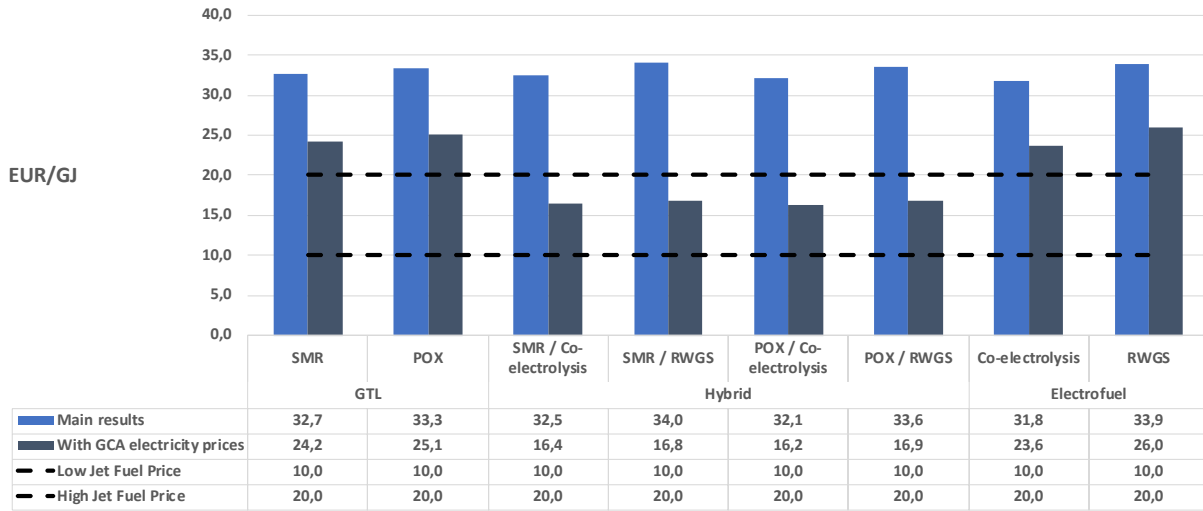
Figure 9.4: *Comparison of jet fuel prices from simulations using the volatile electricity prices of GCA with the main results described in 8.1.1 Jet Fuel Prices. The jet fuel prices with electricity prices from GCA can be seen to be significantly lower than those from the main results, and even lower than the high estimate of the current jet fuel price in 2019.*

9.2.3   Dynamics

With the electricity price changing this significantly, it is interesting to investigate how the production dynamics of the hybrid configuration change. The immediate thought would be that PtL would produce a larger proportion of the total amount of syngas, however, Figure 9.5 shows a different trend. The figure shows the proportion of syngas produced from GtL and PtL with the GCA electricity price compared to the main results for the hybrid scenarios.
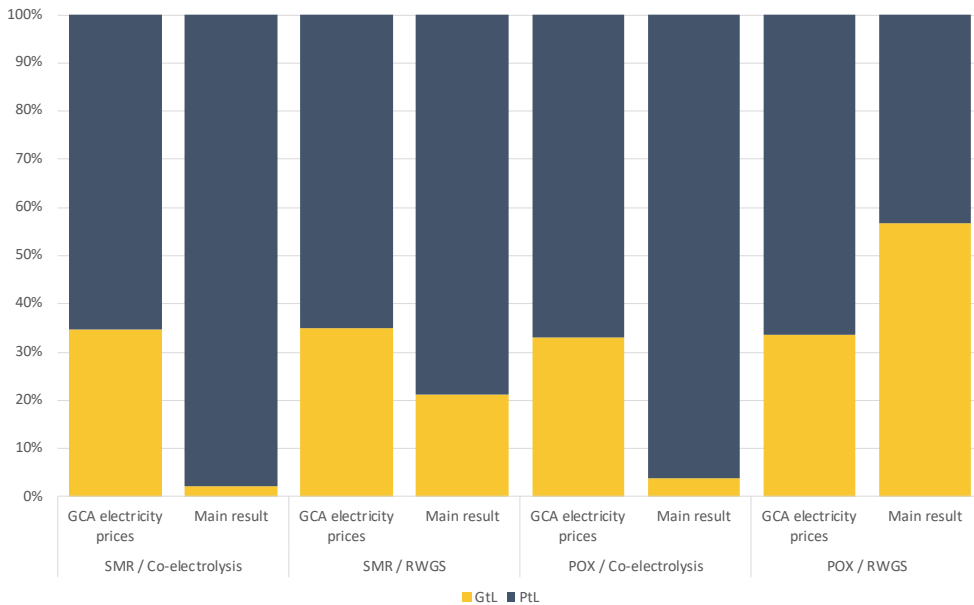
Figure 9.5: *Proportion of syngas produced from GtL and PtL between the scenarios 1.3 SMR / Co-electrolysis, 1.3 SMR / RWGS, 1.3 POX / Co-electrolysis and 1.3 POX / RWGS compared with the corresponding syngas production proportions from the main results with the electricity price from ST.*

Here, it can be seen that contrary to what might appear obvious, GtL produces a larger proportion of the total syngas compared to the simulations with electricity prices from ST. This can be explained by the high spread in the electricity prices. While the average price might be lower, there are many more hours with quite high prices as well, in which syngas can either be produced from GtL or extracted from a storage. However, naturally, syngas can not always be extracted from the storage, if the inventory level is zero. In these hours, the plant would then choose to produce syngas by GtL. Therefore, the proportion of syngas from GtL would be higher, but most of the syngas produced from PtL would still be based on a feedstock of free electricity, which would naturally reduce the overall costs.

It can be seen that the case of scenario *1.6 POX / RWGS* shows a different trend than the remaining - as it did in the main results. Here, while the three other configurations show a larger proportion from GtL when simulating with the GCA prices, this scenario results in a smaller proportion. In the main results, this scenario produced more syngas from GtL when methane was produced from methanation rather than biogas upgrading, which could be explained by the less costly CO_2 that could then be acquired from biogas upgrading, and the fact that the production costs for POX and RWGS showed to be fairly close, making a single parameter more likely to be decisive. The reason why RWGS produces more of the total syngas with the GCA prices can likely be explained by the fact that the average production costs from RWGS and POX were very close in scenario *1.6 POX / RWGS* and that an average reduction in the electricity prices would mean that many of the hours, that in the main scenario would lean towards POX by a slight margin, here is not able to economically compete with the lower electricity price.

Since there is such a spread in the electricity prices it can also be observed from the hourly productions that storages play a larger role. This is due to the fact that e.g. hydrogen and CO_2 storages become significantly more feasible as there are more hours with near free production, in which hydrogen and CO_2 can be stored despite not being demanded in that hour. Therefore, higher investment costs can be justified as the hours with zero-prices on electricity can be better utilized. Figure 9.6 shows the invested storage capacities from the ADAPT module in Sifre from scenario *1.5 POX / Co-electrolysis* with the electricity prices from GCA compared to the storage capacities for the main result of the same scenario.

From the figure, it is clear that storages play a more significant role when the prices fluctuate as they do in GCA. It can be seen that especially CO_2 and hydrogen storages is shown to become more feasible with the GCA electricity prices. The main results showed no desire to invest in any hydrogen storage, while the capacity invested in in this sensitivity scenario is almost 2000 MWh, which approximately corresponds to the hydrogen consumed in six hours of continuous steady syngas production from co-electrolysis. Furthermore, while the storage of CO_2 showed to be the most feasible storage in the main results as well, it was to a different degree. In this sensitivity scenario, the CO_2 storage can be seen to be over 2000 MWh, which would correspond to approximately 7,800 tonne of CO_2.
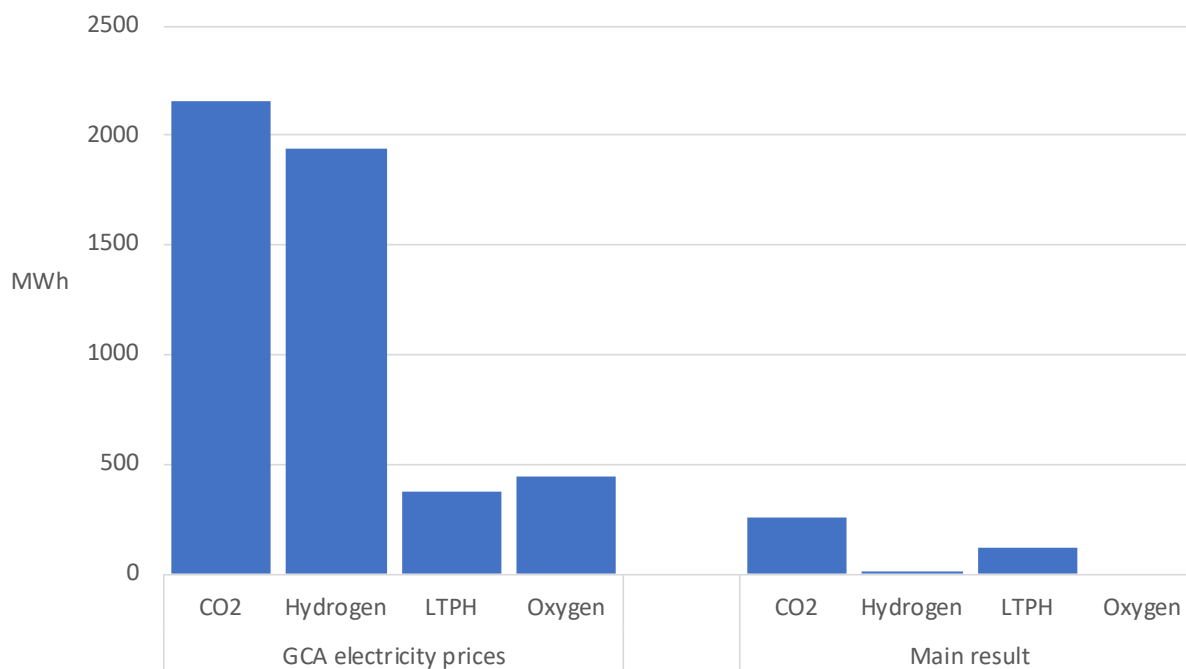
Figure 9.6: *Comparison of the storage capacities for CO_2, hydrogen, LTPH and oxygen for scenario 1.5 POX / Co-electrolysis using the electricity prices of GCA and the storage capacities of the same scenario from the main results.*

9.3   Demand for Negative CO_2 Emission

The closer society comes to being a zero-emission society, the more the shadow price of GHG increase, as the most cost-efficient measures are usually chosen first. This means that removing all GHG emissions can result in a very high socioeconomic cost. Therefore, in the future, it might be more feasible to continue emitting GHGs from certain sources and then installing capacity for capturing this amount from point sources such as biomass or waste incineration or from DAC, and then storing this equivalent amount of biogenic CO_2 so that a net zero GHG emission can be reached by still emitting some fossil GHG. However, this means that the liquid fuel production plant might not be able to purchase CO_2 at the same price as the production cost from CC or DAC, as there might be a market for this CO_2 reduction. The higher the demand for CO_2 reduction, the more costly production methods would be deployed, increasing the price of CO_2. In the main results, this CO_2 market has been simulated, as shown in Figure 7.5, by a demand of CO_2 reduction and a set of biogenic CO_2 producers. Here, the marginal producer would be setting the price of CO_2. The purpose of this sensitivity analysis is to investigate the effect of society's demand for a larger CO_2 reduction, meaning that fuel production plants would have to pay more to acquire CO_2. In order to provide a more in-depth picture of how the jet fuel production would be affected by a higher CO_2 price, three different CO_2 reduction demands have been investigated; 5 Mt, 10 Mt and 15 Mt. The sensitivity analysis has been performed in scenario *2.5 POX / Co-electrolysis*, as it proved to be the most feasible hybrid configuration and in order to include all possible sources of CO_2, an upstream production of methane from biogas upgrading has been assumed.

Recalling from Section *8.1.4 CO₂ as a Commodity*, this study has included nine different CO_2 production costs, in which four different costs for CO_2 reflect CO_2 from biogas upgrading including transportation by different methods and distances, three different CO_2 costs reflect CO_2 from DAC and two different CO_2 costs reflect CO_2 from CC of waste and biomass incineration. In the main results for scenario *2.5 POX / Co-electrolysis* the average cost of CO_2 was 47.5 EUR/tCO₂. Recalling from Figure 7.5 in Section *7.2.8 CO₂ Production and Consumption*, when CO_2 is to be stored, it is imposed an extra cost of 31.8 EUR/tCO₂ [69].

9.3.1 Resulting Jet Fuel Prices

The interesting values to investigate in this sensitivity is the cost of producing CO_2, cost of producing syngas and the resulting jet fuel price with the three national CO_2 reduction demands. It is valuable to investigate if the jet fuel plants could potentially be part of the system that delivers the CO_2 reduction 2050. In order to do so, it will be evaluated what delivering this reduction demand solely from the jet fuel plant will do to the resulting jet fuel price. The resulting prices can be seen in Figure 9.7.

	Main Scenario	5 Mt Reduction	10 Mt Reduction	15 Mt Reduction
CO2 - Reduction demand (EUR/tCO2)	79,3	91,6	97,9	125,0
CO2 - Fuel prodution (EUR/tCO2)	47,5	59,8	66,0	93,2
Syngas	24,0	25,1	25,6	28,1
Jet Fuel	30,2	31,3	32,4	35,0
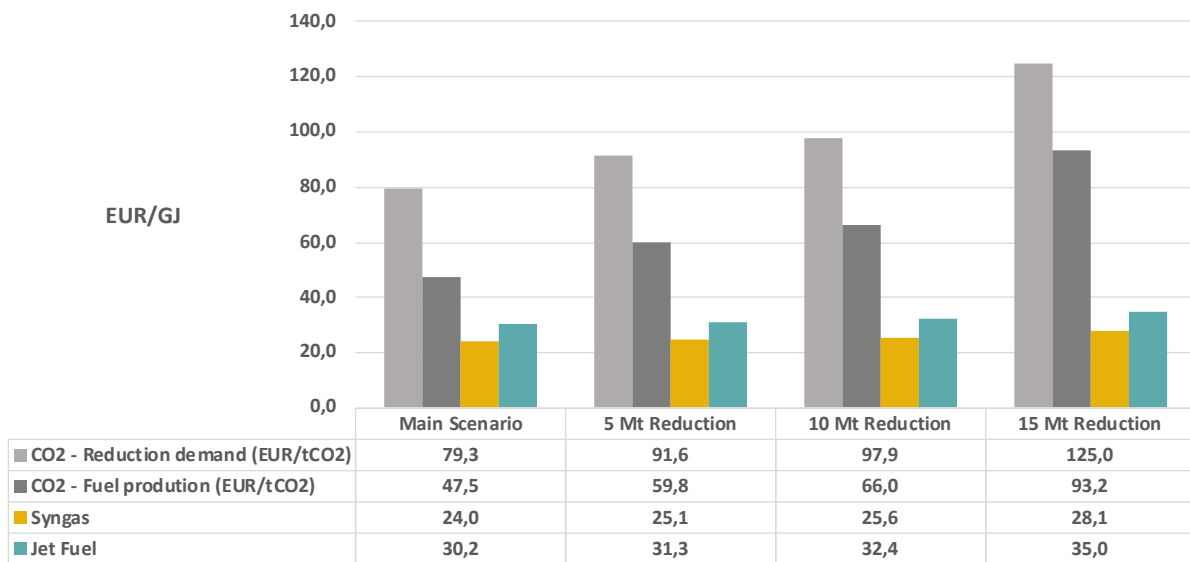
Figure 9.7: *Comparison of the resulting area prices from the main result in scenario 2.5 POX / Co-electrolysis along with the resulting area prices for the sensitivity of having to acquire more costly CO₂ when the demand is higher. While the area price of CO₂ increase significantly, the resulting syngas and jet fuel price is more robust to changes in CO₂ costs.*

The figure shows that as the demand for CO_2 reductions increase, so does the jet fuel price. This is mainly due to the higher production cost of CO_2. It can be seen that while the cost of CO_2 increases significantly, especially when the emission reduction increases from 10 Mt to 15 Mt, the syngas and jet fuel price is more robust to this change. From 10 Mt to 15 Mt, the CO_2 cost increases by more than 40%, while the resulting jet fuel price only increase by less than 10%, since the cost of CO_2 only pose a smaller part of the total jet fuel price, the jet fuel price is less affected by larger changes in the cost of CO_2.

As mentioned earlier, in order to supply the demand for CO_2 reduction, a cost of piping and storage must be accounted for. Therefore, the CO_2 price at the liquid fuel production site still dictates the price of CO_2

related to the reduction demand, but this price is however 31.8 EUR/tCO$_2$ higher due to the cost of piping and storage. This price difference can be seen in Figure 9.7. The CO$_2$ reduction price resembles that shadow price of carbon capture and storage (CCS).

9.3.2   Dynamics

It can be seen in Figure 9.7 that the CO$_2$ price is relatively constant from the main results through the sensitivity scenario with a required 10 Mt CO$_2$ reduction. This can be explained by this CO$_2$ being provided by CO$_2$ sources that are relatively close in cost per tCO$_2$. Figure 9.8 shows the CO$_2$ consumption from the main result and the three sensitivity scenarios based on scenario *2.5 POX / Co-electrolysis*. It is interesting to investigate which CO$_2$ resources are activated first. Recalling from Figure 8.6 in Section *8.1.4 CO$_2$ as a Commodity*, the CO$_2$ merit order showed that the least costly CO$_2$, by a significant margin, could be acquired from collecting CO$_2$ from biogas upgrading, as it was assumed that the fuel costs of biogas and electricity would be covered by the revenue from selling methane, and therefore, the cost of CO$_2$ would be zero. Therefore, the only cost connected with acquiring this CO$_2$ at the fuel production plant, would be the transportation, in which piping would outperform trucking for both 30 and 100 km distances. However, only approximately 1,000 kt can be acquired from biogas upgrading, meaning that even for the main result, other sources should be activated, increasing the price of the CO$_2$ area. This would in most cases be CO$_2$ from waste incineration at an average cost of 45 EUR/tCO$_2$. Figure 9.8 shows, that exclusively for jet fuel production, the plant consumes 2,450 kt of CO$_2$. Here, the majority of CO$_2$ is produced from CC of waste incineration with almost 1,500 kt. In the same scenario, 58 and 2 tonne would be acquired from DAC and CC of biomass incineration, respectively.

In Figure 9.8 it can be seen that already in the main scenario, almost all of the potential of CC from waste and biogas has been utilized. When a reduction demand of 5 Mt CO$_2$ is included, it will mostly be supplied from the more costly DAC unit, as it increases from 58 tonne to more than 4,600 kt, effectively supplying the majority of the reduction demand. When the reduction demand is at 5 Mt CO$_2$, CC from biomass only activates in relatively few hours, similar to the main result. CC from biomass will only be utilized fully when the reduction demand increases to 15 Mt, while DAC increases to more than 12 Mt. For the reduction demand of 15 Mt, the resulting DAC capacity has been found to be 411 MW, which corresponds to almost 1,5 kt CO$_2$ per hour, or 35 kt per day.

In Figure 9.7, it could be seen that the average yearly cost of CO$_2$ increased with the increasing demand for CO$_2$ reduction. This can be explained by the fact that, as the consumption of CO$_2$ increases, more costly production units must be activated. For the main result, the marginal supplier in far most hours could be seen to be the CC from waste incineration, as the yearly average cost was found to be 47.5 EUR/tCO$_2$. As mentioned, the cost of waste has been assumed to be zero, which would mean that the production cost of CO$_2$ from waste incineration should be equal to the cost of capture, which has been found to be 45.3 EUR/tCO$_2$ [44], as mentioned in Section *4.2.5 Carbon Capture*.

	Main	5 Mt Reduction	10 Mt Reduction	15 Mt Reduction
■ Biogas	965.215	989.793	990.420	990.443
■ Waste	1.487.849	1.690.607	1.700.940	1.700.941
■ DAC	58	4.656.347	7.981.259	12.300.726
■ Biomass	2	102.996	1.767.346	2.447.638
– Total consumption	2.453.124	7.439.743	12.439.965	17.439.747
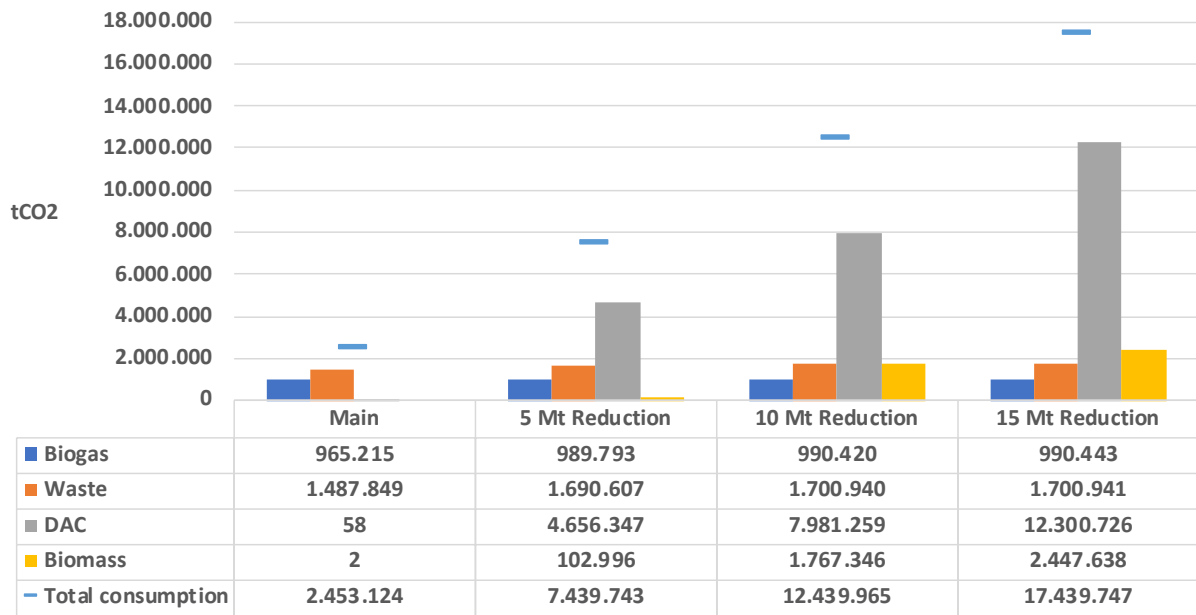
Figure 9.8: *Total consumption of CO_2 both the main result and the sensitivity of providing 5, 10 and 15 Mt negative CO_2 emissions. The columns show which source the CO_2 is acquired from, and it can be seen that the first source to be fully utilized is from biogas upgrading, which is close to fully collected in all scenarios - both the main result and the sensitivities. Then, CO_2 from waste is collected, and lastly, DAC and CC from biomass is utilized, in which DAC will be used first, and likely when the electricity prices are low.*

In Figure 9.9 the yearly average prices of CO_2 can be seen as an overlay on the CO_2 merit curve that was shown in Section *8.1.4 CO_2 as a Commodity*. Here, a clear tendency of increasing average CO_2 prices with increasing consumption, can be seen. It is obvious from the figure, that as the reduction demand of CO_2 increases, the more often the more costly CO_2 sources must be activated. In the main result, the yearly average cost of CO_2 can be seen to be 47.5 EUR/tCO_2, as previously mentioned, which is slightly higher than the merit curve would suggest. This can be explained by the smaller portion of CO_2 that is produced from DAC and CC of biomass incineration, as shown in Figure 9.8. This would mean, that in those hours the marginal supplier would be either of these two, increasing the price of all CO_2, resulting in this slightly higher average cost.

However, the average yearly CO_2 cost for both 5 Mt and 10 Mt can be seen to be lower than either of the suggested marginal supplier. This can be explained by the fact that in many hours during the year, a less costly production unit will be the marginal supplier at a significantly lower cost, e.g. DAC in hours where the electricity cost is 0 EUR/MWh, which means that the yearly cost is more likely closer to a weighted average of all activated production unit below the demand. Furthermore, the more CO_2 that is produced from DAC the more fluctuations will be seen in the CO_2 prices, as DAC is very dependent on the electricity price.

The average cost of CO_2 when society has a demand for CO_2 reductions of 15 Mt can be seen to increase to 93 EUR/tCO_2. When the demand increases to this high amount, it is likely that the DAC unit is unable to utilize the synergies of the fuel production plant, as can be seen in the figure, in which the 15 Mt demand

lies outside the potential for DAC with utilization of LTPH. This means that there are many hours during a year in which the highest electricity prices would result in significantly higher CO_2 prices due to the DAC being the marginal supplier of CO_2.
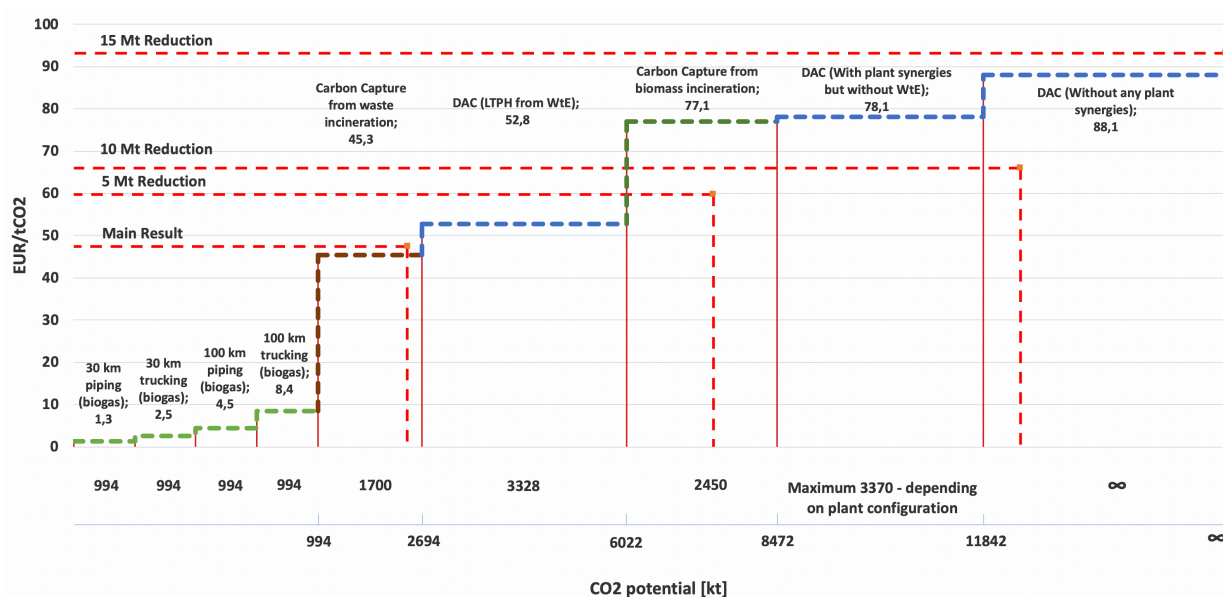
Figure 9.9: *Illustration of the activated CO_2 sources for the consumption in the main result compared with the consumptions when a 5 Mt, 10 Mt and 15 Mt CO_2 reduction demand is included. As mentioned in Section 8.1.4 CO_2 as a Commodity, the price set for each source is a yearly average, in which the hourly costs varies with especially electricity price. Therefore, the average area prices for CO_2 with different consumptions will not fit directly with the price of the marginally activated source, but rather be a weighting of all activated production units. However, the figure clearly shows that the higher consumption of CO_2 results in increasing yearly average CO_2 prices as the more costly sources are activated more often.*

While the specific values do not fit perfectly on the yearly average prices, nor should they, as explained earlier, the overall tendency is clear. A large increase in the average price of CO_2 can be seen from the main result to a demand for reductions of 5 Mt CO_2, which fits with the more significant increase in price from CC from waste incineration to CC from biomass incineration. Furthermore, a much less significant increase can be seen when increasing the reduction demand from 5 Mt to 10 Mt, due to the fact that much of this extra CO_2 consumption would be supplied by either CC of biomass incineration or DAC without the possibility of utilizing LTPH from waste incineration of which the average cost per tCO_2 is very similar. Lastly, the larger increase from increasing the demand from 10 Mt to 15 Mt can be seen by the more significant increase in average cost for the DAC unit that can not utilize any synergies from fuel production, and which would be forced to produce at higher electricity prices as well.

9.4   Future Development of Electric Steam-Methane Reforming

A technology, within liquid fuel production, that has been gaining increasingly interest is the electric steam-methane reforming (eSMR) technology by Haldor Topsoe [103]. Compared to the conventional SMR technology, eSMR has several benefits. First, conventional SMR is driven by a HTPH source in order to heat up the methane-steam mixture in the reactor. In order to produce this HTPH, gaseous hydrocarbons are

combusted in order to reach the temperature level of approximately 900 °C. The eSMR technology is fully electrically driven by direct resistive heating of the tubes that the methane-steam mixture flows within [104]. Another benefit with this electrification of the reformer is that no combustion space is required making the eSMR unit a 100 times smaller than a conventional SMR unit [103]. Furthermore, eSMR can operate using raw biogas instead of methane so that neither biogas upgrading nor methanation is required in order to produce syngas. This possibility of running the eSMR unit on biogas is primarily a decentral solution where the production of syngas and the crude oil from LTFT is produced on the biogas production site. However, eSMR can also be implemented on a central production site of liquid fuels, where it utilizes methane as fuel input instead of biogas.

In this sensitivity analysis both the decentral and central solution of producing liquid fuels through eSMR will be investigated in several liquid fuel production configurations. These configurations include the ones where conventional SMR is already a part of the production chain, i.e. pure GtL using SMR and the hybrid productions configurations with SMR and co-electrolysis, and SMR and RWGS. In these production configurations, the conventional SMR unit is replaced by an eSMR unit.

9.4.1   Sensitivity Analysis Framework

Since the eSMR technology is still in the development phase and there are trade secrets related to the technology, an approximation of the technology has been assumed. The approximation differs depending on whether it is in a decentral liquid fuel production configuration or a central configuration. As mentioned earlier, the decentral eSMR uses biogas as fuel input. The proportion between biogas and electricity in the fuel consumption of the unit has been assumed to have the same proportion as the one between methane and HTPH in the conventional SMR unit, i.e. 81.3% methane and 18.7% HTPH. Because of the higher carbon content in the biogas, the eSMR unit is assumed to produce syngas with a H_2:CO ratio of 2:1 instead of 3:1 as in the conventional SMR unit. Therefore, the decentral eSMR unit does not require a RWGS unit in order to adjust the H_2:CO ratio in the syngas.

The approximation of the central eSMR is rather similar to the conventional SMR. The only difference between the two units is, that instead of HTPH the eSMR uses electricity as fuel input. The output from the eSMR unit is assumed to be same as conventional SMR i.e. syngas with a H_2:CO ratio of 3:1. The total effeciency of the two eSMR units have been assumed to be the same as the conventional SMR unit, with a total efficiency of 85.5%.

Even though it might be expected that the CAPEX and OPEX of eSMR are lower compared to conventional SMR due to the simpler and smaller unit setup, the CAPEX and OPEX are assumed to be the same as for conventional SMR. This is because no economical figures of eSMR are available. An overview of the energy inputs, outputs, total efficiencies, CAPEX and OPEX of the different eSMR units and the conventional SMR unit can be seen in Table 9.1.

In order to be able to evaluate the eSMR technology in a liquid fuel production configuration, the results are compared with the conventional SMR technology in a liquid fuel production configuration. For the centrally located liquid fuel production plants, the scenario with eSMR can be directly compared to the

Table 9.1: *The table gives an overview of the input and output energies, total efficiencies, CAPEX and OPEX of the conventional SMR unit and the decentral and central eSMR units used in Sifre and ADAPT.*

	Inputs [% energy of total input]	Outputs [% energy of total input]	Total efficiency [total output /total input]	CAPEX [M€/MW]	OPEX [€/MW/y]
Steam Methane Reforming (SMR)	Methane = 81.28% HTPH = 18.72%	Syngas (3:1) = 85.45%	85.45%	0.064	3,210
Electric Steam Methane Reforming (eSMR) (Decentral)	Biogas = 81.28% Electricity = 18.72%	Syngas (2:1) = 85.45%	85.45%	0.064	3,210
Electric Steam Methane Reforming (eSMR) (Central)	Methane = 81.28% Electricity = 18.72%	Syngas (3:1) = 85.45%	85.45%	0.064	3,210

main results that include conventional SMR. However, this is not the case for the decentrally located liquid fuel production. Therefore, results for liquid fuel production by both SMR and eSMR have been generated in order to compare the decentral eSMR solution with the decentral SMR solution. Some of the surrounding framework conditions have been adjusted for this purpose since every liquid fuel production configuration until now has been a part in a centrally located system. Some of the synergies that can be found centrally are not the same as for a decentral production site. In this sensitivity analysis is has been assumed, that no waste and biomass incineration are located at the decentral liquid fuel production site. This means that the utilization of LTPH and captured CO_2 from waste and biomass incineration is not a possibility at the decentral production site. However, excess heat from the production units within the liquid fuel production chain, methanation, LTFT etc., can still be recirculated for use internally. Obviously this is only relevant for the conventional SMR unit that uses HTPH and not the eSMR unit.

9.4.2   Sensitivity Analysis Results

The resulting yearly average jet fuel prices for every scenario with eSMR, including its respective comparable scenario with SMR, can be seen in Figure 9.10. As mentioned earlier, the eSMR sensitivity analysis have been conducted on all scenarios that included a conventional SMR unit, where that SMR unit has been replaced by either the decentral or central eSMR unit depending on the surrounding system. Therefore, the sensitivity analysis have been conducted on three different types of liquid fuel production configurations - pure GtL with either SMR or eSMR, hybrid where SMR or eSMR are combined with co-electrolysis and hybrid where SMR or eSMR are combined with RWGS.

First, consider only the decentral scenarios. Generally throughout the decentral scenarios, a clear pattern can

be seen. The jet fuel price of every decentral scenario with eSMR is lower than the corresponding scenario with SMR. Recalling from Section *9.4.1 Sensitivity Analysis Framework* the main difference between the decentral eSMR and SMR units are the fuel inputs and outputs. Where conventional SMR has methane and HTPH as fuel inputs, eSMR has raw biogas and electricity. Since methane is produced by raw biogas through either biogas upgrading or methanation, the resulting methane price is obviously higher than the price of raw biogas. Recalling from Section *8.1.3 Upstream Methane Production* methanation results in a higher methane price compared to biogas upgrading. Therefore, it can also be seen that the jet fuel price difference between decentral SMR and eSMR is generally higher in the methanation scenarios. This is because the decentral eSMR uses biogas, which has a fixed fuel price of 17.6 EUR/GJ, as primary fuel throughout every scenario whereas decentral SMR uses methane, and since the methane price is generally higher in the methanation scenarios this results in a higher jet fuel price difference than the biogas upgrading scenarios.

Furthermore, the price difference between the decentral eSMR and SMR scenarios also comes from the fact that the SMR unit uses HTPH, which has to be produced through a gas boiler using either methane, fuel gas or hydrogen. Compared to having just an input of electricity to the unit this results in higher fuel costs for the conventional SMR unit compared to the eSMR unit.

| | GtL | | Hybrid | | | |
| | eSMR or SMR | | eSMR / SMR combined with Co-electrolysis | | eSMR / SMR combined with RWGS | |
	Methanation	Biogas Upgrading	Methanation	Biogas Upgrading	Methanation	Biogas Upgrading
Decentral SMR	32,8	26,9	34,2	33,8	37,6	36,8
Decentral eSMR	25,3	25,3	30,3	30,6	33,8	34,0
Central SMR	32,7	26,9	32,5	29,9	34,0	33,5
Central eSMR	35,2	27,3	31,9	31,4	34,2	33,3
Low Jet Fuel Price	10	10	10	10	10	10
High Jet Fuel Price	20	20	20	20	20	20

Figure 9.10: *The figure shows the yearly average jetfuel prices for every scenario with eSMR, including its respective comparable scenario with SMR. The results for "Central SMR" are equivalent to the respective scenario results in the main scenarios.*

When considering the central scenarios, the jet fuel price pattern is not as clear as with the decentral scenarios. One of the reasons for this is that the central eSMR unit is not as different from the conventional SMR unit with the only difference being that the HTPH fuel input is replaced by an input of electricity in the eSMR unit. The two different units both have methane is their primary fuel input. Furthermore, on the central production sites it is assumed that low-priced LTPH from waste and biomass incineration can

be utilized an boosted in temperature through a gas boiler in order to produce HTPH for the SMR unit. Therefore, the central eSMR unit does not have the same advantages as the decentral eSMR does. The result of this is a jet fuel price difference that does not show any clear pattern since the jet fuel price from using eSMR is higher in three scenarios and the jet fuel price from using SMR is higher in the other three scenarios. The largest price difference in the central scenarios can be found in the pure GtL scenario with methanation, where the jet fuel price from using conventional SMR is 2.5 EUR/GJ lower than when using eSMR.

Finally, comparing decentral liquid fuel production with central production through either SMR and eSMR it can be seen, that throughout the hybrid scenarios there are no clear winner among decentral eSMR and central SMR or eSMR. Decentral SMR, however, is outperformed in every hybrid scenario. With that said, the hybrid configurations with either SMR or eSMR in combination with co-electrolysis results in lower jet fuel prices compared to the hybrid configuration with RWGS.

When considering pure GtL, the decentral production using eSMR seem to perform better than the other production solutions, resulting in lower jet fuel prices. It should however be mentioned, that the pure GtL solution is not scale-able to the entire Danish demand of jet fuel due to the biogas constraint. As with the main scenarios, the pure GtL scenarios in this sensitivity analysis only have to supply a demand of 25 PJ jet fuel.

The syngas production proportion between GtL and PtL in the hybrid scenarios of this sensitivity analysis have also been investigated. The results can be seen in Figure 9.11. Recalling from the results of the main scenarios in Section *8.1.2 Hybrid Configurations*, the syngas production proportion from GtL in the hybrid configurations with an upstream production of methane by biogas upgrading tend to be between 50-60%. The exact same result can be seen with every biogas upgrading scenario in this sensitivity analysis, as the syngas production proportion from GtL in every hybrid configuration located centrally or decentrally, with either eSMR or SMR falls between 50-60%. Furthermore, the methanation scenarios also show roughly the same result as the main scenarios - PtL has a higher influence in the methanation scenarios. This can be explained by the price of methane which tends to be higher in the methanation scenarios as explained earlier. That is with the exception of the decentral eSMR which uses biogas instead of methane as a fuel input. Therefore, the syngas production proportion from GtL, in the decentral hybrid configurations using eSMR, tends to be higher because of the lower cost of biogas compared to methane. There is however one outlier i.e. the decentral hybrid configuration using SMR and RWGS in the methanation scenario. In this scenario 96.5% of the syngas needed for jet fuel production is produced in the SMR unit. This behaviour is unexpected since the price of methane in the methanation scenarios tends to be higher than in the biogas upgrading scenarios. However, the production proportion from GtL being higher than in the hybrid configuration with SMR and co-electrolysis does seem plausible, since the production cost of co-electrolysis is lower than RWGS. An explanation of the fact, that the production proportion from GtL, in the corresponding scenario with SMR and RWGS and biogas upgrading, is lower than in the methanation scenario might be found in the fact that

when producing methane for GtL the secondary product is CO_2 which can be utilized in PtL. This synergy can not be found when using methanation which might be the reason that the proportion from GtL is higher.
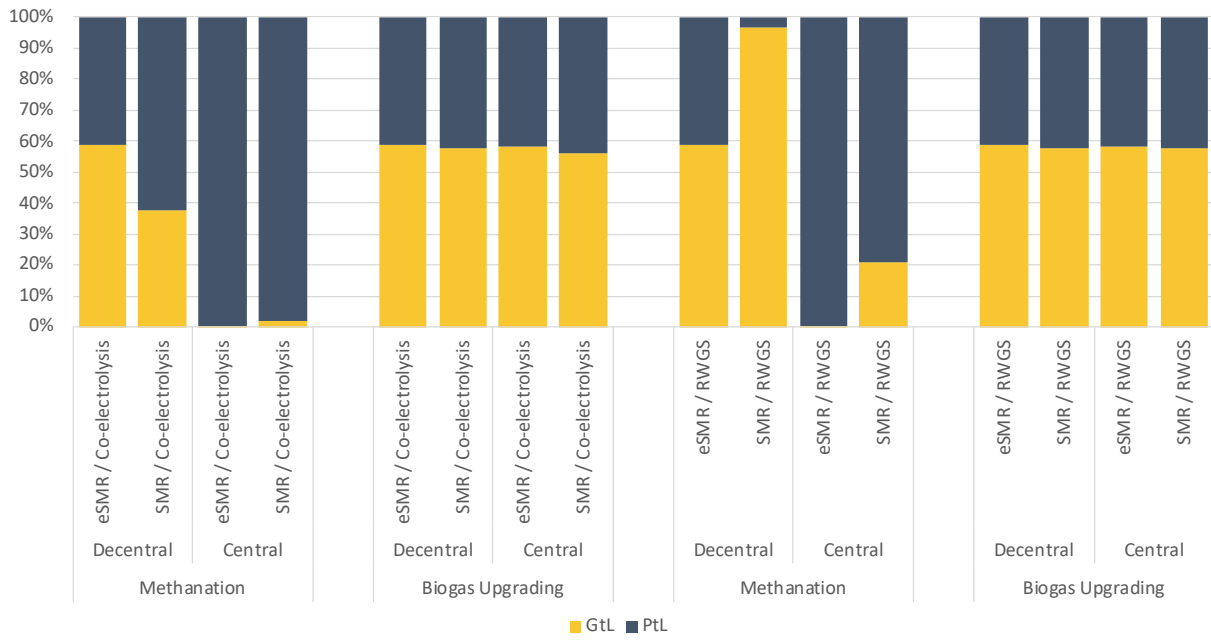
Figure 9.11: *The figure shows the syngas production proportion between GtL and PtL in the hybrid scenarios of this sensitivity analysis. As with the results for the jet fuel prices, the results for SMR in centrally located hybrid configurations are equivalent to the respective scenario results in the main scenarios.*

10   Discussion

Many assumptions, limitations, inclusions and adaptations has been made to realize the goal of this study, which give reason to discussion. Obviously, the validity of the results are of central concern, and in order to be as transparent as possible, this discussion will be used to cover uncertainties, thoughts and the choices made in the project. All significant elements will be touched upon and their individual potential influence on the result will be discussed. The discussion will be split in sub-headings to provide a better overview and help the reader.

10.1   Assumptions and Delimitations

As mentioned, many assumptions are inevitably made when doing large studies of future prospects. Especially when doing studies on potential futures with a temporal scope of 2050. However, that does not prove these analyses less valuable, as they help shape the path towards that future. In such a study, the chosen assumptions potentially have a large impact on the results, and in many cases, these assumptions are based on estimates - well-documented and reasoned estimates, however.

10.1.1   Technology Data

The data for the different technologies that has been used in this study, has been made from a larger literature study of the field of syngas production, gas-to-liquid (GtL), power-to-liquid (PtL) and more. This study made up the majority of the first part of the project period, in order to provide a well-documented value-chain for fuel production, and account for potential efficiency considerations that could otherwise show a more positive case than reality would support. In this study, most literature, from which the efficiencies were chosen, were based on practical experience from tests and experiments. Naturally, it is difficult to predict the future development of a technology - especially those that are still not fully commercialized. The economics of central technologies, such as co-electrolysis, could potentially change significantly if the efficiency were to either be 10% lower or 10% higher, since it was found that the majority of costs were associated to the fuel consumption of electricity and methane. Coming up with qualified lower and higher estimates for potential efficiencies would be a time-consuming process, especially doing it individually for every technology in every scenario, and therefore, this was considered out of the scope. However, the model has been made in such a manner that if new technology data is available, the original data can easily be substituted with new and simulated within the same framework.

Direct air capture (DAC) is a technology that is still in its earlier development stages, and only a few plants, of which some are only pilot projects, are currently running, with the first plant deployed in 2017. The technology data for DAC has been based on assumptions made from the literature study. Climeworks, a company that has been pioneers within the development of DAC units, has predicted a future cost per tCO_2 below 100 USD. This prediction is fairly close to the data used in this project, with smaller differences in the assumption of electricity and heat prices.

10.1.2   Biogas Potential

As described earlier, the amount of biogas has been based on [11], in which the total biogas production potential was found to be 94 PJ. In this report it has been assumed, that 85% of that biogas potential will be economically feasible, resulting in a total of 80 PJ produced. In order to account for other significant consumptions of renewable gas, the general consumptions from [18] has been assumed, which account for gas for the industry, transportation and electricity network balancing. In that report, 20 PJ were found to be used for heavy-duty transportation. However, a recent internally study at Energinet suggests, that hydrogen will be the more feasible solution for this heavy-duty transportation. This assumption builds on the prediction that hydrogen will be available for fueling, and the infrastructure to support this has not been included in the analysis. It is, however peripheral to this study, and the costs for the hydrogen fuelling stations would not directly affect the prices of jet fuel. That being said, the demand for hydrogen for heavy-duty transportation might cause a higher demand for infrastructure of hydrogen. Infrastructural costs are generally recovered by imposing tariffs on the transported energy, which means that, if the demand for hydrogen was higher, e.g. by a demand from heavy-duty transportation, the tariff that were to be imposed on the consumed amount of hydrogen would be lower since the investment cost of the hydrogen infrastructure would be recovered by more units of energy. In Section *8.2 Case Study of Funen* it was found that, hydrogen infrastructure could generally reduce the price of jet fuel, in which potential strains in the electricity network could also be mitigated by hydrogen piping. Having the synergy between the production of liquid fuels and the heavy-duty transportation, i.e. a shared use of hydrogen infrastructure, could potentially lower the jet fuel price even more.

10.1.3   Infrastructural Costs

The cost of infrastructure can potentially be substantial. In this study, infrastructural costs for hydrogen and CO_2 piping has been included in specific analyses regarding these. The costs of potential infrastructural expansions in both the gas and electrical network have, however, not been included in the modelling. This is because when working with a temporal scope of 2050, it is difficult to give reasonable estimate of potential infrastructural expansions, and the need for expansions would not necessarily be due to liquid fuel production only. In 2050 there might be other demands that could induce a need for infrastructural expansions which is why the investment costs for such expansions should not necessarily be imposed onto the jet fuel price. The natural gas grid does not extent to all areas of Denmark, and for fuel production plants to be located at the central locations, some expansion of this grid would be needed, e.g. natural gas piping from outside Aarhus to the site at which the waste incineration is currently located. However, the costs that can be found when injecting upgraded or methanated biogas to the grid has been included in the modelling as part of the CAPEX and OPEX. In order to utilize all biogas for methane production and transport using the gas grid, every biogas plant must be connected to said grid. An analysis of these potential costs could be considered a study all by it self, and including it in the modelling of jet fuel in Sifre would eventually impose the cost of the infrastructural expansion on the cost of jet fuel, which would not necessarily be the case in reality.

10.1.4   Location of Refining of Syncrude

Using FT for fuel production is a well-known method that is deployed several places in the world. In this study, the FT unit and the refining has been assumed to be located at the same location - partly due to modelling simplification and partly due to the focus of presenting prospects from utilization of synergies that can be found. However, refining of syncrude would not necessarily have to be located together with the syncrude production. Today, oil is extracted from the underground and transported to the refining site via tanker or oil pipeline. The refining of syncrude and conventional crude oil is comparable in many ways, and having fewer large refineries could prove feasible due to economies of scale [105], [106]. Today, two large oil refineries are located in Denmark, and these two refineries produce what corresponds to more than 40% of the total Danish energy consumption yearly [107]. In this study, entirely new equipment for refining of syncrude has been assumed, however, the existing refineries could potentially be retrofitted slightly in which no new refining plants would be required - though the current refineries would likely need some adjustments. This would reduce the overall investment costs of the fuel production. A future study with a comparison between retrofitting existing oil refineries and the central-location refineries from this study, that utilizes synergies but does not gain from economies of scale, would be interesting.

10.1.5   Modelling

A model can always be made more realistic and more detailed and delimiting is done to every model. The *Fuel Production Model* that has been made for this study is no exception, and several assumptions were made, in order to delimit the analysis, reduce the modelling time and keep the transparency of the results. With the use of Sifre to simulate the jet fuel prices, it has been necessary to fix the market prices of gasoline and ethanol from the LTFT synthesis. These prices has been assumed to be equal to second generation bio-ethanol, and the revenue from selling them has been deducted from the cost of production and thereby reducing the jet fuel price. In reality, a market for both gasoline and ethanol should be modelled, which would result in prices that are dependent on the demand. This demand has been considered out of the scope of this study. However, an analysis of the value of each outputs could be interesting, comparing the value of gasoline to jet fuel, and the fact that revenues from gasoline could force a production of jet fuel.

10.2   Results

Many different results have been found and documented in Sections *8 Simulation Results* and *9 Sensitivity Analysis*. Naturally, the validity of the results is of central concern and therefore, it is relevant to discuss findings from the modelling.

10.2.1   Main Results

Throughout the result section, the primary focus has been to investigate the effect on the jet fuel prices. Here, pure GtL and PtL plants have been compared to configurations in which both pathways are combined in the so-called hybrid configurations, that can been shortened to X-to-liquid. In general, it can be seen that

the lowest jet fuel prices can be found by pure GtL when the methane is produced by biogas upgrading. However, as it was described in the main result section, this configuration would not be able to supply the full demand of jet fuel in Denmark, and would therefore not be a viable solution, exclusively. Therefore, comparing these jet fuel prices can distort the picture of the hybrid configurations. More accurately, the jet fuel price from GtL with methanation should be a focus for comparison, as it is closer to being able to satisfy the total demand, though still falling short. This is where the hybrid solution shows its value. The hybrid configuration would indeed prove valuable. The lowest jet fuel price that is not from pure GtL was shown, in Figure 8.1, to be scenario *2.3 SMR / Co-electrolysis* at 29.9 EUR/GJ. In this scenario, the consumption of biogas falls within the limit of the biogas constraint. This result is valuable as it shows, that when the hybrid configuration is used, the methane used for GtL can be produced by biogas upgrading instead of methanation resulting in a lower methane price, while PtL can utilize the CO_2 produced secondarily from biogas upgrading, resulting in relatively low jet fuel prices while still being able to supply the entire demand of 50 PJ. When comparing this jet fuel price to the ones from pure GtL using methanation, it can be seen that, by quite a margin, the hybrid configuration can produce jet fuel at lower costs - more specifically, the jet fuel price would be between 8-10% lower from the hybrid configuration, compared to the two GtL configurations. The hybrid configurations would likely prove even more advantageous if ancillary services had been modelled, in which the plants could actually be paid to not produce from electricity, or to ramp up production from electricity depending on demand - this would not be possible in neither pure GtL nor PtL. Furthermore, the result of the Funen case study showed that when producing 5 PJ of jet fuel solely by PtL, a significant amount of strain is imposed on the electricity network. This result can likely be scaled to parts of the energy system of Denmark, meaning that using pure PtL to produce the entire demand of jet fuel would most likely strain the electricity network increasing the need for electricity infrastructure expansions. However, this could be mitigated through the hybrid plant configuration.

10.2.2   Case Study of Funen

The case study with hydrogen production at the western coast of Jutland is subject to some assumptions that can be discussed. First of all, the economies of scale of the hydrogen production and every conversion unit associated with the hydrogen production, i.e. electric boilers and heat pumps used for production of LTPH, is assumed to result in a 25% decrease in the investment cost and the fixed and variable O&M costs. This decrease might not be true, but since an analysis of the economies of scale for hydrogen production has been out of the scope of this study, the 25% decrease was used as a best estimate of what the benefits from economies of scale might be. Also, the original investment cost of the hydrogen pipe used in this study is merely an indicative investment cost excluding the cost of compressing the hydrogen to a higher pressure. The cost of compression is significant compared to the pipe cost and therefore an assumed cost of compression has been added to the pipe investment cost. This added cost resembles the cost of compressing upgraded biogas in order to inject it into the natural gas grid, and a deeper analysis of the compression costs related to hydrogen compression might have resulted in another cost.

Generally, the results showed, that the assumptions made for the analysis of hydrogen piping have a rather

important impact in the resulting jet fuel price. For the Funen case study, the hydrogen piping solution implemented for the hybrid plant configuration with POX and RWGS resulted in a jet fuel price of 25.4 EUR/GJ, which is equivalent to the lowest jet fuel price from the main scenarios - jet fuel produced solely by POX with an upstream methane production by biogas upgrading - with a price of 25.2 EUR/GJ. The average jet fuel price through every scenario with hydrogen piping was 27 EUR/GJ. Therefore, if these assumptions can be deemed reasonable, piping of hydrogen is seemingly a socioeconomically feasible supply of hydrogen and solution to avoid strain in the electricity network. However, an element that the hydrogen piping solution did not account for, is the fact that the production of hydrogen at the western coast of Jutland is a consequence from the need to balance the production of electricity from the NSWPH with the electricity demand. Throughout every hydrogen piping scenario, the supply of hydrogen from the western coast of Jutland to the liquid fuel production site in Odense, remained completely constant. This is because the actual production of electricity from the NSWPH, and the fluctuations that comes with it, has not been modelled. In reality, if the supply of hydrogen to the liquid fuel production would have to be independent from the production of electricity in the NSWPH, a large-scale hydrogen storage in the form of a cavern would be necessary, which is also something that Energinet is currently investigating [17]. This means that the resulting hydrogen price would be higher than the price found in this study, since this added cost for a large-scale hydrogen storage and the added cost of hydrogen infrastructure that follows with it, has not been accounted for. If this could alter the results significantly is difficult to determine, but it is certain that it would induce an increased hydrogen price resulting in higher jet fuel prices.

10.3   CO$_2$ Market

A simplified version of the market of CO$_2$ has been included in the modelling of the jet fuel production. This has been done to further investigate the sources of CO$_2$ that could prove most feasible in the future. However, the actual market price and market demand for CO$_2$ is very difficult to predict - especially since seeing CO$_2$ as a valuable commodity still lies far from the conception of CO$_2$ today. In order to fully investigate the cost of the CO$_2$, more sources of production could be taken into account, but most importantly, the demand for CO$_2$ should be further investigated.

This study has given preliminary results that could point towards a potential price of CO$_2$, but many factors would eventually end up setting the price of CO$_2$. The area of CO$_2$ should, in reality, likely be split in two separate sections; one with the trading of the physical CO$_2$ and one with trading of negative CO$_2$ emissions - perhaps in the form of certificates.

A market of certificates for negative CO$_2$ emissions would likely arise from the feasibility aspect that was brought up in Section *9.3 Demand for Negative CO$_2$ Emission*, in which it was described that reaching a total zero-emission society would likely be sub-optimal to being net-zero emitting, or climate neutral, in which some fossil emission is allowed as long as there is an equal amount of negative emissions, in the form of capturing and storing biogenic CO$_2$ from either bio-energy carbon capture and storage (BECCS) or DAC, resulting in net-zero emissions.

The market for physical CO_2 and the market for negative CO_2 emissions would not share the same price, but would likely be co-dependent. When considering the physical CO_2 market, the price on this market is dependent on the combined demand for physical CO_2, e.g. including the demand for CO_2 related to liquid fuel production and the demand related to producing certificates for negative CO_2 emissions. The price on the CO_2 market would then be set by the marginal producer of physical CO_2 that is deployed in order to supply the combined demand of CO_2. On the other CO_2 market - the market for certificates of negative CO_2 emissions - there would be a set of suppliers which are able to transport and store biogenic CO_2 at different prices. However, all these suppliers would be dependent on the price of CO_2 that is set on the physical CO_2 market. These suppliers would then only compete on the costs associated with transporting and storing CO_2, and the price on this market would then be set by the marginal supplier of negative CO_2 emissions, i.e. the last supplier that is deployed in order to transport and store the amount of biogenic CO_2 that matches the demand for certificates of negative CO_2 emissions. In this way the two markets would be co-dependent. The marginal supplier of physical CO_2 is likely to be either CC or DAC.

Uncovering all of the mechanisms that would exist on these two CO_2 markets would require an extensive analysis of several sectors such as agriculture, transportation, heat and power production etc. This has been considered out of the scope, and the simplified version of the market serves as an indication.

Being able to sell CO_2 from biogas upgrading in a market for physical CO_2 would likely reduce the marginal production cost of methane from biogas upgrading. For the specific biogas upgrading plant this would either result in a larger producer surplus or a lower price of methane, depending on if that specific plant were the marginal supplier.

Had a more in-depth analysis of a potential market for CO_2 been analyzed and used in the model, it could have been interesting to analyze if sources such as biomass would even be used for incineration with CC. In the future, even more applications could make use of biomass - perhaps with a higher willingness to pay for said biomass. Having modelled a full market for CO_2, it would be able to analyze if the biomass resource would be more feasible to burn and capture CO_2 from, or be used for other processes, such as pyrolysis to make an oil that similarly to syncrude can be used for fuel production.

10.4   Choosing a Pathway with Methane

The focus of this study has been to investigate the prospects of using the pathway of GtL and PtL for jet fuel production in 2050. This has been done to uncover the prospects for the complete production of the future Danish demand within a climate net-neutral energy system. However, since international aviation is not part of the 70% GHG reduction goal for 2030, the focus of the future jet fuel production is of somewhat less focus in the coming years. Therefore, this study aims at uncovering a jet fuel pathway that could still consider the 2030 goals of emission reductions. This has been done be incorporating technologies within the value chain that are more commercially mature that could, on the way towards taking part in the jet fuel value chain, provide emission reductions within other sectors that are included in the 70% goal. This

idea arose as it was found that bio- and electromethane could play a significant role in the production of jet fuel, and also help reduce the emissions from the industry, balancing of the electrical grid and other sectors significantly. The proposed framework for jet fuel production has thus considered a 2030 way point towards sustainable jet fuel production by utilizing commercially proven intermediate technologies.

The reason why looking as far as 2050 is relevant, while it is very unpredictable, is that it helps mitigate decisions, that might make sense on short-term, while they prove sub-optimal on a long-term. Therefore, having a 2050 system configuration to move towards helps making the most viable decision along the way towards 2050, while it might be slightly more costly in 2030.

10.5   Sensitivity Analysis

10.5.1   Global Climate Action Electricity Price

The sensitivity analysis shows that the largest sensitivities in the results can be found from the assumption of the fuel costs. Here, it was shown that especially the electricity cost could affect the jet fuel prices - and by a large margin. Using the electricity prices from the TYNDP scenario *Global Climate Action* (GCA), the jet fuel price could even reach those of today's fossil jet fuel prices, which is one of the major challenges with sustainable jet fuel production. While the result is interesting, and shows that, given large flexibility and many zero-cost hours of electricity, the jet fuel can reach very competitive prices, it should be noted that such prices are still relatively difficult to predict. The GCA prices are based on an energy system in which no PtX is included, which would likely smoothen the duration curve of electricity, since it would help balance the production and consumption side of electricity, creating fewer hours with zero-prices.

10.5.2   Electric Steam-Methane Reforming

Generally, throughout this study the main focus has been a central production of liquid fuels through different production configurations. A decentral production of liquid fuels was only a focus in the sensitivity analysis regarding the *electric steam-methane reforming* (eSMR) technology in Section *9.4 Future Development of Electric Steam-Methane Reforming*. This is because the eSMR technology is well suited for a decentral production of syngas since it is able to utilize raw biogas as the primary fuel input. The results showed that the solution with eSMR applied in decentral production of liquid fuels did in fact outperform the conventional SMR technology in several plant configurations, and more interestingly, it was also able to compete with the central production of liquid fuels in every scenario, while actually resulting in lower jet fuel prices in most of the scenarios. This begs the question; is a central production of liquid fuels, which has been the primary focus of this study, actually the most feasible method? As with the upstream methane production, which might very likely be a combination of conventional biogas upgrading and methanation in the future, it is very likely that the production of liquid fuels would be produced by a combination of decentrally and centrally located production plants. With that said, the decentral scenarios did assume that the final liquid products could be produced at the same site as where the syncrude from LTFT was produced. It is, however,

unlikely that the refining of syncrude would be located decentrally together with the syncrude production. As mentioned earlier in the discussion, only two large-scale refineries are located in Denmark indicating that refining clearly benefits from economies of scale, which is why it may not be feasible to place several decentral refineries together with a decentral production of syncrude. This means that there are some costs that have not been accounted for in the eSMR analysis, e.g. the cost of transportation of syncrude from the decentral production site to a centrally located refinery. Furthermore, there are some of the synergies that would not necessarily be the same when refining are not placed at the same site as the production of syncrude, e.g. re-circulation of fuel gas for use in production of HTPH. However, since the eSMR does not use HTPH as fuel input, this synergy is not utilized nearly as much in the eSMR scenarios as in the main scenarios meaning that this assumption might not alter the resulting jet fuel prices significantly.

10.6   LUP-Model

In earlier stages of the project period, the study was supposed to focus on an optimization of the distribution of the total jet fuel production capacity in Denmark. In order to do so, the production of jet fuel were to be modelled in two different models - one, which should be used to find the more feasible plant configuration and one in which the entire Danish energy system were modelled alongside with the purpose of investigating the optimal distribution of the production capacity among five specific locations, considering DH demands, grid constraints and biogas availability. This model was to be modelled within the full framework of *long-term development plan* (LUP), which is an ongoing Sifre model development at Energinet. Unfortunately, this model was not able to be completed in time, due to a significant amount of errors in Sifre that could not be resolved within the time frame, and the related analysis had to be abandoned. The model would have incorporated both local electricity and gas production and consumption alongside every other framework condition for the entirety of the Danish energy system. The idea was then, that Sifre and ADAPT would be able to optimize the production capacities for jet fuel production, of the chosen production pathway, between the five largest DH networks in Denmark; Copenhagen, Aalborg, Aarhus, Odense and TVIS in the Triangle Region. However, due to errors in Sifre, such a model was found to take significantly more time than initially expected and therefore, the work was abandoned.

11   Conclusion

The purpose of this study has been to investigate the feasibility of implementing gas-to-liquid and power-to-liquid pathways to produce the Danish demand for jet fuel of 50 PJ in 2050, and analyzing potential future framework conditions that can affect this jet fuel price. The focus has been to utilize synergies that can be found by locating the liquid fuel production plants near existing infrastructure and waste and biomass incineration to benefit from heat and CO_2, and investigating the sensitivity of the framework conditions has been of central concern. The main conclusion in this study is that, combining GtL and PtL to a hybrid configuration mitigate the potential challenges that arise from producing jet fuel exclusively from either pathway, without compromising the socioeconomic prodcuction cost, and thereby the jet fuel price.

In this study, the jet fuel price has been one of the primary dependent variables used for comparison of different liquid fuel production plant configurations. From the main scenarios it can be concluded, that the pathway resulting in the lowest jet fuel price is pure GtL by using POX with a biomethane feedstock produced by conventional biogas upgrading, resulting in a jet fuel price of 25.2 EUR/GJ. In fact, it was generally the scenarios that incorporated an upstream production of methane by biogas upgrading which resulted in the lowest jet fuel prices, since the price of biomethane in these scenarios is 11% lower on average than the price of bio- and electromethane in the corresponding scenario with an upstream production of methane by methanation of CO_2 in the biogas. When producing jet fuel purely by PtL, the price has been found to be 31.8 and 33.9 EUR/GJ for co-electrolysis and RWGS, respectively. Many aspects regarding the hybrid production plant configurations has been uncovered throughout this study. Generally, the hybrid plant configurations that included co-electrolysis could produce jet fuel at a price somewhere between those from pure GtL and pure PtL, while including RWGS would result in jet fuel prices almost equal to those from pure PtL. The lowest jet fuel price among all hybrid configurations was 29.9 EUR/GJ, which was in the scenario including SMR and co-electrolysis and upstream methane production from biogas upgrading. However, considering the average jet fuel price between an upstream methane production from biogas upgrading and methanation for each respective hybrid configuration, the hybrid configuration including POX and co-electrolysis resulted in the same price as SMR and co-electrolysis around 31.2 EUR/GJ.

Even though the jet fuel from pure GtL using biogas upgrading is the lowest, this price is not comparable to the price of the hybrid configurations since pure GtL with a methane feedstock from either biogas upgrading or methanation can not supply the entire demand of jet fuel due to the biogas constraint. This is also the reason why the jet fuel demand in the pure GtL was set to 25 PJ and not the Danish demand of 50 PJ. Generally, the hybrid plant configuration showed several advantages over both pure GtL or pure PtL. The flexible production in hybrid plant configurations become beneficial in relation to both the biogas constraint and potential strain on the electricity network. In every scenario with a hybrid configuration, the plant was able to produce the entire demand of 50 PJ while staying well within the limit of the biogas constraint, since the plant makes use of PtL to accommodate this constraint. Furthermore, results from the Funen case study indicated, that producing the entire demand of jet fuel purely from PtL might create a significant

amount of strain on the electricity network. This can be mitigated by the hybrid plant configuration, which optimizes its production of syngas based on both the biogas constraint and the available capacity in the electricity network. It can therefore be concluded from this study, that the hybrid configuration including co-electrolysis and either SMR or POX is a strong candidate for the future production of synthetic jet fuel in Denmark.

Throughout this study, several synergies related to central liquid fuel production have been uncovered and utilized. First, when locating the production centrally, the plant has a possibility of utilizing both LTPH and captured CO_2 from waste and biomass incineration. In every main scenario, the maximum waste incineration capacity of 665 MW was invested in. However, biomass incineration was not found as feasible and is only being invested in to a small degree, due to the higher fuel price compared to waste. Furthermore, locating refining and production of syncrude centrally, together, makes it possible to recirculate fuel gas from refining - a synergy that is unlikely to be found for decentral syncrude production, due to economies of scale. Furthermore, locating the production of liquid fuels centrally gives access to some of the larger DH networks in Denmark, to which excess heat from liquid fuel production can be sold. It also gives access to larger connections to both the electricity and gas grid in Denmark. In the case study of Funen it was found, that using a hybrid configuration with co-electrolysis and POX for a production of 5 PJ jet fuel, the electricity load exclusively from co-electrolysis could be as high as 300 MW in several hours, and 350 MW for exclusively RWGS, which means the locating large-scale liquid fuel production decentrally would most likely create strain on large parts of the electricity distribution network. Therefore, if the production of liquid fuels were to benefit greatly from economies of scale it would be a requirement that the production is located centrally. This study does not include a deeper comparative analysis between decentral and central production of liquid fuels. However, the results from the eSMR sensitivity analysis indicates, that locating the production of liquid fuels centrally does in fact benefit from all of these synergies given the fact that every scenario including decentral hybrid configurations using conventional SMR resulted in higher jet fuel prices than their corresponding scenario with a central production of liquid fuels using SMR.

From the case study of Funen, it can be concluded that if utilizing the pure PtL pathway for liquid fuel production, strain on the electricity network is a real concern. This study investigates three different measures for mitigating strain: hydrogen storage, hydrogen piping and the hybrid plant configuration. All measures proved to be technically feasible solutions for strain mitigation, but resulted in quite different jet fuel prices. Implementing a hydrogen storage resulted in the highest jet fuel price of 43.7 EUR/GJ which is significantly higher than every price in the main scenarios. The jet fuel prices resulting from implementing a hybrid plant configuration was lower compared to hydrogen storage, with an average price of 31.3 EUR/GJ between every hybrid configuration, which is fairly close to the jet fuel prices from the main scenarios. Finally, the strain mitigation solution with a hydrogen production at the western coast of Jutland and piping to Odense resulted in the lowest jet fuel prices, with an average of 26.8 EUR/GJ between every scenario with a hybrid plant configuration that included RWGS. When using pure PtL with RWGS, the jet fuel price resulted in 27.2

EUR/GJ. It can therefore be concluded, that the hydrogen piping solution is the most socioeconomically feasible solution for strain mitigation, but this solution is, however, also subject to several assumptions that must be considered. The hybrid plant configuration proved to be a close candidate in terms of resulting jet fuel prices.

Throughout the result sections, it has been found that especially the fuel consumption cost contributes to the resulting jet fuel price - especially the cost of consuming methane and electricity. The study shows that the resulting jet fuel prices are especially sensitive to changes in the yearly electricity prices, as they are significantly reduced with the electricity prices from the 10-year network development plan scenario Global Climate Action. The simulation with electricity prices from GCA showed that, with the more fluctuating prices, which is a product of large production of renewable energy resources from wind and solar, the jet fuel prices could greatly benefit from using power-to-liquid in the hours where the electricity price is zero, and shift to GtL when the fluctuation reach high prices. Furthermore, the large number of zero-cost hours for electricity means that the plants can greatly benefit from storages of hydrogen and CO_2 to better benefit from the zero-cost hours of electricity.

In case of the prices from GCA being the actual electricity prices in 2050, the jet fuel prices can be lowered to such a degree, that it would be competitive to today's prices, with an average jet fuel price for hybrid scenarios at 16.6 EUR/GJ - approximately 50% lower than the jet fuel prices that has been found with electricity prices from Sustainable Transition. Furthermore, it was found that hybrid configurations would benefit significantly more from the fluctuating electricity price than other configurations.

While it has been found that the electricity price can greatly affect the jet fuel price, the results also showed that in case the fuel production plant is not located with waste and biomass incineration, and therefore can not utilize LTPH and CO_2 from this, the jet fuel prices does not change significantly as it was found to increase from 31.8, in the main result, to 33.7 EUR/GJ - an increase of approximately 6%.

For the purpose of producing 50 PJ of jet fuel, it has been found that CO_2 from biogas upgrading, carbon capture of waste incineration and, to a smaller degree, direct air capture and CC from biomass incineration, is able to cover the demand of alternative carbon resources that is needed to comply with the constraint of renewable gas, produced by biogas, for gas-to-liquid. It has been found that CO_2 from biogas upgrading and CC of waste incineration is generally the more economically feasible sources, and that this CO_2 will always be used first to the degree of which it is produced. CO_2 from biogas has been found to be more feasible when transported from the biogas upgrading plant to the liquid fuel production plants via pipe, rather than trucking. Both these two sources have been found to be constrained to a point where other sources are often required. For plant configurations that require more CO_2, it has been found that the costs of CO_2 from CC of biomass incineration and DAC are relatively close when LTPH from the plant can be used for DAC, in which it can reach a production cost of 52.8 EUR/tCO_2.

Furthermore, it was found that liquid fuel production plants can participate in a potential future market for both physical CO_2 and in a market purposed with balancing fossil emissions through e.g. certificates of negative emissions to reach climate net-neutrality. It was found that almost 10 Mt of negative emissions could be produced via production units that utilize liquid fuel plant synergies to reduce costs. However, the supply of negative emissions has been found to increase the CO_2 prices resulting in an increase of the jet fuel price by 12.3 and 18.5 EUR/GJ for 5 Mt and 10 Mt, respectively.

Lastly, it can be concluded that the Sifre model has been developed in such a manner, that it is easy to investigate how changing parameters - if it be the framework conditions, technical or economical specifications of conversion units etc. - will affect the production of jet fuel in Denmark. Therefore, the model has a high potential for future analyses, and can easily be updated continuously.

Bibliography

[1] E. C. Wormslev and M. K. Broberg, "Sustainable Jet Fuel for Aviation", NIRAS, Tech. Rep., Jan. 2020.

[2] European Union, *Reducing emissions from aviation*. [Online]. Available: `https://ec.europa.eu/clima/policies/transport/aviation_en` (visited on 06/01/2020).

[3] Global Carbon Atlas, *CO2 emissions*. (visited on 06/06/2020).

[4] International Civil Aviation Organization, *Trends in Emissions that affect Climate Change*. [Online]. Available: `https://www.icao.int/environmental-protection/Pages/ClimateChange_Trends.aspx` (visited on 06/01/2020).

[5] A. W. Mortensen and K. D. Rasmussen, "The tragedy of the planet? Characterizing climate change as a tragedy of the commons type of challenge", Master's thesis, 2018.

[6] Energinet, *North Sea Wind Power Hub-konsortium fremlægger mulig løsning til at opfylde klimamål*. [Online]. Available: `https://energinet.dk/Om-nyheder/Nyheder/2019/07/09/North-Sea-Wind-Power-Hub-konsortium-fremlaegger-mulig-losning-til-at-opfylde-klimamaal` (visited on 06/01/2020).

[7] The Danish Parliament, "Aftale om klimalov", Tech. Rep. december, 2019, p. 14 001.

[8] Energinet, *Winds of Change*, 2019.

[9] A. W. Mortensen, H. Wenzel, K. D. Rasmussen, and S. S. Justesen, "Nordic GTL – a pre-feasibility study on sustainable aviation fuel from biogas, hydrogen and CO2", Tech. Rep., Oct. 2019.

[10] T. Birkmose, K. Hjort-Gregersen, J. Hinge, and R. Hørfarter, "Kortlægning af hensigtsmæssig lokalisering af nye biogasanlæg i Danmark - Udpegning af områder med særlige muligheder for biogas", Tech. Rep., Dec. 2015.

[11] H. Wenzel, J. M. Triolo, L. V. Toft, and N. Østergaard, "Energiafgrødeanalysen", Syddansk Universitet & SEGES, Tech. Rep., 2020.

[12] A. D. Klerk, "Fischer-Tropsch Refining", PhD thesis, Feb. 2008.

[13] T. D. Rasmussen and M. Broe, "Sustainable Transportation in a future 100 % Renewable Danish Energy System", Master's thesis, 2018.

[14] S. F. Rasmussen, "Implementation of Fischer-Tropsch Jet Fuel Production in the Danish Energy System", 2019.

[15] R. D. Andersen and R. K. Rasmussen, "Feasibility Study of Sustainable Jet Fuel Production on Funen", Master's thesis, 2019.

[16] A. V. Laursen and J. B. Pedersen, "Strategic Energy Planning of Funen , Denmark - System Perspectives for 2035 & 2050", 2018.

[17] Energinet, "Systemperspektiver ved 70-procentmålet og storskala havvind", Tech. Rep., 2020.

[18] ——, "Systemperspektiv 2035", Tech. Rep., 2018.

[19] Klimarådet, "Kendte veje og nye spor til 70 procents reduktion", Tech. Rep., 2020.

[20] H. Lund, B. V. Mathiesen, J. Z. Thellufsen, P. Sorknæs, and I. R. Skov, "IDAs Klimasvar: Transport- og energiløsninger 2030", Tech. Rep., 2020.

[21] X. D. Peng, "Analysis of the thermal efficiency limit of the steam methane reforming process", *Industrial and Engineering Chemistry Research*, vol. 51, no. 50, pp. 16 385–16 392, 2012, ISSN: 08885885. DOI: 10.1021/ie3002843.

[22] X. Zhang, Y. Song, G. Wang, and X. Bao, "Co-electrolysis of CO2 and H2O in high-temperature solid oxide electrolysis cells: Recent advance in cathodes", *Journal of Energy Chemistry*, vol. 26, no. 5, pp. 839–853, 2017, ISSN: 20954956. DOI: 10.1016/j.jechem.2017.07.003. [Online]. Available: https://doi.org/10.1016/j.jechem.2017.07.003.

[23] Y. Wang, T. Liu, L. Lei, and F. Chen, "High temperature solid oxide H2O/CO2 co-electrolysis for syngas production", *Fuel Processing Technology*, vol. 161, pp. 248–258, Jun. 2017, ISSN: 03783820. DOI: 10.1016/j.fuproc.2016.08.009. [Online]. Available: https://linkinghub.elsevier.com/retrieve/pii/S0378382016303502.

[24] A. P. E. York and T. Xiao, "Brief Overview of the Partial Oxidation of Methane to Synthesis Gas", *Topics in Catalysis*, 2003.

[25] J. Baltrusaitis and W. L. Luyben, "Methane Conversion to Syngas for Gas-to-Liquids (GTL): Is Sustainable CO2 Reuse via Dry Methane Reforming (DMR) Cost Competitive with SMR and ATR Processes?", *ACS Sustainable Chemistry and Engineering*, vol. 3, no. 9, pp. 2100–2111, 2015, ISSN: 21680485. DOI: 10.1021/acssuschemeng.5b00368.

[26] R. Krishna and S. T. Sie, "Design and scale-up of the Fischer-Tropsch bubble column slurry reactor", *Fuel processing technology*, vol. 64, no. 1, pp. 73–105, 2000, ISSN: 03783820. DOI: 10.1016/S0378-3820(99)00128-9.

[27] A. Mahmood, S. Bano, J. H. Yu, and K. H. Lee, "Performance evaluation of SOEC for CO2/H2O co-electrolysis: Considering the effect of cathode thickness", *Journal of CO2 Utilization*, vol. 33, pp. 114–120, Apr. 2019, ISSN: 22129820. DOI: 10.1016/j.jcou.2019.05.014.

[28] F. G. Albrecht, D. H. König, N. Baucks, and R. U. Dietrich, "A standardized methodology for the techno-economic evaluation of alternative fuels – A case study", *Fuel*, vol. 194, pp. 511–526, 2017, ISSN: 00162361. DOI: 10.1016/j.fuel.2016.12.003. [Online]. Available: http://dx.doi.org/10.1016/j.fuel.2016.12.003.

[29] G. Herz, E. Reichelt, and M. Jahn, "Techno-economic analysis of a co-electrolysis-based synthesis process for the production of hydrocarbons", *Applied Energy*, vol. 215, no. August 2017, pp. 309–320, 2018, ISSN: 03062619. DOI: 10.1016/j.apenergy.2018.02.007. [Online]. Available: https://doi.org/10.1016/j.apenergy.2018.02.007.

[30] W. L. Becker, R. J. Braun, M. Penev, and M. Melaina, "Production of Fischer-Tropsch liquid fuels from high temperature solid oxide co-electrolysis units", *Energy*, vol. 47, no. 1, pp. 99–115, 2012, ISSN: 03605442. DOI: `10.1016/j.energy.2012.08.047`. [Online]. Available: `http://dx.doi.org/10.1016/j.energy.2012.08.047`.

[31] D. J. Ramberg, Y. H. Henry Chen, S. Paltsev, and J. E. Parsons, "The economic viability of gas-to-liquids technology and the crude oil–natural gas price relationship", *Energy Economics*, vol. 63, pp. 13–21, 2017, ISSN: 01409883. DOI: `10.1016/j.eneco.2017.01.017`. [Online]. Available: `http://dx.doi.org/10.1016/j.eneco.2017.01.017`.

[32] D. F. Rodríguez Vallejo and A. De Klerk, "Improving the interface between Fischer-Tropsch synthesis and refining", *Energy and Fuels*, vol. 27, no. 6, pp. 3137–3147, 2013, ISSN: 08870624. DOI: `10.1021/ef400560z`.

[33] L. Pastor-Pérez, F. Baibars, E. Le Sache, H. Arellano-García, S. Gu, and T. R. Reina, "CO2 valorisation via Reverse Water-Gas Shift reaction using advanced Cs doped Fe-Cu/Al2O3 catalysts", *Journal of CO2 Utilization*, vol. 21, no. August, pp. 423–428, 2017, ISSN: 22129820. DOI: `10.1016/j.jcou.2017.08.009`.

[34] F. Ghodoosi, M. R. Khosravi-Nikou, and A. Shariati, "Mathematical Modeling of Reverse Water-Gas Shift Reaction in a Fixed-Bed Reactor", *Chemical Engineering and Technology*, vol. 40, no. 3, pp. 598–607, 2017, ISSN: 15214125. DOI: `10.1002/ceat.201600220`.

[35] M. Fasihi, D. Bogdanov, and C. Breyer, "Techno-Economic Assessment of Power-to-Liquids (PtL) Fuels Production and Global Trading Based on Hybrid PV-Wind Power Plants", *Energy Procedia*, vol. 99, pp. 243–268, Mar. 2016, ISSN: 18766102. DOI: `10.1016/j.egypro.2016.10.115`. [Online]. Available: `http://dx.doi.org/10.1016/j.egypro.2016.10.115`.

[36] R. W. Baker, B. Freeman, J. Kniep, Y. I. Huang, and T. C. Merkel, "CO2 Capture from Cement Plants and Steel Mills Using Membranes", *Industrial and Engineering Chemistry Research*, vol. 57, no. 47, pp. 15 963–15 970, 2018, ISSN: 15205045. DOI: `10.1021/acs.iecr.8b02574`.

[37] D. J. Ramberg, "General Equilibrium Impacts of New Energy Technologies on Sectoral Energy Usage by", PhD thesis, 2015, ISBN: 4000109855.

[38] C. M. Kalamaras and A. M. Efstathiou, "Hydrogen Production Technologies: Current State and Future Developments", *Conference Papers in Energy*, vol. 2013, pp. 1–9, 2013. DOI: `10.1155/2013/690627`.

[39] X. Zhou, C. Chen, and F. Wang, "Modeling of non-catalytic partial oxidation of natural gas under conditions found in industrial reformers", *Chemical Engineering and Processing: Process Intensification*, vol. 49, no. 1, pp. 59–64, 2010, ISSN: 02552701. DOI: `10.1016/j.cep.2009.11.006`.

[40] N. Shaigan, W. Qu, D. G. Ivey, and W. Chen, "A review of recent progress in coatings, surface modifications and alloy developments for solid oxide fuel cell ferritic stainless steel interconnects", *Journal of Power Sources*, vol. 195, no. 6, pp. 1529–1542, 2010, ISSN: 03787753. DOI: `10.1016/j.jpowsour.2009.09.069`.

[41] Batelle Memorial Institute, "Manufacturing Cost Analysis of 1 kW and 5 kW Solid Oxide Fuel Cell (SOFC) for Auxilliary Power Applications", Tech. Rep., 2014.

[42] M. Korobitsyn, F. vab Berkel, and G. Christie, "Review of Synthesis Gas Processes", no. December, 2000.

[43] K. Chattopadhyay and H. L. Frandsen, "Techno-economic assessment of SOEC - Identifying potentials for grid integration", Tech. Rep., 2019.

[44] Global CCS Institute, "Waste-to-Energy with CCS: A pathway to carbon-negative power generation", Tech. Rep., 2018.

[45] S. Siegemund, M. Trommler, O. Kolb, V. Zinnecker, P. Schmidt, W. Weindorf, W. Zittel, T. Raksha, and J. Zerhusen, "E-Fuels study. The potential of electricity-based fuels for low-emission transport in the EU", Tech. Rep., 2017.

[46] P. R. Schmidt, W. Zittel, W. Weindorf, and T. Raksha, "Empowering a sustainable mobility future with zero emission fuels from renewable electricity", Tech. Rep., 2016.

[47] NIRAS, "CCS og CCU Potentialer", Tech. Rep., 2020.

[48] P. M. Maitlis and A. de Klerk, Eds., *Greener Fischer-Tropsch Processes for Fuels and Feedstocks*. Weinheim, Germany: Wiley-VCH Verlag GmbH & Co. KGaA, Feb. 2013, ISBN: 9783527656837. DOI: `10.1002/9783527656837`. [Online]. Available: `http://doi.wiley.com/10.1002/9783527656837`.

[49] Energistyrelsen, "Samfundsøkonomiske beregningsforudsætninger for energipriser og emissioner", Tech. Rep., 2019.

[50] ——, "Analyseforudsætninger til energinet", Tech. Rep., 2019.

[51] P. Henriksen, personal communication, Apr. 8, 2020.

[52] Centralkommunernes Transmissionsselskab, "Årsberetning 2018", Tech. Rep., 2018.

[53] HOFOR, "Årsrapport 2018", Tech. Rep., 2018.

[54] VEKS, "Årsrapport 2018", Tech. Rep., 2019.

[55] Affaldvarme Aarhus, "Årsrapport 2018", Tech. Rep., 2018.

[56] Fjernvarme Fyn, "Årsberetning 2018", Tech. Rep., 2018.

[57] Aalborg Forsyning, "Miljøredegørelse 2018", Tech. Rep., 2018.

[58] TVIS, *Fjernvarme i Trekantområdet*. [Online]. Available: `https://www.tvis.net/fire-kommuner/` (visited on 04/29/2020).

[59] Energi- Forsynings- og Klimaministeriet, *Bekendtgørelse om bæredygtig produktion af biogas. BEK nr 448 af 20/05/2016*, 2018.

[60] Danish Energy Agency, *Biogas in Denmark*. [Online]. Available: `https://ens.dk/en/our-responsibilities/bioenergy/biogas-denmark` (visited on 06/09/2020).

[61] Energinet, "Baggrundsrapport: Systemperspektiv 2035", Tech. Rep., 2018.

[62] N. de Vries, "Safe and effective application of ammonia as a marine fuel", Master's thesis, 2019.

[63] Maersk, *Alcohol, Biomethane and Ammonia are the best-positioned fuels to reach zero net emissions.* [Online]. Available: `https://www.maersk.com/news/articles/2019/10/24/alcohol-biomethane-and-ammonia-are-the-best-positioned-fuels-to-reach-zero-net-emissions` (visited on 05/17/2020).

[64] Energistyrelsen and Energinet, "Technology Data for Renewable Fuels", Tech. Rep., 2017.

[65] International Energy Agency, "Putting CO2 to Use: Creating value from emissions", Tech. Rep. September, 2019, p. 86. [Online]. Available: `https://www.iea.org/reports/putting-co2-to-use`.

[66] Danish Energy Agency, "Kapacitet til affaldsforbraending i Danmark", Tech. Rep., Apr. 2018.

[67] Miljøministeriet, "Danmark uden affald II", Tech. Rep., Feb. 2015.

[68] J. C. Svendsen, personal communication, Apr. 8, 2020.

[69] S. Budinis, S. Krevor, N. M. Dowell, N. Brandon, and A. Hawkes, "An assessment of CCS costs, barriers and potential", *Energy Strategy Reviews*, vol. 22, Nov. 2018, ISSN: 2211467X. DOI: `10.1016/j.esr.2018.08.003`. [Online]. Available: `https://linkinghub.elsevier.com/retrieve/pii/S2211467X18300634`.

[70] E. S. Rubin, J. E. Davison, and H. J. Herzog, "The cost of CO2 capture and storage", *International Journal of Greenhouse Gas Control*, vol. 40, pp. 378–400, Sep. 2015, ISSN: 17505836. DOI: `10.1016/j.ijggc.2015.05.018`. [Online]. Available: `https://linkinghub.elsevier.com/retrieve/pii/S1750583615001814`.

[71] Energinet, *Tariffer og Gebyrer*. [Online]. Available: `https://energinet.dk/El/Elmarkedet/Tariffer` (visited on 04/28/2020).

[72] Energistyrelsen and Energinet, "Technology Data for Energy Plants", Tech. Rep., 2016.

[73] M. Münster and H. Lund, "Comparing Waste-to-Energy technologies by applying energy system analysis", *Waste Management*, vol. 30, no. 7, pp. 1251–1263, 2010, ISSN: 0956053X. DOI: `10.1016/j.wasman.2009.07.001`.

[74] M. Münster and P. Meibom, "Long-term affected energy production of waste to energy technologies identified by use of energy system analysis", *Waste Management*, vol. 30, no. 12, pp. 2510–2519, 2010, ISSN: 0956053X. DOI: `10.1016/j.wasman.2010.04.015`.

[75] Forening Biogasbranchen, *Produktion*. [Online]. Available: `https://biogasbranchen.dk/om-biogas/produktion` (visited on 04/16/2020).

[76] H. Iskov and S. Kneck, "Using the natural gas network for transporting hydrogen - 10 years of experience", Tech. Rep., 2017.

[77] Danish Gas Technology Centre, *DGC med i lovende test af brint i gasnettet.* [Online]. Available: `https://www.dgc.dk/nyhed/2019/dgc-med-i-lovende-test-af-brint-i-gasnettet` (visited on 05/12/2020).

[78] Energistyrelsen, "Havvindspotentialet i Danmark", Tech. Rep., 2019. [Online]. Available: `https://ens.dk/ansvarsomraader/vindenergi/fakta-om-vindenergi`.

[79] Energinet, *Gas composition and quality for transmission, yearly Data.* [Online]. Available: `https://www.energidataservice.dk/dataset/gascompositionyearly` (visited on 04/14/2020).

[80] Energistyrelsen and Energinet, "Technology Data for Energy Transport", 2017.

[81] S. Biollaz, A. Calbry-Muzyka, T. Schildhauer, J. Witte, and A. Kunz, "Direct Methanation of Biogas", Tech. Rep., 2017.

[82] Climeworks, *Our Technology.* [Online]. Available: `https://www.climeworks.com/our-technology/` (visited on 05/13/2020).

[83] Carbon Engineering, *Our Technology.* [Online]. Available: `https://carbonengineering.com/our-technology/` (visited on 05/13/2020).

[84] ORYX GTL Limited, *Whats GTL.* [Online]. Available: `https://oryxgtl.com.qa/whats-gtl/` (visited on 05/13/2020).

[85] Chevron, *Gas-to-liquids.* [Online]. Available: `https://www.chevron.com/stories/gas-to-liquids` (visited on 05/13/2020).

[86] OLTIN YO'L GTL, *What Is GTL - The Technology.* [Online]. Available: `https://www.oltinyolgtl.com/what-is-gtl/` (visited on 05/13/2020).

[87] PetroSA, *GTL Technology.* [Online]. Available: `http://www.petrosa.co.za/innovation_in_action/Pages/GTL-TECHNOLOGY.aspx` (visited on 05/13/2020).

[88] Global Syngas Technologies Council, *Syngas Production.* [Online]. Available: `https://www.globalsyngas.org/syngas-production/` (visited on 05/13/2020).

[89] A. de Klerk, *Fischer-Tropsch Refining.* Weinheim, Germany: Wiley-VCH Verlag GmbH & Co. KGaA, Jul. 2011, ISBN: 9783527635603. DOI: `10.1002/9783527635603`. [Online]. Available: `http://doi.wiley.com/10.1002/9783527635603`.

[90] International Energy Agency, "The Future of Hydrogen", Tech. Rep., Jun. 2019.

[91] U. IEA, "International Energy Outlook 2017", Tech. Rep., 2017. DOI: `www.eia.gov/forecasts/ieo/pdf/0484(2016).pdf`. arXiv: `EIA-0484(2013) [DOE]`. [Online]. Available: `https://www.eia.gov/outlooks/archive/ieo17/`.

[92] Shell, *Introduction to Pearl GTL.* [Online]. Available: `https://www.shell.com.qa/en_qa/about-us/projects-and-sites/pearl-gtl.html` (visited on 05/13/2020).

[93] European Union, "Official Journal of the European Union - L 140", *Official Journal of the European Union*, vol. 52, 2009. [Online]. Available: `https://eur-lex.europa.eu/legal-content/EN/TXT/PDF/?uri=OJ:L:2009:140:FULL&from=LT`.

[94] Energinet, *Energinets Modeller*. [Online]. Available: `https://energinet.dk/Analyse-og-Forskning/Beregningsmodeller` (visited on 05/17/2020).

[95] ——, "SIFRE: Simulation of Flexible and Renewable Energy sources", Tech. Rep. [Online]. Available: `https://energinet.dk/Analyse-og-Forskning/Beregningsmodeller`.

[96] ——, "ADAPT: Analyseværktøj for et Samfundsøkonomisk Effektivt Energisystem", Tech. Rep., 2014. [Online]. Available: `https://energinet.dk/Analyse-og-Forskning/Beregningsmodeller`.

[97] Finansministeriet, "Den Samfundsøkonomiske Diskonteringsrente", Tech. Rep., 2018. [Online]. Available: `https://fm.dk/media/10174/dokumentationsnotat-_-den-samfundsoekonomiske-diskonteringsrente.pdf`.

[98] Nord Pool, *No. 52/2013 - Nord Pool Spot to introduce new minimum and maximum price caps*. [Online]. Available: `https://www.nordpoolgroup.com/message-center-container/newsroom/exchange-message-list/2013/Q3/No-522013---Nord-Pool-Spot-to-introduce-new-minimum-and-maximum-price-caps/` (visited on 05/28/2020).

[99] B. Metz, O. Davidson, H. de Coninck, M. Loos, and L. Meyer, *The IPCC special report on carbon dioxide capture and storage*. 2006, pp. 1611–1618, ISBN: 9608758424.

[100] ENTSO-E and ENTSOG, "TYNDP 2018: Scenario Report. Main Report", Tech. Rep., 2018, p. 30. [Online]. Available: `https://www.entsoe.eu/Documents/TYNDP%20documents/TYNDP2018/Scenario_Report_2018_Final.pdf?Web=1`.

[101] European Comission, *2030 climate & energy framework*. [Online]. Available: `https://ec.europa.eu/clima/policies/strategies/2030_en` (visited on 06/10/2020).

[102] ——, *2050 long-term strategy*. [Online]. Available: `https://ec.europa.eu/clima/policies/strategies/2050_en` (visited on 06/08/2020).

[103] Haldor Topsoe, *Topsoe to build demonstration plant to produce cost-competitive CO2-neutral methanol from biogas and green electricity*, 2019. [Online]. Available: `https://blog.topsoe.com/topsoe-to-build-demonstration-plant-to-produce-cost-competitive-co2-neutral-methanol-from-biogas-and-green-electricity` (visited on 06/04/2020).

[104] S. T. Wismann, J. S. Engbæk, S. B. Vendelbo, F. B. Bendixen, W. L. Eriksen, K. Aasberg-Petersen, C. Frandsen, I. Chorkendorff, and P. M. Mortensen, "Electrified methane reforming: A compact approach to greener industrial hydrogen production", *Science (New York, N.Y.)*, vol. 364, no. 6442, pp. 756–759, 2019, ISSN: 10959203. DOI: `10.1126/science.aaw8775`.

[105] R. Pirog, "Petroleum Refining: Economic Performance and Challenges for the Future", Tech. Rep., 2007.

[106] Canadian Fuels Association, "The Economics of Petroleum Refining", Tech. Rep. December, 2013. [Online]. Available: `https : / / www . canadianfuels . ca / website / media / PDF / Publications / Economics-fundamentals-of-Refining-December-2013-Final-English.pdf`.

[107] Drivkraft Danmark, *Raffinaderierne leverer effektiv og stabil energi til danskerne hver dag*. [Online]. Available: `https://www.drivkraftdanmark.dk/viden/raffinaderierne-leverer-effektiv-og-stabil-energi-til-danskerne-hver-dag/` (visited on 06/13/2020).

APPENDICES

A   Potential Biogas Share by Municipality Assigned on Bidding Zones

Municipality	Manure	Waste	Natural areas	Straw	Total	Bidding zone
Ringkøbing-Skjern	56,5%	2,2%	2,2%	39,1%	3,1%	VestJL
Lolland	9,5%	0,0%	0,0%	90,5%	2,8%	SydSJ
Aalborg	35,0%	7,5%	2,5%	55,0%	2,6%	NordJL
Guldborgsund	15,4%	2,6%	0,0%	82,1%	2,6%	SydSJ
Vejle	35,9%	7,7%	2,6%	53,8%	2,5%	ØstJL
Haderslev	42,9%	0,0%	0,0%	57,1%	2,3%	SydJL
Hjørring	51,4%	2,9%	2,9%	42,9%	2,3%	NordJL
Viborg	67,6%	2,9%	5,9%	23,5%	2,3%	ØstJL
Herning	54,3%	2,9%	2,9%	40,0%	2,2%	VestJL
Tønder	78,8%	0,0%	3,0%	18,2%	2,1%	SydJL
Randers	22,6%	0,0%	3,2%	74,2%	2,0%	ØstJL
Sønderborg	33,3%	3,3%	0,0%	63,3%	2,0%	SydJL
Thisted	53,3%	0,0%	3,3%	43,3%	2,0%	NordvestJL
Næstved	13,3%	3,3%	0,0%	83,3%	2,0%	SydSJ
Hedensted	27,6%	3,4%	0,0%	69,0%	1,9%	ØstJL
Skive	44,8%	3,4%	0,0%	51,7%	1,9%	NordvestJL
Brønderslev	48,1%	0,0%	0,0%	51,9%	1,9%	NordJL
Varde	89,3%	3,6%	7,1%	0,0%	1,8%	VestJL
Bornholm	28,6%	3,6%	0,0%	67,9%	1,8%	Bornholm
Slagelse	11,1%	3,7%	0,0%	85,2%	1,8%	SydSJ
Aabenraa	69,2%	3,8%	0,0%	26,9%	1,8%	SydJL
Norddjurs	30,8%	0,0%	0,0%	69,2%	1,8%	ØstJL
Faaborg-Midtfyn	30,8%	3,8%	0,0%	65,4%	1,8%	Fyn
Kalundborg	15,4%	3,8%	0,0%	80,8%	1,7%	VestSJ
Kolding	28,0%	0,0%	0,0%	72,0%	1,7%	SydJL
Vesthimmerlands	73,1%	0,0%	3,8%	23,1%	1,7%	NordJL
Jammerbugt	38,5%	3,8%	3,8%	53,8%	1,7%	NordJL
Favrskov	28,0%	4,0%	0,0%	68,0%	1,7%	ØstJL
Vordingborg	16,0%	0,0%	0,0%	84,0%	1,6%	SydSJ
Vejen	68,0%	0,0%	0,0%	32,0%	1,6%	SydJL
Assens	36,0%	4,0%	0,0%	60,0%	1,6%	Fyn
Holstebro	52,0%	4,0%	4,0%	40,0%	1,6%	VestJL
Holbæk	16,7%	4,2%	0,0%	79,2%	1,6%	VestSJ
Nordfyns	27,3%	0,0%	0,0%	72,7%	1,5%	Fyn
Syddjurs	27,3%	0,0%	4,5%	68,2%	1,4%	ØstJL
Morsø	38,1%	0,0%	0,0%	61,9%	1,4%	NordvestJL
Esbjerg	81,0%	9,5%	0,0%	9,5%	1,4%	VestJL
Mariagerfjord	57,1%	4,8%	4,8%	33,3%	1,3%	ØstJL
Århus	15,0%	25,0%	0,0%	60,0%	1,3%	ØstJL
Horsens	35,0%	5,0%	0,0%	60,0%	1,3%	ØstJL
Lemvig	52,6%	0,0%	0,0%	47,4%	1,3%	VestJL
Frederikshavn	35,0%	5,0%	5,0%	55,0%	1,3%	NordJL
Silkeborg	42,1%	5,3%	5,3%	47,4%	1,2%	ØstJL
Rebild	63,2%	0,0%	0,0%	36,8%	1,2%	ØstJL
Faxe	5,9%	5,9%	0,0%	88,2%	1,1%	SydSJ
Svendborg	29,4%	0,0%	0,0%	70,6%	1,1%	Fyn
Ikast-Brande	56,3%	6,3%	0,0%	37,5%	1,0%	ØstJL
Skanderborg	33,3%	6,7%	0,0%	60,0%	1,0%	ØstJL
Langeland	21,4%	0,0%	0,0%	78,6%	0,9%	Fyn
Nyborg	28,6%	7,1%	0,0%	64,3%	0,9%	Fyn

Figure A.1: *Potential biogas share by municipality with assigned bidding zones (Part 1) - See next page for Part 2. Source: [10].*

Municipality	Manure	Waste	Natural areas	Straw	Total	Bidding zone
Middelfart	53,8%	0,0%	0,0%	46,2%	0,9%	Fyn
Odder	23,1%	0,0%	0,0%	76,9%	0,8%	ØstJL
Struer	41,7%	0,0%	0,0%	58,3%	0,8%	VestJL
Ringsted	15,4%	0,0%	0,0%	84,6%	0,8%	VestSJ
Stevns	15,4%	0,0%	0,0%	84,6%	0,8%	SydSJ
Billund	50,0%	8,3%	0,0%	41,7%	0,8%	VestJL
Sorø	20,0%	0,0%	0,0%	80,0%	0,7%	VestSJ
Odense	20,0%	30,0%	0,0%	50,0%	0,7%	Fyn
Odsherred	18,2%	9,1%	0,0%	72,7%	0,7%	VestSJ
Kerteminde	20,0%	0,0%	0,0%	80,0%	0,7%	Fyn
Lejre	11,1%	0,0%	0,0%	88,9%	0,7%	VestSJ
Køge	10,0%	10,0%	0,0%	80,0%	0,7%	VestSJ
Roskilde	11,1%	11,1%	0,0%	77,8%	0,6%	VestSJ
Frederikssund	12,5%	12,5%	0,0%	75,0%	0,5%	NordSJ
København	0,0%	100,0%	0,0%	0,0%	0,5%	KBH
Gribskov	20,0%	20,0%	0,0%	60,0%	0,3%	NordSJ
Fredericia	25,0%	0,0%	0,0%	75,0%	0,3%	SydJL
Hillerød	0,0%	25,0%	0,0%	75,0%	0,3%	NordSJ
Ærø	33,3%	0,0%	0,0%	66,7%	0,3%	Fyn
Samsø	25,0%	0,0%	0,0%	75,0%	0,3%	ØstJL
Egedal	0,0%	33,3%	0,0%	66,7%	0,2%	NordSJ
Greve	0,0%	50,0%	0,0%	50,0%	0,2%	VestSJ
Høje Taastrup	0,0%	33,3%	0,0%	66,7%	0,1%	VestSJ
Fredensborg	0,0%	50,0%	0,0%	50,0%	0,1%	NordSJ
Halsnæs	0,0%	0,0%	0,0%	100,0%	0,1%	NordSJ
Helsingør	0,0%	50,0%	0,0%	50,0%	0,1%	NordSJ
Solrød	0,0%	0,0%	0,0%	100,0%	0,1%	VestSJ
Allerød	0,0%	0,0%	0,0%	100,0%	0,1%	NordSJ
Rødovre	0,0%	100,0%	0,0%	0,0%	0,1%	NordSJ
Furesø	0,0%	100,0%	0,0%	0,0%	0,1%	NordSJ
Frederiksberg	0,0%	100,0%	0,0%	0,0%	0,1%	KBH
Rudersdal	0,0%	100,0%	0,0%	0,0%	0,1%	NordSJ
Ishøj	0,0%	0,0%	0,0%	100,0%	0,1%	VestSJ
Tårnby	0,0%	100,0%	0,0%	0,0%	0,1%	KBH
Lyngby-Taarbæk	0,0%	100,0%	0,0%	0,0%	0,1%	NordSJ
Gladsaxe	0,0%	100,0%	0,0%	0,0%	0,1%	NordSJ
Gentofte	0,0%	100,0%	0,0%	0,0%	0,1%	NordSJ
Hvidovre	0,0%	100,0%	0,0%	0,0%	0,1%	NordSJ
Ballerup	0,0%	100,0%	0,0%	0,0%	0,1%	NordSJ
Brøndby	0,0%	0,0%	0,0%	0,0%	0,0%	NordSJ
Hørsholm	0,0%	0,0%	0,0%	0,0%	0,0%	NordSJ
Albertslund	0,0%	0,0%	0,0%	0,0%	0,0%	NordSJ
Herlev	0,0%	0,0%	0,0%	0,0%	0,0%	NordSJ
Glostrup	0,0%	0,0%	0,0%	0,0%	0,0%	NordSJ
Dragør	0,0%	0,0%	0,0%	0,0%	0,0%	KBH
Vallensbæk	0,0%	0,0%	0,0%	0,0%	0,0%	NordSJ
Læsø	0,0%	0,0%	0,0%	0,0%	0,0%	NordJL
Christiansø	0,0%	0,0%	0,0%	0,0%	0,0%	Bornholm
Fanø	0,0%	0,0%	0,0%	0,0%	0,0%	SydJL
Total	36,7%	5,1%	1,8%	56,3%	100,0%	

Figure A.2: *Potential biogas share by municipality with assigned bidding zones (Part 2). Source: [10].*

B   Technology Data

The figures show the applied energy balances for the central conversion units used for the production of jet fuel. As mentioned in Section *7.1 Sifre and ADAPT Methodology*, Sifre requires a heating value for CO_2 and oxygen, which means that the energy balances has been slightly modified because of this. The energy balance for the actual Sifre units can be seen in the parentheses, while the original energy balance is shown as the main value in the figures. All energy balances are made as a proportion of a total input of 1 PJ energy, meaning that e.g. *Biogas: 0.96* means that out of a total input of 1 PJ, 0.96 PJ is biogas.

Biogas Upgrading
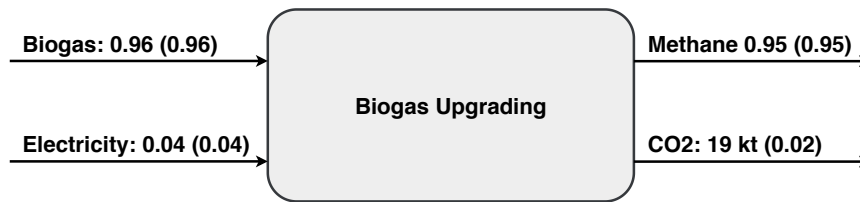
Figure B.1: *Energy balance of biogas upgrading [72].*

Table B.1: *ADAPT input for biogas upgrading [64]. The cost includes both the scrubbing of CO_2 and injection to the natural gas grid.*

Biogas Upgrading	Unit	ADAPT
Investment cost	M€/MW	0.487
Fixed O&M cost	€/MW/year	12,255
Variable O&M cost	€/MWh	-

Methanation

Figure B.2: *Energy balance of methanation [81].*

Table B.2: *ADAPT input for methanation of biogas [64].*

Methanation	Unit	ADAPT
Investment cost	M€/MW	0.713
Fixed O&M cost	€/MW/year	25,394
Variable O&M cost	€/MWh	2.385

Steam-Methane Reforming

Figure B.3: *Energy balance of steam-methane reforming [21].*

Table B.3: *ADAPT input for steam-methane reforming [42].*

Steam-Methane Reformer	Unit	ADAPT
Investment cost	M€/MW	0.064
Fixed O&M cost	€/MW/year	3,210
Variable O&M cost	€/MWh	-

Partial Oxidation
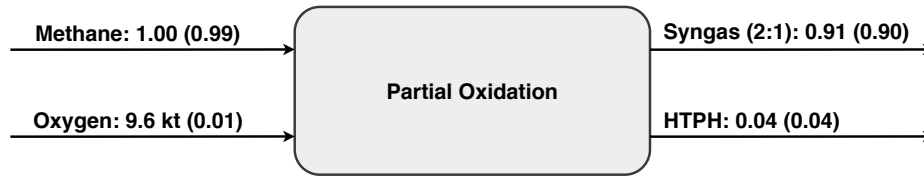
Figure B.4: *Energy balance of partial oxidation [24].*

Table B.4: *ADAPT input for partial oxidation [31], [42].*

Partial Oxidation	Unit	ADAPT
Investment cost	M€/MW	0.039
Fixed O&M cost	€/MW/year	1,926
Variable O&M cost	€/MWh	-

Reverse Water-Gas Shift for adjusting Syngas
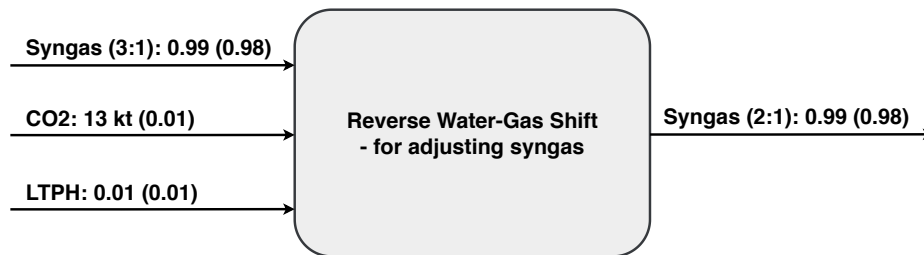
Figure B.5: *Energy balance of reverse water-gas shift for H_2:CO ratio adjustment. The energy balance has been made from stoichiometric calculations.*

Table B.5: *ADAPT input for reverse water-gas shift. It has been assumed to be the same for both adjusting and producing syngas [25].*

Reverse Water-Gas Shift	Unit	ADAPT
Investment cost	M€/MW	0.006
Fixed O&M cost	€/MW/year	298
Variable O&M cost	€/MWh	-

Reverse Water-Gas Shift for producing Syngas
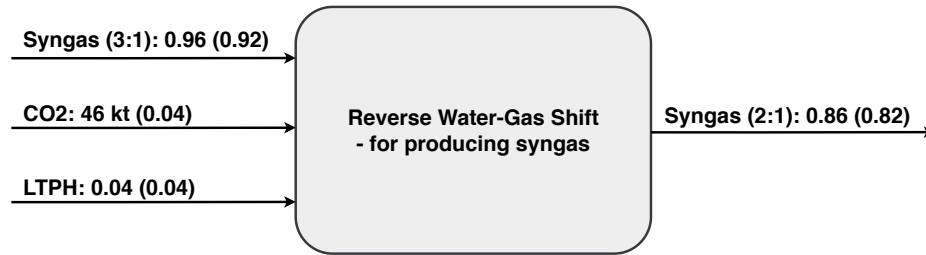
Figure B.6: *Energy balance of reverse water-gas shift for syngas production. The energy balance is made from the stoichiometic calculations with an assumption of 10% hydrogen loss.*

Table B.6: *ADAPT input for reverse water-gas shift. It has been assumed to be the same for both adjusting and producing syngas [25].*

Reverse Water-Gas Shift	Unit	ADAPT
Investment cost	M€/MW	0.006
Fixed O&M cost	€/MW/year	298
Variable O&M cost	€/MWh	-

Electrolysis (SOEC)
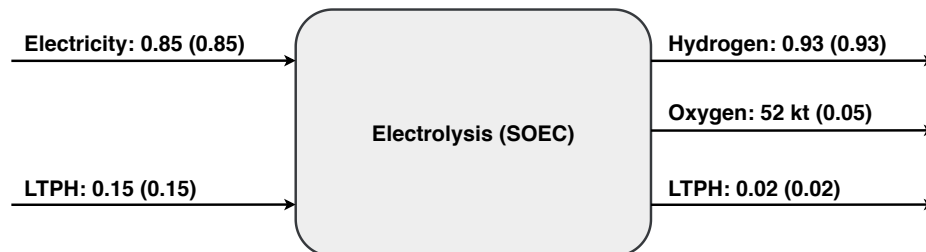
Figure B.7: *Energy balance of solid oxide electrolyzer cell [72].*

Table B.7: *ADAPT input for electrolysis (SOEC) [64].*

Electrolysis (SOEC)	Unit	ADAPT
Investment cost	M€/MW	0.475
Fixed O&M cost	€/MW/year	14,246
Variable O&M cost	€/MWh	-

Co-electrolysis
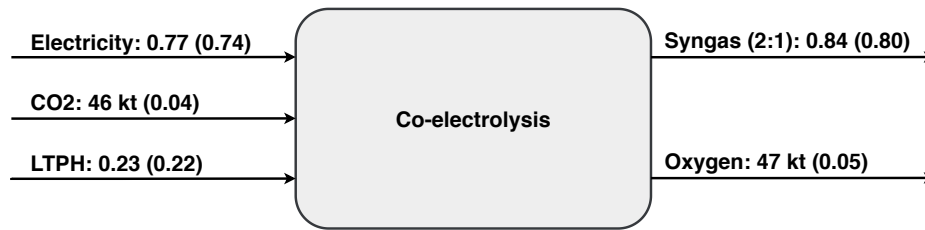
Figure B.8: *Energy balance of solid oxide electroyzer cell operated as co-electrolysis of CO_2 and water [30].*

Table B.8: *ADAPT input for co-electrolysis [64]. Has been assumed to be similar to that of regular electrolysis of water after talks with the Technical University of Denmark.*

Co-electrolysis (SOEC)	Unit	ADAPT
Investment cost	M€/MW	0.475
Fixed O&M cost	€/MW/year	14,246
Variable O&M cost	€/MWh	-

Low-Temperature Fischer-Tropsch
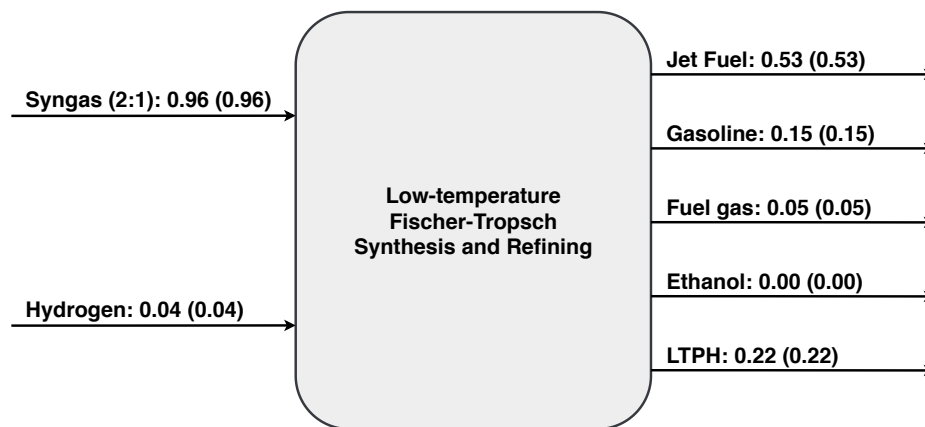
Figure B.9: *Energy balance of low-temperature Fischer-Tropsch [12].*

Table B.9: *ADAPT input for low-temperature Fischer-Tropsch and refining [31]. The cost of the Fischer-Tropsch synthesis and refining has been based on the cost of the Pearl GTL in Qatar [92].*

Low-temperature Fischer-Tropsch	Unit	ADAPT
Investment cost	M€/MW	0.309
Fixed O&M cost	€/MW/year	15,475
Variable O&M cost	€/MWh	-

Direct Air Capture

Figure B.10: *Energy balance of temperature swing adsorption direct air capture [13].*

Table B.10: *ADAPT input for direct air capture (temperature swing adsorption) [82].*

Direct Air Capture	Unit	ADAPT
Investment cost	M€/MW	2.859
Fixed O&M cost	€/MW/year	57,185
Variable O&M cost	€/MWh	-

Waste Incineration

Figure B.11: *Energy balance of waste incineration [72]. The energy balance includes a carbon capture rate of 75% [47], while the actual content of CO_2 is approximately 95 kt/PJ.*

Table B.11: *ADAPT input for waste incineration [72].*

Waste Incineration	Unit	ADAPT
Investment cost	M€/MW	1.358
Fixed O&M cost	€/MW/year	54,542
Variable O&M cost	€/MWh	4.527

Biomass Incineration
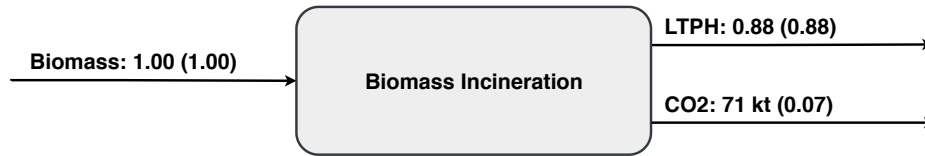
Figure B.12: *Energy balance of a biomass boiler [72]. The energy balance includes a carbon capture rate of 75% [47], while the actual content of CO_2 is approximately 95 kt/PJ.*

Table B.12: *ADAPT input for bionass incineration [72].*

Biomass Incineration	Unit	ADAPT
Investment cost	M€/MW	0.346
Fixed O&M cost	€/MW/year	26,056
Variable O&M cost	€/MWh	0.773

C   Sifre and ADAPT Input Data

C.1   Production Units

Biogas Upgrading
– **Type:** Backpressure (Methane and CO_2 (offsite))
– **Cb:** 50.45
– **Production efficiency, B:** 3.77
– **Fuel consumption:** 95.93% Biogas, 4.07% Electricity
– **ADAPT, Investment cost:** 0.487 M€/MW
– **ADAPT, Fixed O&M cost:** 12,255 €/MW/y
– **ADAPT, Lifetime cost:** 15 years
– **Variable O&M:** 0.0 €/MWh
– **Minimum Production Limit:** 15%

Methanation
– **Type:** Backpressure (Methane and LTPH)
– **Cb:** 8.80
– **Production efficiency, B:** 4.01
– **Fuel consumption:** 53.79% Biogas, 46.21% Hydrogen
– **ADAPT, Investment cost:** 0.713 M€/MW
– **ADAPT, Fixed O&M cost:** 25,394 €/MW/y
– **ADAPT, Lifetime cost:** 25 years
– **Variable O&M:** 2.385 €/MWh
– **Minimum Production Limit:** 15%

Electrolysis (SOEC)
– **Type:** Backpressure (Gas mix 1 and LTPH)
– **Cb:** 65.47
– **Production efficiency, B:** 3.67
– **Fuel consumption:** 85.00% Electricity, 15.00% LTPH
– **ADAPT, Investment cost:** 0.475 M€/MW
– **ADAPT, Fixed O&M cost:** 14,246 €/MW/y
– **ADAPT, Lifetime cost:** 25 years
– **Variable O&M:** 0.0 €/MWh
– **Minimum Production Limit:** 15%

Co-electrolysis (SOEC)
– **Type:** Backpressure (Syngas (2:1) and Oxygen)
– **Cb:** 17.80
– **Production efficiency, B:** 4.47
– **Fuel consumption:** 73.93% Electricity, 21.71% LTPH, 4.36% CO_2
– **ADAPT, Investment cost:** 0.475 M€/MW
– **ADAPT, Fixed O&M cost:** 14,246 €/MW/y
– **ADAPT, Lifetime cost:** 25 years
– **Variable O&M:** 0.0 €/MWh
– **Minimum Production Limit:** 15%

Steam-methane reforming (SMR)

– **Type:** Condensation (Syngas (3:1))
– **Production efficiency, B:** 4.21
– **Fuel consumption:** 81.28% Methane, 18.72% HTPH
– **ADAPT, Investment cost:** 0.064 M€/MW
– **ADAPT, Fixed O&M cost:** 3,210 €/MW/y
– **ADAPT, Lifetime cost:** 20 years
– **Variable O&M:** 0.0 €/MWh
– **Minimum Production Limit:** 15%

Electric steam-methane reforming (eSMR) (Decentral)
– **Type:** Condensation (Syngas (2:1))
– **Production efficiency, B:** 4.21
– **Fuel consumption:** 81.28% Biogas, 18.72% Electricity
– **ADAPT, Investment cost:** 0.064 M€/MW
– **ADAPT, Fixed O&M cost:** 3,210 €/MW/y
– **ADAPT, Lifetime cost:** 20 years
– **Variable O&M:** 0.0 €/MWh
– **Minimum Production Limit:** 15%

Electric steam-methane reforming (eSMR) (Central)
– **Type:** Condensation (Syngas (3:1))
– **Production efficiency, B:** 4.21
– **Fuel consumption:** 81.28% Methane, 18.72% Electricity
– **ADAPT, Investment cost:** 0.064 M€/MW
– **ADAPT, Fixed O&M cost:** 3,210 €/MW/y
– **ADAPT, Lifetime cost:** 20 years
– **Variable O&M:** 0.0 €/MWh
– **Minimum Production Limit:** 15%

Partial oxidation (POX)
– **Type:** Backpressure (Syngas (2:1) and HTPH)
– **Cb:** 23.86
– **Production efficiency, B:** 3.99
– **Fuel consumption:** 99.05% Methane, 0.95% Oxygen
– **ADAPT, Investment cost:** 0.039 M€/MW
– **ADAPT, Fixed O&M cost:** 1,926 €/MW/y
– **ADAPT, Lifetime cost:** 20 years
– **Variable O&M:** 0.0 €/MWh
– **Minimum Production Limit:** 15%

Air separation unit (ASU)
– **Type:** Condensation (Oxygen)
– **Production efficiency, B:** 18.95
– **Fuel consumption:** 100.00% Electricity
– **ADAPT, Investment cost:** 3.449 M€/MW
– **ADAPT, Fixed O&M cost:** 103,465 €/MW/y
– **ADAPT, Lifetime cost:** 20 years
– **Variable O&M:** 0.0 €/MWh
– **Minimum Production Limit:** 15%

Reverse water-gas shift (RWGS) 1
– **Type:** Condensation (Syngas (2:1))
– **Production efficiency, B:** 3.69
– **Fuel consumption:** 97.57% Syngas (3:1), 1.26% CO_2, 1.18% HTPH
– **ADAPT, Investment cost:** 0.006 M€/MW
– **ADAPT, Fixed O&M cost:** 298 €/MW/y
– **ADAPT, Lifetime cost:** 25 years
– **Variable O&M:** 0.0 €/MWh
– **Minimum Production Limit:** 15%

Reverse water-gas shift (RWGS) 2
– **Type:** Condensation (Syngas (2:1))
– **Production efficiency, B:** 4.37
– **Fuel consumption:** 91.774% Hydrogen, 4.242% CO_2, 3.984% HTPH
– **ADAPT, Investment cost:** 0.006 M€/MW
– **ADAPT, Fixed O&M cost:** 298 €/MW/y
– **ADAPT, Lifetime cost:** 25 years
– **Variable O&M:** 0.0 €/MWh
– **Minimum Production Limit:** 15%

Low-temperature Fischer-Tropsch (LTFT) + Refining
– **Type:** Backpressure (Fuel mix 1 and LTPH)
– **Cb:** 3.32
– **Production efficiency, B:** 4.92
– **Fuel consumption:** 95.98% Syngas (2:1), 4.02% Hydrogen
– **ADAPT, Investment cost:** 0.309 M€/MW
– **ADAPT, Fixed O&M cost:** 15,475 €/MW/y
– **ADAPT, Lifetime cost:** 25 years
– **Variable O&M:** 0.0 €/MWh
– **Minimum Production Limit:** 15%

Direct air capture (DAC) - temperature swing adsorption (TSA)
– **Type:** Backpressure (CO_2 (DAC) and DH)
– **Cb:** 0.56
– **Production efficiency, B:** 25.92
– **Fuel consumption:** 87.50% LTPH, 12.50% Electricity
– **ADAPT, Investment cost:** 2.859 M€/MW
– **ADAPT, Fixed O&M cost:** 57,185 €/MW/y
– **ADAPT, Lifetime cost:** 25 years
– **Variable O&M:** 0.0 €/MWh
– **Minimum Production Limit:** 15%

HTPH Gas Boiler
– **Type:** Condensation (HTPH)
– **Production efficiency, B:** 3.79
– **Fuel consumption:** 100.00% Methane, 100.00% Hydrogen, 100.00% Fuel gas
– **ADAPT, Investment cost:** 0.050 M€/MW
– **ADAPT, Fixed O&M cost:** 1,877 €/MW/y
– **ADAPT, Lifetime cost:** 25 years
– **Variable O&M:** 0.994 €/MWh
– **Minimum Production Limit:** 15%

LTPH to HTPH Gas Boiler
– **Type:** Condensation (HTPH)
– **Production efficiency, B:** 3.79
– **Fuel consumption:** 100.00% Methane, 100.00% Hydrogen, 100.00% Fuel gas, 50.00% LTPH
– **ADAPT, Investment cost:** 0.050 M€/MW
– **ADAPT, Fixed O&M cost:** 1,877 €/MW/y
– **ADAPT, Lifetime cost:** 25 years
– **Variable O&M:** 0.994 €/MWh
– **Minimum Production Limit:** 15%

LTPH Electric Boiler
– **Type:** Condensation (LTPH)
– **Production efficiency, B:** 3.64
– **Fuel consumption:** 100.00% Electricity
– **ADAPT, Investment cost:** 0.077 M€/MW
– **ADAPT, Fixed O&M cost:** 1,016 €/MW/y
– **ADAPT, Lifetime cost:** 25 years
– **Variable O&M:** 0.442 €/MWh
– **Minimum Production Limit:** 15%

LTPH Heat Pump
– **Type:** Condensation (LTPH)
– **Production efficiency, B:** 1.76
– **Fuel consumption:** 100.00% Electricity
– **ADAPT, Investment cost:** 1.031 M€/MW
– **ADAPT, Fixed O&M cost:** 2,208 €/MW/y
– **ADAPT, Lifetime cost:** 20 years
– **Variable O&M:** 1.943 €/MWh
– **Minimum Production Limit:** 15%

Wood Chip Boiler
– **Type:** Backpressure (LTPH and CO_2 (biomass - uncaptured))
– **Cb:** 12.43
– **Production efficiency, B:** 4.09
– **Fuel consumption:** 100.00% Wood Chips
– **ADAPT, Investment cost:** 0.346 M€/MW
– **ADAPT, Fixed O&M cost:** 26,056 €/MW/y
– **ADAPT, Lifetime cost:** 25 years
– **Variable O&M:** 0.773 €/MWh
– **Minimum Production Limit:** 15%

Waste Boiler
– **Type:** Backpressure (LTPH and CO_2 (waste - uncaptured))
– **Cb:** 12.33
– **Production efficiency, B:** 4.09
– **Fuel consumption:** 100.00% Waste
– **ADAPT, Investment cost:** 1.358 M€/MW
– **ADAPT, Fixed O&M cost:** 54,542 €/MW/y
– **ADAPT, Lifetime cost:** 25 years
– **Variable O&M:** 4.527 €/MWh
– **Minimum Production Limit:** 15%

Carbon capture (CC) (biomass)
– **Type:** Condensation (CO_2 (biomass - captured))
– **Production efficiency, B:** 3.60
– **Fuel consumption:** 100.00% CO_2 (biomass - uncaptured)
– **Production cost:** 163.2 €/MWh (modelled as a tax in Sifre)
– **Minimum Production Limit:** 0%

Carbon capture (CC) (waste)
– **Type:** Condensation (CO_2 (waste - captured))
– **Production efficiency, B:** 3.60
– **Fuel consumption:** 100.00% CO_2 (waste - uncaptured)
– **Production cost:** 163.2 €/MWh (modelled as a tax in Sifre)
– **Minimum Production Limit:** 0%

CO_2 Piping and Storage
– **Type:** Condensation (CO_2 (CO_2 Reduction))
– **Production efficiency, B:** 3.60
– **Fuel consumption:** 100.00% CO_2 (biogas), 100.00% CO_2 (DAC), 100.00% CO_2 (biomass - uncaptured), 100.00% CO_2 (waste - uncaptured)
– **Production cost:** 114.6 €/MWh (modelled as a tax in Sifre)
– **Minimum Production Limit:** 0%

Gas Splitter 1
– **Type:** Backpressure (Hydrogen and Oxygen)
– **Cb:** 17.85
– **Production efficiency, B:** 3.80
– **Fuel consumption:** 100.00% Gas mix 1
– **Minimum Production Limit:** 0%

Fuel Splitter 1
– **Type:** Backpressure (Jet fuel and Fuel mix 2)
– **Cb:** 2.64
– **Production efficiency, B:** 4.96
– **Fuel consumption:** 100.00% Fuel mix 1
– **Minimum Production Limit:** 0%

Fuel Splitter 2
– **Type:** Backpressure (Gasoline and Fuel mix 3)
– **Cb:** 3.25
– **Production efficiency, B:** 4.71
– **Fuel consumption:** 100.00% Fuel mix 2
– **Minimum Production Limit:** 0%

Fuel Splitter 3
– **Type:** Backpressure (Fuel gas and Ethanol)
– **Cb:** 21.08
– **Production efficiency, B:** 3.77
– **Fuel consumption:** 100.00% Fuel mix 3
– **Minimum Production Limit:** 0%

CO$_2$ Mixer
- **Type:** Condensation (CO$_2$ (fuel production))
- **Production efficiency, B:** 3.60
- **Fuel consumption:** 100.00% CO$_2$ (biogas), 100.00% CO$_2$ (DAC), 100.00% CO$_2$ (waste - captured),

  100.00% CO$_2$ (biomass - captured)
- **Minimum Production Limit:** 0%

C.2   Energy Storages

Oxygen Storage
- **ADAPT, Investment cost:** 0.591 M€/MWh
- **ADAPT, Fixed O&M cost:** 0.0 €/MWh/y
- **ADAPT, Lifetime cost:** 30 years
- **Charge efficiency:** 99.00%
- **Discharge efficiency:** 99.00%
- **Loss:** 0.10 %/hour

Hydrogen Storage
- **ADAPT, Investment cost:** 0.023 M€/MWh
- **ADAPT, Fixed O&M cost:** 441.6 €/MWh/y
- **ADAPT, Lifetime cost:** 30 years
- **Charge efficiency:** 90.00%
- **Discharge efficiency:** 100.00%
- **Loss:** 0.10 %/hour

Syngas (2:1) Storage
- **ADAPT, Investment cost:** 0.083 M€/MWh
- **ADAPT, Fixed O&M cost:** 0.0 €/MWh/y
- **ADAPT, Lifetime cost:** 30 years
- **Charge efficiency:** 99.00%
- **Discharge efficiency:** 99.00%
- **Loss:** 0.10 %/hour

Syngas (3:1) Storage
- **ADAPT, Investment cost:** 0.083 M€/MWh
- **ADAPT, Fixed O&M cost:** 0.0 €/MWh/y
- **ADAPT, Lifetime cost:** 30 years
- **Charge efficiency:** 99.00%
- **Discharge efficiency:** 99.00%
- **Loss:** 0.10 %/hour

CO$_2$ Storage
- **ADAPT, Investment cost:** 0.000137 M€/MWh
- **ADAPT, Fixed O&M cost:** 22.5 €/MWh/y
- **ADAPT, Lifetime cost:** 20 years
- **Charge efficiency:** 99.00%
- **Discharge efficiency:** 99.00%
- **Loss:** 0.10 %/hour

Fuel gas Storage
– **ADAPT, Investment cost:** 0.023 M€/MWh
– **ADAPT, Fixed O&M cost:** 441.6 €/MWh/y
– **ADAPT, Lifetime cost:** 30 years
– **Charge efficiency:** 90.00%
– **Discharge efficiency:** 100.00%
– **Loss:** 0.10 %/hour

HTPH Storage
– **ADAPT, Investment cost:** 0.0028 M€/MWh
– **ADAPT, Fixed O&M cost:** 0.0 €/MWh/y
– **ADAPT, Lifetime cost:** 25 years
– **Charge efficiency:** 90.00%
– **Discharge efficiency:** 90.00%
– **Loss:** 1.00 %/hour

LTPH Storage
– **ADAPT, Investment cost:** 0.0028 M€/MWh
– **ADAPT, Fixed O&M cost:** 0.0 €/MWh/y
– **ADAPT, Lifetime cost:** 25 years
– **Charge efficiency:** 90.00%
– **Discharge efficiency:** 90.00%
– **Loss:** 1.00 %/hour

Natural Gas Grid
– **Charge efficiency:** 99.00%
– **Discharge efficiency:** 99.00%
– **Loss:** 0.01 %/hour

C.3   Interconnection Lines

Hydrogen Pipe (Western Jutland (VestJL) to Odense)
– **ADAPT, Investment cost:** 0.2511 M€/MW
– **ADAPT, Lifetime cost:** 50 years
– **Distance:** 150 km

CO_2 Pipe (offsite to onsite)
– **Transportation cost:** 4.80 €/MWh (1.33 €/tonne) (modelled as a tariff of the interconnection line)
– **Distance:** 30 km

CO_2 Pipe (offsite to onsite)
– **Transportation cost:** 9.60 €/MWh (2.67 €/tonne) (modelled as a tariff of the interconnection line)
– **Distance:** 60 km

CO_2 Pipe (offsite to onsite)
– **Transportation cost:** 16.00 €/MWh (4.44 €/tonne) (modelled as a tariff of the interconnection line)
– **Distance:** 100 km

CO$_2$ Trucking (offsite to onsite)
– **Transportation cost:** 9.10 €/MWh (2.53 €/tonne) (modelled as a tariff of the interconnection line)
– **Distance:** 30 km

CO$_2$ Trucking (offsite to onsite)
– **Transportation cost:** 18.2 €/MWh (5.06 €/tonne) (modelled as a tariff of the interconnection line)
– **Distance:** 60 km

CO$_2$ Trucking (offsite to onsite)
– **Transportation cost:** 30.3 €/MWh (8.43 €/tonne) (modelled as a tariff of the interconnection line)
– **Distance:** 100 km

D   Sifre Modelling

This appendix includes figures illustrating the design of the Sifre model. Due to the size of the model, the decentral and central production sites have been split up in each their figure. The decentral production site, *offsite*, seen in Figure D.3, illustrates how methane is produced by either biogas upgrading or methanation. Whether biogas upgrading or methanation is used for methane production depends on the specific scenario. The central production site, *onsite*, seen in Figure D.4, illustrates how liquid fuels, including jet fuel, are produced. Whether the liquid fuels are produced with a syngas feedstock from SMR, POX, RWGS or co-electrolysis depends on the specific scenario.

D.1   Sifre Model - Legends
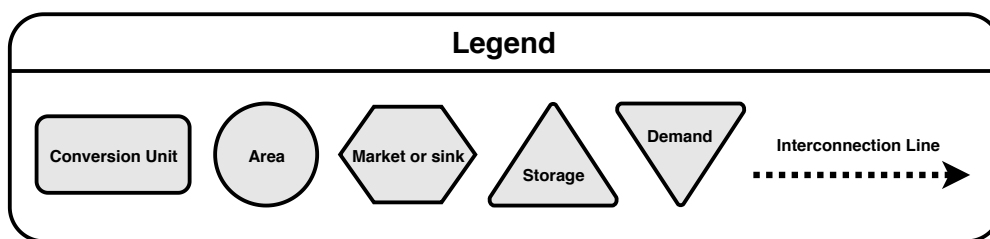
Figure D.1: *The figure shows the main legend for the boxes and interconnection line for both Figure D.3 and D.4.*
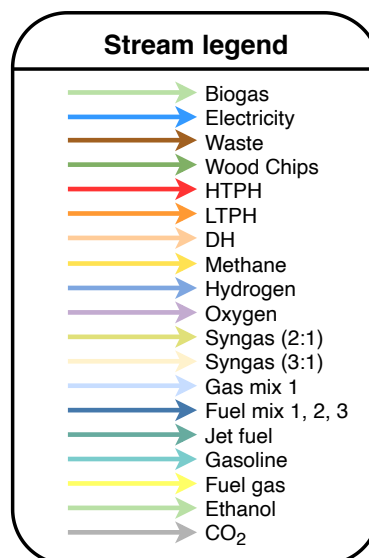
Figure D.2: *The figure shows the stream legend for both Figure D.3 and D.4.*

D.2   Sifre Model - Offsite
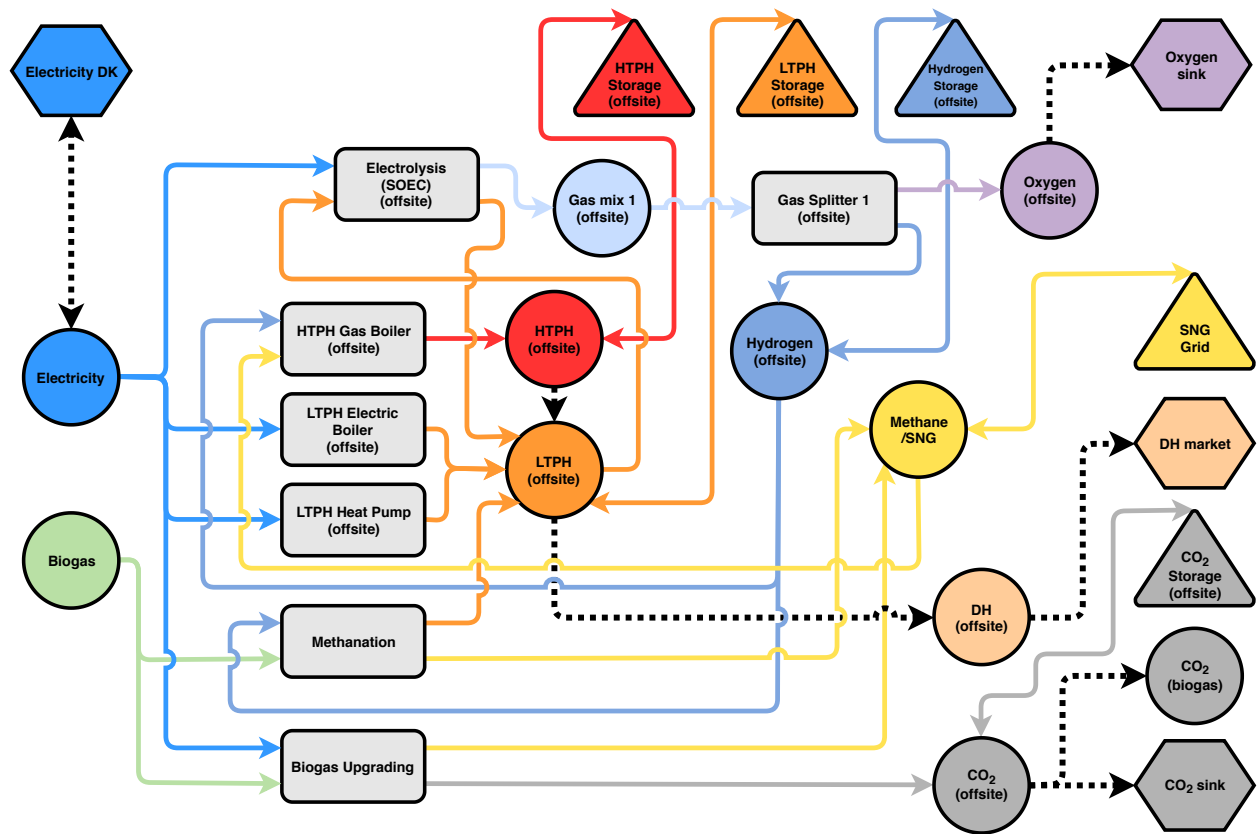
Figure D.3: *The figure illustrates how the decentral production site, offsite, has been modelled in Sifre. Whether biogas upgrading or methanation is used for methane production depends on the scenario.*

D.3 Sifre Model - Onsite
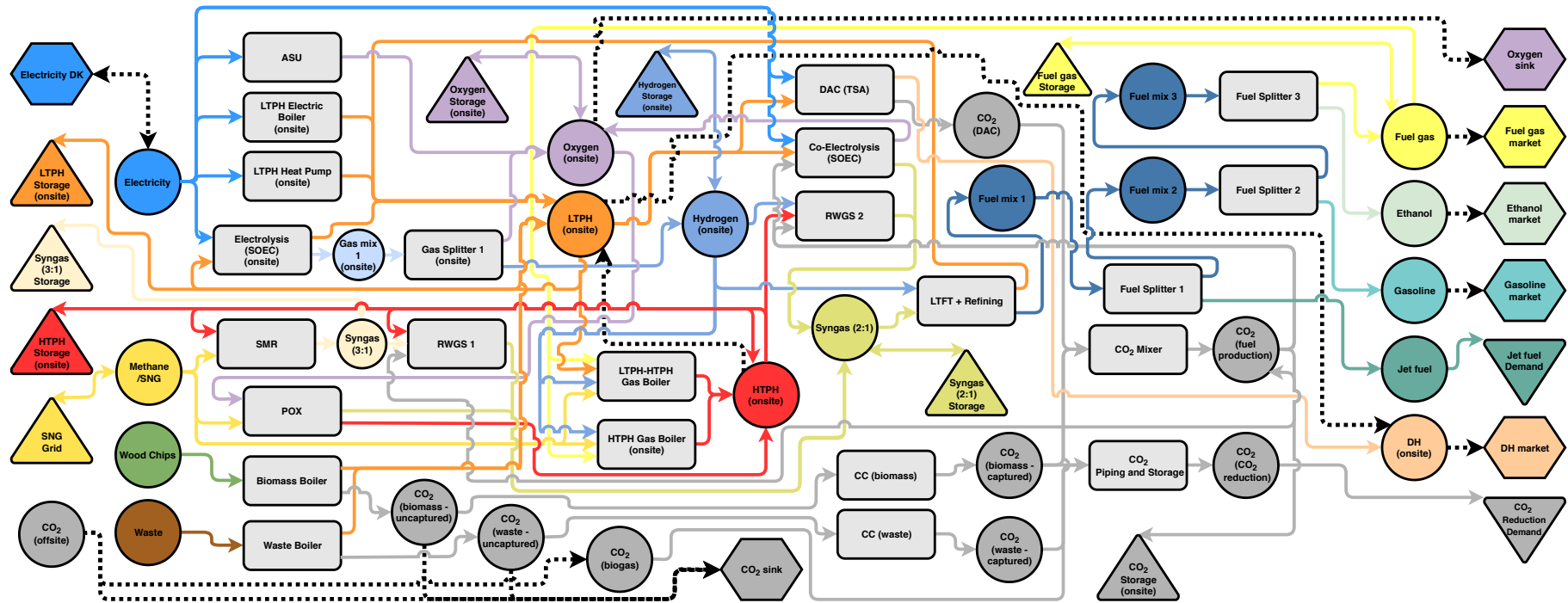
Figure D.4: *The figure illustrates how the central production site, onsite, has been modelled in Sifre. Whether the liquid fuels are produced with a syngas feedstock from SMR, POX, RWGS or co-electrolysis depends on the scenario.*

E   Collection of ADAPT results

Table E.1: *The table shows the invested capacities of production units in ADAPT for all main scenarios with a feedstock of methane produced by methanation. All capacities, except for DAC and ASU, have been given in MW-primary output while DAC and ASU have been given in produced tonne/hour.*

Production unit	Unit	Scenario							
		1.1	*1.2*	*1.3*	*1.4*	*1.5*	*1.6*	*1.7*	*1.8*
Biogas Upgrading	*MW*	-	-	-	-	-	-	-	-
Methanation	*MW*	1370	1580	57	579	119	1807	2	2
Electrolysis (offsite)	*MW*	744	859	32	315	65	982	1	1
Electrolysis (onsite)	*MW*	176	63	128	3262	127	3360	127	3496
SMR	*MW*	1433	-	130	900	-	-	-	-
POX	*MW*	-	1433	-	-	409	2544	-	-
ASU	*t/hr*	-	42	-	-	-	-	-	-
RWGS 1	*MW*	1433	-	134	900	-	-	-	-
RWGS 2	*MW*	-	-	-	2667	-	2749	-	2865
Co-electrolysis	*MW*	-	-	2864	-	2865	-	2865	-
DAC	tCO_2/hr	-	-	343	268	339	83	344	337
LTFT + Refining	*MW*	1092	1092	2184	2184	2184	2184	2184	2184
Waste Boiler	*MW*	665	665	665	665	665	665	665	665
Biomass Boiler	*MW*	-	-	56	-	40	-	69	-
HTPH Gas Boiler (offsite)	*MW*	-	-	1	-	-	-	-	-
HTPH Gas Boiler (onsite)	*MW*	-	-	59	-	21	128	-	-
LTPH to HTPH Gas boiler	*MW*	331	-	1	277	-	-	-	139
LTPH Electric Boiler (offsite)	*MW*	-	-	2	-	-	-	-	-
LTPH Electric Boiler (onsite)	*MW*	-	-	50	-	61	-	-	-
LTPH Heat Pump (offsite)	*MW*	-	-	-	-	-	-	-	-
LTPH Heat Pump (onsite)	*MW*	-	-	-	-	-	-	-	-

Table E.2: *The table shows the invested capacities of production units in ADAPT for all main scenarios with a feedstock of methane produced by biogas upgrading. All capacities, except for DAC and ASU, have been given in MW-primary output while DAC and ASU have been given in produced tonne/hour.*

Storage	Unit	Scenario							
		2.1	*2.2*	*2.3*	*2.4*	*2.5*	*2.6*	*2.7*	*2.8*
Biogas Upgrading	*MW*	1420	1576	1590	1590	1590	1590	2	2
Methanation	*MW*	-	-	-	-	-	-	-	-
Electrolysis (offsite)	*MW*	-	-	-	-	-	-	-	-
Electrolysis (onsite)	*MW*	176	63	127	2935	127	3496	127	3496
SMR	*MW*	1433	-	1957	2421	-	-	-	-
POX	*MW*	-	1433	-	-	2514	2544	-	-
ASU	*t/hr*	-	42	-	-	-	-	-	-
RWGS 1	*MW*	1433	-	1957	2421	-	-	-	-
RWGS 2	*MW*	-	-	-	2389	-	2865	-	2866
Co-electrolysis	*MW*	-	-	1939	-	2865	-	2866	-
DAC	*tCO$_2$/hr*	-	-	30	13	-	-	344	337
LTFT + Refining	*MW*	1092	1092	2184	2184	2184	2184	2184	2184
Waste Boiler	*MW*	665	665	665	665	665	665	665	665
Biomass Boiler	*MW*	-	-	-	-	-	-	69	-
HTPH Gas Boiler (offsite)	*MW*	-	-	-	-	-	-	-	-
HTPH Gas Boiler (onsite)	*MW*	-	-	-	-	-	128	3	-
LTPH to HTPH Gas boiler	*MW*	331	-	452	580	-	-	-	139
LTPH Electric Boiler (offsite)	*MW*	-	-	-	-	-	-	-	-
LTPH Electric Boiler (onsite)	*MW*	-	-	-	-	-	-	2	-
LTPH Heat Pump (offsite)	*MW*	-	-	-	-	-	-	-	-
LTPH Heat Pump (onsite)	*MW*	-	-	-	-	-	-	-	-

Table E.3: *The table shows the invested capacities of storages in ADAPT for all main scenarios with a feedstock of methane produced by methanation. All capacities, except for the oxygen and CO_2 storages, have been given in MWh while the oxygen and CO_2 storages have been given in tonne.*

Production unit	Unit	Scenario							
		1.1	*1.2*	*1.3*	*1.4*	*1.5*	*1.6*	*1.7*	*1.8*
LTPH Storage (offsite)	*MWh*	-	-	41	-	-	-	-	-
LTPH Storage (onsite)	*MWh*	-	-	53	-	119	-	-	-
HTPH Storage (offsite)	*MWh*	-	-	54	-	-	-	-	-
HTPH Storage (onsite)	*MWh*	-	-	39	537	1	1014	-	-
Hydrogen Storage (offsite)	*MWh*	-	-	11	-	-	-	-	-
Hydrogen Storage (onsite)	*MWh*	-	-	14	-	-	-	-	-
Oxygen Storage (offsite)	*t*	-	-	-	-	-	-	-	-
Oxygen Storage (onsite)	*t*	-	-	-	-	-	-	-	-
CO₂ Storage (offsite)	*tCO₂*	-	-	-	-	-	-	-	-
CO₂ Storage (onsite)	*tCO₂*	-	-	731	2785	931	16315	-	-
Fuel gas Storage	*MWh*	-	-	7	159	-	-	-	-
Syngas (2:1) Storage	*MWh*	-	-	7	-	-	-	-	-
Syngas (3:1) Storage	*MWh*	-	-	5	-	-	-	-	-

Table E.4: *The table shows the invested capacities of storages in ADAPT for all main scenarios with a feedstock of methane produced by biogas upgrading. All capacities, except for the oxygen and CO_2 storages, have been given in MWh while the oxygen and CO_2 storages have been given in tonne.*

Storage	Unit	Scenario							
		2.1	*2.2*	*2.3*	*2.4*	*2.5*	*2.6*	*2.7*	*2.8*
LTPH Storage (offsite)	*MWh*	-	-	-	-	-	-	-	-
LTPH Storage (onsite)	*MWh*	-	-	-	2	-	-	3	2
HTPH Storage (offsite)	*MWh*	-	-	-	-	-	-	-	-
HTPH Storage (onsite)	*MWh*	-	-	221	186	-	811	3	2
Hydrogen Storage (offsite)	*MWh*	-	-	-	-	-	-	-	-
Hydrogen Storage (onsite)	*MWh*	-	-	-	1	-	-	2	1
Oxygen Storage (offsite)	*t*	-	-	-	-	-	-	-	-
Oxygen Storage (onsite)	*t*	-	-	-	-	-	-	-	-
CO₂ Storage (offsite)	*tCO₂*	-	-	5484	8967	10759	8628	48	40
CO₂ Storage (onsite)	*tCO₂*	-	-	416	1318	7107	7916	44	38
Fuel gas Storage	*MWh*	-	-	140	114	-	-	1	-
Syngas (2:1) Storage	*MWh*	-	-	-	-	-	-	1	-
Syngas (3:1) Storage	*MWh*	-	-	-	-	-	-	-	-